Translational control of a set of mRNAs by RNA-binding protein Bfr1p at the ER in budding yeast.

Dissertation

der Mathematisch-Naturwissenschaftlichen Fakultät

der Eberhard Karls Universität Tübingen

zur Erlangung des Grades eines

Doktors der Naturwissenschaften

(Dr. rer. nat.)

vorgelegt von

Manchalu Srinivas

Achampet, Indien

Tübingen

2019

Gedruckt mit Genehmigung der Mathematisch-Naturwissenschaftlichen

Fakultät der Eberhard Karls Universität Tübingen

Tag der mündlichen Qualifikation: 28.01.2020

Dekan: ..... …….Prof. Dr. Wolfgang Rosentiel

1.Berichterstatter: ..... …..Prof. Dr. Ralf-Peter Jansen

2.Berichterstatter:.....Prof. Dr. Doron Rapaport

Table of Contents

List of abbreviations

Asc1p - Absence of growth suppressor of Cyp1 protein

ASH1 - Asymmetric synthesis of HO gene

BFR1/Bfr1p –Brefeldin A resistance gene/protein

BSA - Bovine serum albumin

cDNA - Complementary DNA

CHX - Cycloheximide

CLIP - Cross-linking immunoprecipitation

CLN3 – Cyclin gene

Ct – Cycle threshold

C-terminus – Carboxyl-terminus

DCP1, *DCP2*/Dcp1p, Dcp2p – mRNA decapping gene/protein

DDT - Dichlorodiphenyltrichloroethane

DEB - DNA extraction buffer

DEPC – Diethyl pyrocarbonate

DNA - Deoxyribonucleic acid

DNase - Deoxyribonuclease

dsRBD – double-stranded RNA-binding domain

E. coli – *Escherichia coli*

Eap1p –eIF4E-associated protein

ECL - Enhanced chemiluminescence

EDAC - 1-Ethyl-3-(3-dimethylaminopropyl) carbodiimide

EDC3/Edc3p – Enhancer of mRNA decapping gene/protein

eIF4E - Eukaryotic translation initiation factor 4E

ER – Endoplasmic reticulum

ERAD - Endoplasmic Reticulum-Associated Degradation

FACS - Fluorescence-activated cell sorting

FUS – Fused in sarcoma

G1 – Gap 1 phase of the cell cycle

G418 - Geneticin

GFP - Green fluorescent protein

GTP - Guanosine-5'-triphosphate

HA - Hemagglutinin

HCl - Hydrochloric acid

HDEL- Histidine, Aspartic acid, Glutamic acid and Leucine sequence

HEPES - 4-(2-hydroxyethyl)-1-piperazineethanesulfonic acid

hnRNPA1 – Heterogeneous nuclear ribonucleoprotein A1

HPLC - High Performance Liquid Chromatography

HPV - Human papillomavirus

Hrd1p - HMG-coA Reductase Degradation protein

HSP – Heat shock protein

IgG - Immunoglobulin G

IP - Immunoprecipitation

IRE1/Ire1p – Inositol-requiring enzyme gene/protein

kDa - kilodalton

KH – hnRNP-K Homology

Khd1p - HEterogeneous nuclear rnp K-like protein

KOH - Potassium hydroxide

$MgCl_2$ - Magnesium chloride

mRNA - Messenger RNA

mRNP - messenger ribonucleoprotein

NaCl - Sodium chloride

ncRNA - non-coding RNA

NEB – New England Biolabs

NH_4Cl - Ammonium chloride

OD - Optical density

P-bodies - Processing bodies

PBS - Phosphate-buffered saline

PBS-T – Phosphate buffered saline + 0.1% Tween

PCR - Polymerase chain reaction

PEG - Polyethylene glycol

Pep4p - CarboxyPEPtidase Y-deficient protein

Pgk1p - 3-PhosphoGlycerate Kinase protein

PI – Propidium iodide

POM34/Pom34p –Pore membrane gene/protein

PVDF - Polyvinylidene fluoride or polyvinylidene difluoride

RAP - Ribosome-affinity purification

RBD – RNA-binding domain

RNA - Ribonucleic Acid

RNase - Ribonuclease

RPL/Rpl – Ribosomal protein of the large subunit gene/protein

RPS/Rps – Ribosomal protein of the small subunit gene/protein

RRM – RNA-recognition motif

RT-qPCR – Reverse transcription quantitative polymerase chain reaction

S phase – Synthesis phase of the cell cycle

S. cerevisiae – *Saccharomyces cerevisiae*

S. pombe – *Schizosaccharomyces pombe*

SC medium – Synthetic complete medium

SCP160/Scp160p –*S. cerevisiae* protein involved in the control of ploidy gene/protein

Scs2p - Suppressor of Choline Sensitivity protein

SD medium - Synthetic Drop-Out Medium

SDS - Sodium dodecyl sulfate

Sec61p – SECretory protein

SESA – A protein network consisting of Smy2p, Eap1p, Scp160p, and Asc1p

SG – Stress granule

SMY2/Smy2p –Suppressor of *myo2-66* gene/protein

SPB – Spindle pole body

SRP – Signal recognition particle

SS – Signal sequence

ssDNA - Salmon Sperm DNA

STI1/Sti1p – Stress inducible gene/protein

TAP- Tandem affinity purification

TE – Tris- Ethylenediaminetetraacetic acid

TEMED – Tetramethylethylenediamine

TM – Transmembrane domain

tRNA – Transfer RNA

UPOM - Unfolded O-mannosylation

UPR – Unfolded Protein Response

UTR – Untranslated region

UV - Ultraviolet

Xnr1p – eXoRiboNuclease 1 protein

XRN1/Xrn1p – Exoribonuclease gene/protein

yeGFP – yeast enhanced green fluorescent protein

YPED - Yeast extract peptone dextrose

Summary

Translational regulation of mRNA is an important mechanism by which cells modulate protein synthesis. The mRNAs that encode for secreted proteins or proteins of the endomembrane system are translated at the endoplasmic reticulum (ER). In *Saccharomyces cerevisiae*, Brefeldin A resistance factor 1 protein (Bfr1p) was first identified as a multi-copy suppressor of Brefeldin A and proposed to have a function in the secretory pathway. Although *BFR1* is a non-essential gene, *bfr1Δ* cells show several defects, including altered cell shape and size, change in ploidy, induction of P-bodies and chromosomal mis-segregation. However, later studies have shown Bfr1p as a component of polysomes, binding to several hundred mRNAs at the ER and most of these mRNAs encode for secretion or endomembrane proteins. Despite Bfr1p lacking canonical RNA-binding domains, an *in vivo* UV-crosslink of Bfr1p with RNA revealed six residues in Bfr1p that are cross-linked with the RNAs. These studies suggest a potential role of Bfr1p in translational control of mRNAs, however its molecular function remains elusive to date.

In this present study, I show that the Bfr1p's localization to the ER is RNA-dependent and that a point mutation in the RNA-binding residue F239 of Bfr1p alone is enough to affect this localization. Further, I show that the roles of Bfr1p in ploidy maintenance, P-bodies induction and brefeldin A resistance are independent of its interaction with RNA. Consistent with the previous studies, I show that Bfr1p binds to *ERG4* mRNA, which encodes an enzyme involved in the final step of ergosterol biosynthesis and that the RNA-binding mutants of Bfr1p impede this binding. Although *ERG4* mRNA localizes to the ER in *bfr1Δ* cells, the levels of Erg4 protein is strongly reduced, possibly due to its misfolding and subsequent re-translocation to the cytoplasm for degradation via the ERAD pathway. Using ribosome affinity purification (RAP) and

polysome profiling, I demonstrate a reduction in the total ribosomal occupancy on the *ERG4* mRNA in *bfr1Δ* cells and an increased ratio of monosomes to polysome in RNA-binding mutants of Bfr1p, suggesting a role for Bfr1p in translational elongation or protein translocation of the mRNAs that are translating at the ER. Taken together, this study provides further evidence of the proposed role of Bfr1p in translational control with separation from its function in ploidy maintenance.

Zusammenfassung

Die translationale Regulation von mRNA ist ein wichtiger Mechanismus, durch den Zellen die Proteinsynthese modulieren. Die mRNAs, die für sekretierte Proteine oder Proteine des Endomembransystems kodieren, werden am endoplasmatischen Retikulum (ER) translatiert. In Saccharomyces cerevisiae wurde das Brefeldin A Resistenzfaktor 1 Protein (Bfr1p) erstmals als Mehrfachkopiesuppressor von Brefeldin A identifiziert und eine Funktion im Sekretionsweg vorgeschlagen. Obwohl BFR1 ein nicht essentielles Gen ist, zeigen die bfr1Δ Zellen verschiedene Phänotypen, beispielsweise eine veränderte Zellform und Zellgröße, Änderung der Ploidie, Induktion von P-bodies und Chromosomenfehlsegregation. Spätere Studien haben jedoch gezeigt, dass Bfr1p als Bestandteil von Polysomen an verschiedene mRNAs im ER bindet und die Mehrheit dieser mRNAs für Sekretions- oder Endomembranproteine kodiert. Obwohl Bfr1p keine kanonischen RNA-Bindungsdomänen aufweist, ergab eine UV-crosslink, das die RNA in vivo über sechs Aminosäurereste. Diese Studien legen nahe, dass Bfr1p eine potenzielle Rolle bei der Translationskontrolle von mRNAs spielt. Die molekulare Funktion von Bfr1 ist bis heute nicht bekannt.

In dieser vorliegenden Studie zeige ich, dass die Bfr1p Lokalisierung zum ER RNA-abhängig ist und eine Punktmutation F239 von Bfr1p ausreicht, um diese Lokalisierung zu beeinflussen. Außerdem zeige ich, dass die Rolle von Bfr1p bei der Aufrechterhaltung der Ploidie, der Induktion von P-bodies und der Brefeldin A-Resistenz von seinen RNA Wechselwirkungen unabhängig ist. In Übereinstimmung mit den vorherigen Studien zeigte sich, dass Bfr1p an die ERG4 mRNA bindet, die für ein Enzym kodiert, das im letzten Schritt der Ergosterol-Biosynthese beteiligt ist, und dass die RNA-bindenden Mutanten diese Bindung beeinflussen. Obwohl ERG4

mRNA in bfr1Δ Zellen im ER lokalisiert ist, ist der Gehalt an Erg4p möglicherweise aufgrund der Fehlfaltung und dem Abbau über den ERAD Weg im Zytoplasmastask verringest. Mit den Experimenten zur Ribosomenaffinitätsreinigung (RAP) und Polysomenprofilierung konnte eine Verringerung der gesamten ribosomalen Belegung der ERG4 mRNA in bfr1Δ Zellen und ein erhöhtes Verhältnis von Monosomen zu Polysomen in RNA-bindenden Mutanten von Bfr1p nachgewiesen warden. Dies deutet auf eine Rolle von Bfr1p in der Translationselongation hin/oder korrekte Protein Translokation die am ER werden. Zusammengefasst liefert diese Studie weitere Beweise für die oben erwähnten Rolle von Bfr1p bei der Translationskontrolle, wobei Bfr1 ebenfalls einen Einfluss auf die Flufrechterhaltung der Ploidie hat.

1. Introduction

1.1. The RNA-binding proteins

RNA-binding proteins (RBPs) play important roles in different cellular processes such as gene expression, RNA trafficking, translation, and RNA stability. It is predicted that the proteomes of bacteria, archaea, and eukaryotes comprise approximately 3% to 11% of RBPs and in *Saccharomyces cerevisiae*, nearly 500 proteins are predicted to function as RBPs (Scherrer et al. 2010). RBPs bind to double or single-stranded RNA to form ribonucleoprotein particles (RNPs). These proteins are present in both cytoplasm and nucleus. For example, in the nucleus, mRNAs can assemble with RBPs to form mRNP complexes that are exported to the cytoplasm for their translation or degradation. Therefore, RBPs can regulate gene expression in the nucleus and furthermore can control the process of localization, translation, and stability of these mRNAs in the cytoplasm.

Several RBPs have been implicated in neurological diseases. The fragile X mental retardation syndrome is caused by a mutation in the KH2 domain (isoleucine304 to asparagine) of the RNA-binding protein FMRP (Boulle et al. 1993 and Feng et al. 1997). FMRP is responsible for regulating the local translation of proteins involved in synaptic development. *FMR1* knock-out mice show excessive protein production in the brain due to the loss of FMRP which acts as a negative regulator of translation (Feng et al. 1997). Similarly, mutations in the *SMN1* gene causes Spinal Muscular Atrophy (SMA) in humans. SMN (Survival of Motor Neurons) proteins are chaperones and highly conserved from the fission yeast *Schizosaccharomyces pombe* SMN proteins are crucial for the efficient assembly of Sm proteins and small nuclear RNAs (snRNAs) into snRNPs (Liu et al. 1997). SMN proteins bind to upstream of several

RBPs and regulate the splicing process of several RNAs (Chaytow et al. 2018). Recent studies have demonstrated that specific RBPs that contain low-complexity regions and prion-like domains such as TDP-43 and FUS proteins are concentrated by liquid-liquid phase separation in the cytoplasm (Schmidt et al. 2019, Niaki et al. 2019). These proteins form self-templating fibrils and can cause several neurological diseases such as amyotrophic lateral sclerosis and frontotemporal dementia (Shorter 2019).

RBPs are also involved in several other diseases such as cancer. For example, LARP family proteins contain a conserved La domain, and are upregulated in cancers of the head and neck (Sommer et al. 2010). Also, the RBP hnRNP A1 enhances the early splicing of HPV16 mRNA by binding to its splicing silencer (Zhao et al. 2007). The alternative splicing of HPV16 mRNA encodes for a truncated version of E6*I transcript of a full length E6 oncoprotein and is commonly found in oropharyngeal cancers (Paget-Bailly et al. 2019). Lastly, the mRNA cap-binding protein eukaryotic initiation factor 4E (eIF4E) is highly upregulated in several cancers. A specific AU-rich element in the 3'-UTR of eIF4E binds to HuR (Hu family RNA-binding proteins) and stabilizes the mRNA and can correlate with enhanced expression of eIF4E and HuR in malignant cancer specimens (Topisirovic et al. 2009).

Traditionally, it was thought that the protein and RNA interactions occur through well-defined protein domains called RNA-binding domains (RBDs). However, recent developments in high-throughput studies of RNA-protein complexes revealed several proteins that could interact with the RNA even in the absence of these known canonical domains (Hentze et al. 2018). These advancements also shed more light on how intrinsically disordered regions and protein-protein complexes can mediate RNA-protein interactions and play crucial roles in several cellular processes (reviewed in Hentze et al. 2018).

1.1.1. Conventional RNA-binding proteins

In eukaryotes, the canonical RBDs are mainly categorized into four families, the RNA recognition motif (RRM) (Oubridge et al. 1994), the heterologous nuclear RNP K homology (KH) domain (Lewis et al. 2000), the double-stranded RNA-binding domain (dsRBDs) (Ryter and Schultz 1998), and zinc-finger domains (Lu et al. 2003). These RBDs can interact with more than one mRNA and thus allow to regulate several mRNAs by single RBP (Hogan et al. 2018). Here, I briefly described the structure and specificity of RRM and KH domains, two commonly studied RBDs.

1.1.1.1. The RNA recognition motif (RRM)

One of the largest groups of the well-studied RBDs are RRMs that can be found in 0.5-1% of human genes (Venter et al. 2001). The RRM containing RBPs are involved in mRNA processing, the export of mRNA from the nucleus to the cytoplasm and RNA stability (Dreyfuss et al. 2002). The typical RRM consists of 90 amino acids and with a topology of β1-α1-β2-β3-α2-β4 and forms a four-stranded β-sheet folded against two

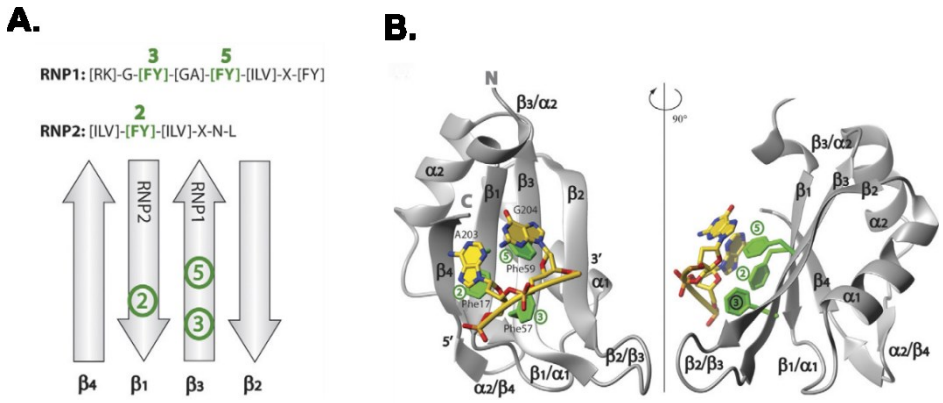

Figure 1. Interaction of RRM with single-stranded RNA/DNA. **A)**. The schematic view of the arrangement of four β sheets in an RRM containing proteins. The highlighted green residues (FY) on β1 and β3 sheets contain two conserved RNP1 and RNP2 aromatic residues that facilitate interaction with the RNA. **B)**. Structure of hnRNP A1 RRM2 interacting with single-stranded telomeric DNA showing how β1 and β3 sheets can accommodate two nucleotides. *The figure and the text are adapted from Cléry et al. (2008).*

α-helices. These four-stranded β sheets facilitate the interaction of RRM with the single-stranded RNA target (**Figure 1A and B**). In general, proteins with RRM binds to more than three nucleotides and recognize longer stranded RNA. The secondary structure elements of the RRM that is β2–β3 loop and the β1–α1 loop can facilitate the binding of the additional RNA. Therefore, in this way, the plasticity of an RRM is achieved for several RNAs (Cléry et al. 2008).

1.1.1.2. hnRNP K homology domains (KH domains)

The KH domains were first identified in the heterogeneous nuclear ribonucleoprotein K homology (hnRNP K) protein and hence given the name KH domains. KH domains are highly conserved and present in archaea, bacteria, and eukaryotes (Valverde et al. 2008). A typical KH domain consists of 70 amino acids and is often found in multiple copies per protein. These domains are capable of binding RNA independently and thus are popular for multi-tasking functions (Nicastro et al. 2015). KH domains are classified into two types (type I and II), and both types have a three-stranded β-sheet

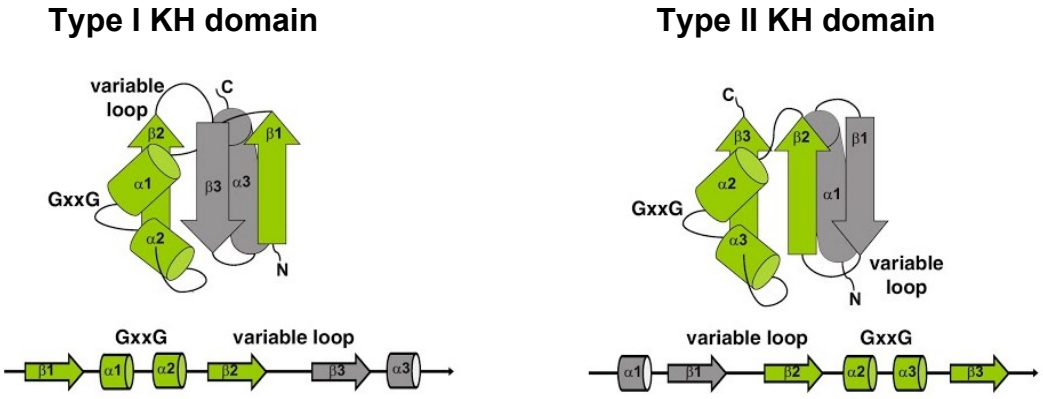

Figure 2. A cartoon representation of the folding and secondary structure of KH domains with three β-sheet and three α-helices. The core structure is represented in green colour (KH motif) and the connecting variable loop in grey colour and with conserved GXXG motif between α1 and α2 loop. *The figure and the text are adapted from Nicastro et al. (2015)*.

packed against three α-helices. The topology of type I is arranged as β-α-α-β-β-α whereas type II is arranged as α-β-β-α-α-β with a signature mark of conserved motif

GXXG in both types **(Figure 2).** This arrangement allows KH domains to interact through hydrophobic interactions with non-aromatic residues and the sugar-phosphate backbone of the single-stranded RNA/DNA to bind GXXG loop either by hydrogen bonding, electrostatic interactions or shape complementary and the specificity is achieved by the conserved hydrophobic region (Lunde et al. 2007).

1.1.2. Unconventional RNA-binding proteins

Methodological developments in capturing RNA-protein interactome led to the identification of several new unconventional RBPs. These new experimental approaches included the use of aptamer-tagged RNA as a bait coupled with Mass spectrometry (MS) (Butter et al. 2009), Photoactive ribonucleoside-enhanced crosslinking and immunoprecipitation (PAR-CLIP) (Hafner et al. 2010), and a PAR-CLIP variant with high-resolution Photo-cross-linking coupled with high-resolution Mass spectrometry (Kramer et al. 2014). These methods revealed that RBPs can have a range of other primary functions than simply binding and regulating RNA, such as enzymatic catalysis or mediators of protein-protein interactions (Hentze et al. 2018).

Among these newly identified unconventional RBPs are proteins with intrinsically disordered regions (IDRs) that contains a motif to bind RNA comprised of aromatic, polar residues such as Tyr together with Gly and Ser (G/S)Y(G/S) (Han et al. 2012, Kato et al. 2012). These residues usually are part of the hydrophobic core of proteins but when they are present on the surface, they can interact with the nucleobases and establish interactions with RNA. In *in vitro* experiments, it was demonstrated that proteins with this motif also could form protein aggregates and induces amyloid-fiber structures. In addition, they are involved in the separation of the liquid-liquid phase *in vivo* (Kato et al. 2012). Also, several studies have shown that phase separation properties of the hnRNP proteins are important for the formation of stress granules

and mutations in these proteins cause several neurological diseases (Xiao et al. 2019, Henning et al. 2015 and Murakami et al. 2015).

One of the newly emerged unconventional RBDs is the Rossmann-fold (R-f) domain, which was especially identified in the proteomes of RNA-binding complexes from cardiomyocytes (Liao et al. 2016). These R-f domains consist of six-stranded parallel β sheets with the interlinking α helices on both sides of these sheets and they interact with mono-or dinucleotides that such as ATP or GTP but can also bind to RNA (Caetano-Anollés et al. 2007, Hentze 1994, Rossmann et al. 1974).

Although these recent studies have identified several new types of RNA-protein interactions, our understanding of the molecular details of these interactions or their biological function remains still unclear.

1.2. The Endoplasmic reticulum, *a factory for protein synthesis of secretion and endomembrane system*

The endoplasmic reticulum (ER) is one of the largest membrane-bound organelles of eukaryotic cells and made up of tubular structures and sheets that are spread throughout the cytoplasm (English and Voeltz 2013). The ER is the major site for the synthesis of secreted or endomembrane proteins (Rapoport 2007, Braakman and Hebert 2013, Reid and Nicchitta 2015, Hoffman et al. 2019), production of lipids and steroids, calcium storage (Clapham 2007), but also participates in the carbohydrate metabolism (Hebert et al. 2005, Fagone and Jackowski 2009). Its physical structure of tubules and sheets can change based on environmental influence and can these changes be important to regulate several functions in the cell (English and Voeltz 2013).

The ER can be divided into two categories. The surface of the ER that contains ribosomes forms a rough structure and is hence called rough endoplasmic reticulum (RER). It is the major site of protein synthesis. The ER with a surface without ribosomes is called smooth endoplasmic reticulum (SER). Here, synthesis of sterols and lipids take place and it stores calcium ions. Based on its location inside the cell, ER can be further categorized into perinuclear ER that surrounds the nuclear envelope and cortical ER, which is present underneath the plasma membrane.

1.2.1. Protein translocation at the ER

Proteins that are to be secreted or inserted into organelles such as ER lumen and plasma membrane are transported across the ER. It is predicted that up to one-third of eukaryotic proteins are passing through the endoplasmic reticulum (Aviram et al. 2016). Since mRNAs are made in the nucleus, they must be exported out of the nucleus in order to be translated by ribosomes to make proteins and targeted to their destination. The targeting of these proteins targeting can be either be co-translational or post-translational targeting.

1.2.1.1. Co-translational translocation to the ER

Targeting of mRNAs to the ER during translation is achieved by signal recognition particle (SRP) and the signal receptor (SR), which is embedded in the ER membrane and recognizes SRP (Waters and Blobel 1986). Both are highly conserved among all the kingdoms (Keenan et al. 2001, Zimmermann et al. 2010).

The delivery of newly synthesized secretion or membrane proteins is a very crucial step because the hydrophobic regions in nascent peptides could be exposed to the aqueous environment in the cytoplasm and thus lead to protein aggregation. Co-

translational targeting of proteins can prevent this problem and make safe delivery to their destinations.

The co-translational delivery of proteins starts with the signal sequence of the newly synthesized peptides that are recognized by the SRP. The SRP binds to the nascent peptide via the S domain as soon as the hydrophobic transmembrane domains (TMD) exits from the ribosomes (Wild et al. 2004 and Reithinger 2013). Simultaneously, the Alu domain of SRP interacts with ribosomes at the elongation factor binding site and slows down the speed of ribosome elongation (**Figure 3**). The complex of ribosome-nascent chain-SRP is then targeted to the ER membrane by the interaction of the S domain of the SRPwith SR (SRα/SRβ) at the ER membrane. The whole complex is stabilized on the ER membrane by binding to GTP. Once the complex is ready to insert or translocate the nascent peptide, the SRP and SR hydrolyze their bound GTP and release from the complex for the next round of co-translational targeting (**Figure 3**).

There are several heat shock proteins that support nascent polypeptides in order to not misfold. For example, in yeast, the absence of SRP can lead to a reduction of protein synthesis and induction of heat shock proteins (Hsp70p) to prevent aggregation of these proteins or help them to fold correctly and target their destination via SRP-independent pathway (Hann and Walter 1991).

1.2.1.2. Post-translational translocation to the ER

In the post-translational targeting pathway, the proteins are fully synthesized in the cytoplasm and subsequently targeted to the ER. Computational analysis in yeast for the secretion proteome from Ast et al. (2013) revealed that up to 43.3% of proteins are predicted to be targeted independently of SRP. Since SRP recognizes the TMDs of a nascent peptide, which needs to be at least 70-80 amino acid residues, peptides with

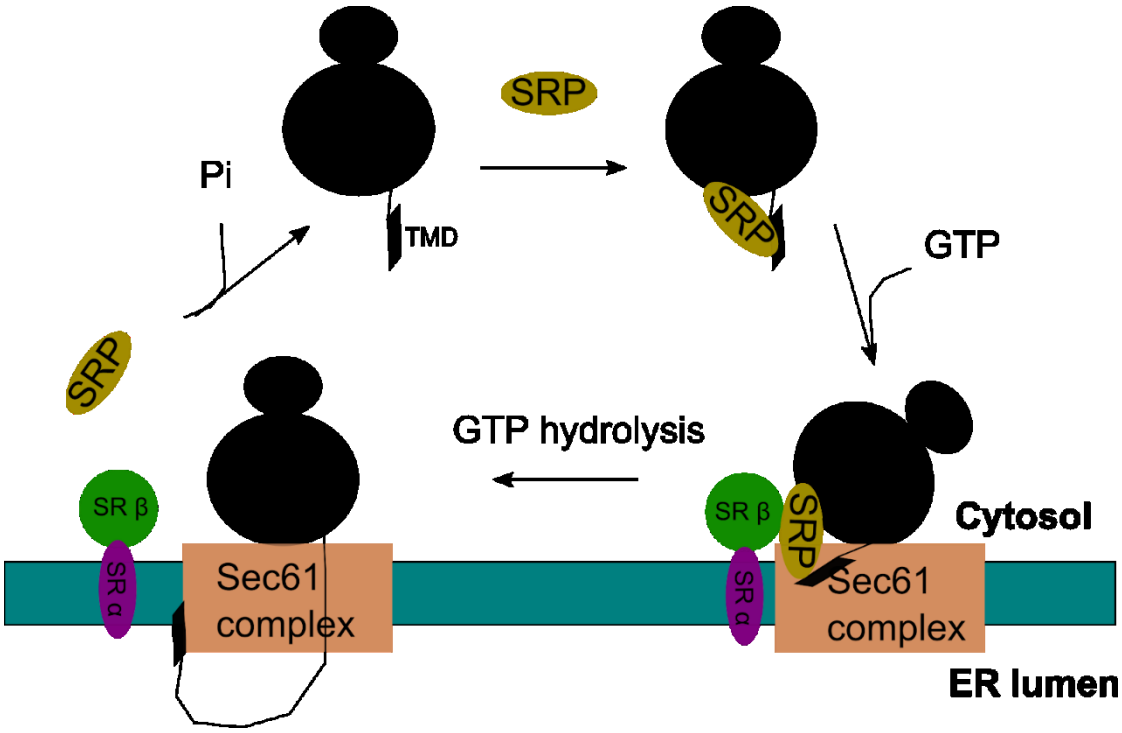

Figure 3. Cartoon representation of SRP-dependent co-translational translocation at the ER. In the cytosol when the ribosomes translate N-terminal TMD of the nascent peptide, the SRP particle binds to the TMD. The stability of complex during targeting is achieved by the presence of GTP. At the ER membrane, SR receptors (SRα/SRβ) which are located close to the Sec61 translocon complex receives the SRP bound ribosomes and initiates the translocation across the ER membrane. After the insertion of targeting peptide, the hydrolysis of GTP leads to the release of SRP from the complex and available for the next round of ribosomes targeting. *Figure adapted from Eichler and Moll (2001).*

shorter sequences cannot be recruited by SRP for targeting to the ER (Ast and Schuldiner 2013; Ast et al. 2013). Also, the tail-anchored (TA) proteins whose TMDs are present at the C-terminus cannot recruit SRP and are targeted post-translationally.

In yeast, the Guided Entry of TA proteins (GET) pathway was proposed as a delivery system for TA proteins to the ER (Schuldiner et al. 2008). GET is also conserved in mammalians and called here the TRC40 pathway (Stefanovic and Hegde 2007). The TA proteins have TMDs with at least 40 amino acid residues at the C-terminus (Shao

and Hedge 2011). As the ribosome completes the translation of the TA proteins, Sgt2p (small glutamine-rich-peptide repeat (TPR)) is the first protein that binds to the nascent

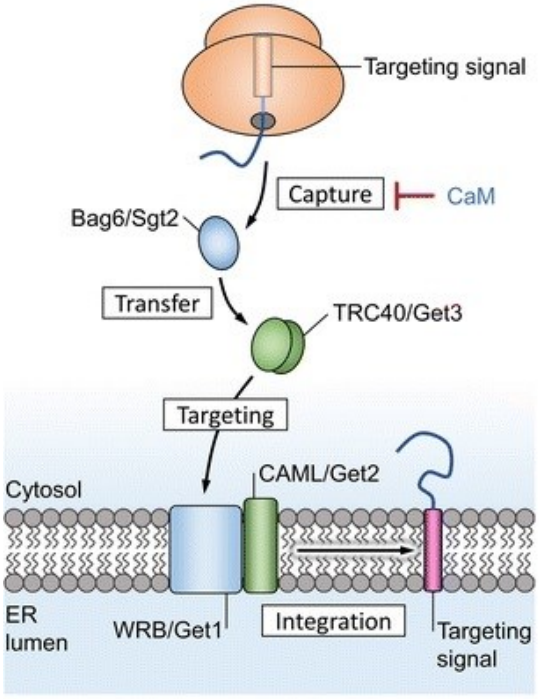

Figure 4. Cartoon representation of the GET pathway for post-translational translocation. As the C-terminal TMD (purple) of TA proteins is synthesized by the ribosomes, the Stg2p recognizes this TMD and binds to form a pre-targeting complex. The Get3p in yeast recognizes this complex and targets them to the ER membrane where the Get1-Get2 complex received this cargo and proceeds for the translocation of peptides across the ER membrane. *The figure and the text are adapted from Puyenbroeck and Vermeire (2018).*

TA protein and prevents it from aggregation **(Figure 4)** (Wang et al. 2010). The Get3 protein, which is a 40kDa ATPase can form a dimer and can create a groove-like structure with open and closed conformation states (Favaloro et al. 2008, Schuldiner et al. 2008, Stefanovic and Hegde 2007). When Get3 is in an open conformation, it can interact with the Stg2p-TA protein complex and recruit it to the ER membrane where it is received by the Get1-Get2 complex. Get3 then releases the TA proteins by ATP hydrolysis (Hu et al. 2009, Schuldiner et al. 2008). There are other pathways of protein delivery to the ER such as translocation of proteins via the Sec61 translocon with the auxiliary essential Sec62-Sec63 and non-essential Sec66 and Sec72

components of ER membrane which can be also targeted co-translationally but in SRP-independent manner (Deshaies and Schekman 1987and 1989, Rothblatt et al. 1989, Sadler et al. 1989) in yeast. In this SRP-independent pathway, the newly synthesized proteins in the cytoplasm are recognized by chaperone proteins like Hsp70 or Hsp90 that target them to the ER membrane. As the complex reaches the ER membrane, the signal sequence (SS) in these proteins is recognized by Sec61 translocon and the chaperone proteins are now released from the complex (Plath and Rapoport 2000). Then, the segment of a targeted protein that has to be inserted into the ER membrane binds to the Kar2 protein through the J domain of the Sec61 translocon in the lumen to ensure successful translocation of target protein across the ER (Brodsky and Schekman 1993, Sadler et al. 1989).

1.2.1.3. Protein quality control (PQC) at the ER

Each step in the delivery of proteins to the ER is critical for the cells. A mistake during translocation of proteins across the ER leads to misfolding or aggregation of proteins that could be toxic for the cells. Several neurological diseases such as Alzheimer's and Parkinson's have been linked to protein aggregation (Hetz et al. 2013). Stress generated by the accumulation of misfolded proteins in the ER is called 'ER stress'. This can be because of oxygen stress (hypoxia), nutrient deprivation or abnormal levels of calcium. To ensure a balance between the protein-folding capacity and protein-folding demands, cells keep track of the levels of misfolded proteins (Hetz and Papa 2017). As the accumulation of misfolded proteins increases, an intracellular response mechanism in cells kicks in to restore ER homeostasis. This so called Unfolded Protein Response (UPR) can stop the production of misfolded proteins, increase the production of ER chaperones to help proteins to refold correctly, initiate apoptosis in case of the severe load of misfolded proteins in the ER, and re-translocate

wrongly folded proteins back to the cytoplasm for their degradation by proteasomes in the ER-associated Degradation (ERAD) pathway (Hetz and Papa 2017).

1.2.1.3.1. The Unfolded Protein Response

In yeast, misfolding of proteins is monitored by a 126 kDa ER transmembrane sensor protein called Ire1p (Cox and Walter 1996, Mori et al. 1993). It is highly conserved

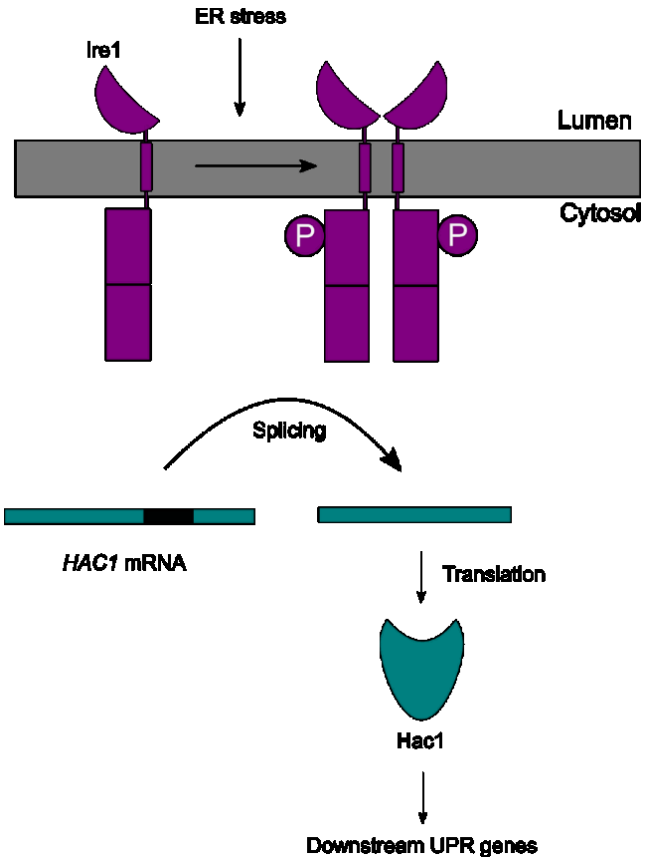

Figure 5. Activation of *S.cerevisiae* Ire1p upon ER stress to induce the UPR. Once activated, Ire1p changes its confirmation by *trans*-autophosphorylation and oligomerization, which leads to splicing of *HAC1* pre-mRNA. The ribosomes translate the spliced *HAC1* to produce Hac1p that induces expression of downstream genes involved in the UPR pathway. *The figure and the text are adapted from Wu et al. (2014)*.

among eukaryotes. Ire1p is activated by binding directly to misfolded proteins in the ER lumen (**Figure 5**). The cytosolic part of Ire1p has two functional domains with kinase and RNAse activities. As soon as the Ire1p is activated, it undergoes conformational changes by oligomerization followed by *trans*-autophosphorylation via its cytosolic kinase domain. Once Ire1 is in an active conformation, the RNAse of Ire1

cleaves the intron of the *HAC1* pre-mRNA. The spliced *HAC1* mRNA is translated by the cytosolic ribosomes to produce Hac1 protein (**Figure 5**). Hac1p acts as a transcription factor for many genes of the UPR pathway (nearly 400 genes, belongs to ER chaperone, lipid biosynthesis, and ERAD) and induces their gene expression to fully restore ER homeostasis.

1.2.1.3.1.1. The ER-associated Degradation (ERAD) pathway

When the levels of misfolded proteins increase, it is also necessary to degrade these proteins before they become unhealthy for the cells. To degrade misfolded ER or membrane proteins they need to be re-translocated to the cytoplasm by the so-called ERAD pathway (Baldridge and Rapoport 2016). Genetic and biochemical studies in budding yeast and mammalian systems led to the identification of the components of the ERAD pathway and an E3 ubiquitin ligase complex as its core component (Bordallo et al. 1998, Bays et al. 2001, Ruggiano et al. 2014). The ubiquitin system is a process of attachment of a small protein of 76 amino acid residues called ubiquitin to the misfolded protein and is composed of three steps process. These steps include the activating proteins called E1, the conjugating proteins called E2 and the ligases involved in the degradation called E3 (Pickart 2001).

In yeast, substrate recognition by the E3 ligase system is based on the location of misfolded proteins (ER lumen or cytosolic side of ER). Two models have been proposed: 1.) ERAD-C substrates in the ER lumen are degraded via the Doa10 complex, whereas 2.) ERAD-M substrates on the cytosolic side of the ER are degraded via the Hrd1 complex (Taxis et al. 2003, Vashist and Ng 2004, Carvalho et al. 2006). In the mammalian system most studied, E3 ligases are Hrd1 and Gp78 which are homologous to yeast but targets different kinds of substrate (Christianson et al. 2011 and Zhang et al. 2015).

The Doa10 complex contains Cue1-Ubc7 as a core complex with Cdc48, Npl4, Ufd1, Ubx2 as cofactors, whereas the Hrd1 consists of Hrd3, Der1, Yos9, Kar2 and Usa1 as cofactors (**Figure 6**).

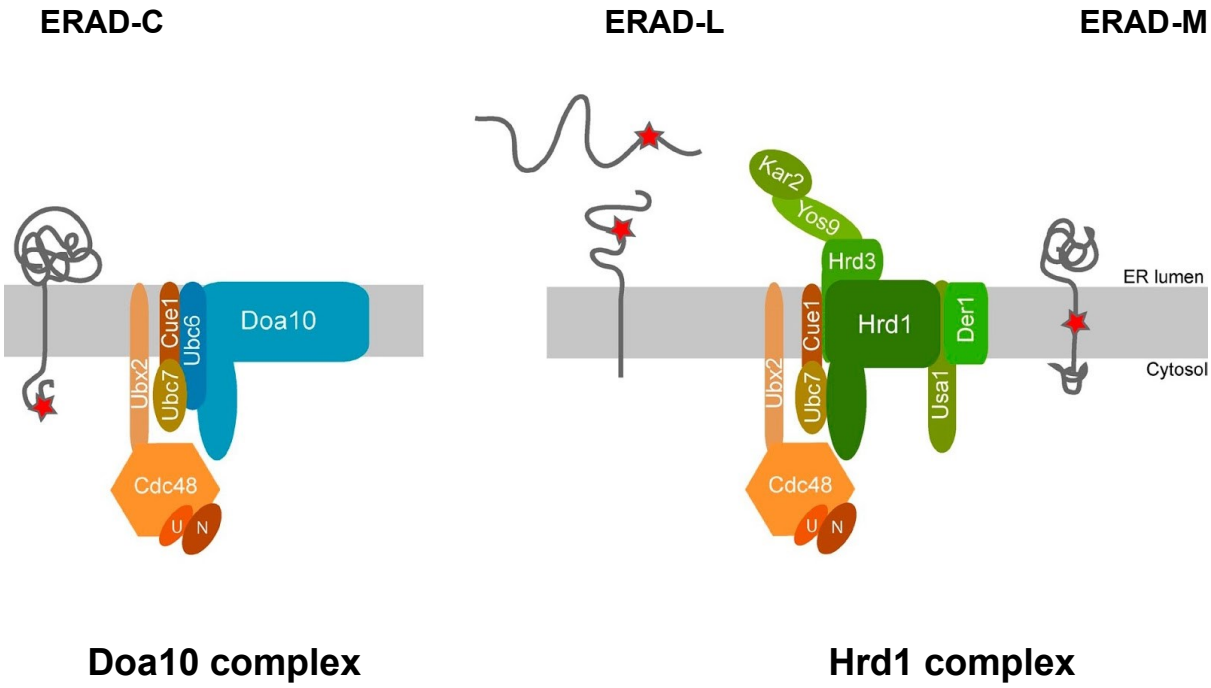

Figure 6. Three categories of the ERAD pathway in *S.cerevisiae.* A cartoon figure showing three different substrates for degradation by ERAD along with their core components and co-factors of the Doa10 complex and Hrd1 complex. The red-colored star indicates the misfolded domain of the nascent peptide. The ERAD is categorized into three categories based on the recognition of the location of its substrates as; ERAD-C (cytoplasmic side of the ER), ERAD-L (in the ER lumen) whereas ERAD-M (across the membrane of the ER). The ERAD-L and ERAD-M is processed by the Hrd1 complex and ERAD-C are processed by the Doa10 complex. *The figure and text are adapted from the Ruggiano et al. (2014).*

The Der1 protein dislocates the misfolded protein from the luminal part of the Sec61p translocon. Yos9p, together with Hrd3p and Kar2p then recognizes the polypeptides that are needed to be degraded by the ubiquitin ligase Hrd1p. Then, Hrd1p together with Hrd3p binds directly to initiate their degradation and called as ERAD-L pathway (**Figure 6**) (Plemper et al. 1997, Bhamidipati et al. 2005, Kim et al. 2005, Szathmary et al. 2005, Carvalho et al. 2006, Denic et al. 2006). The proteins of the ER membrane that are needed to be degraded via ERAD-M are also transported back to the cytosol

by the Hrd1/Hrd3 complex, but the factors involved in this process still remain elusive (Rugginao et al. 2014).

The Doa10 complex of ERAD-L is dedicated to the degradation of peptides that are on the cytosolic face of the ER (Huyer et al. 2004, Vashist and Ng 2004, Nakatsukasa et al. 2008). The Doa10 complex localizes to the ER and to the inner nuclear membrane (Swanson et al. 2001, Deng and Hochstrasser, 2006). The chaperone proteins that mediate this process are Hsp70p and Hsp40p, which recognizes the ubiquitin of the peptides that are needed to be degraded by Doa10 complex (Nakatsukasa et al. 2008).

1.3. Brefeldin A resistance factor 1 protein (Bfr1p): *An unconventional RBP proposed to play roles in the secretion pathway, ploidy control, and translation.*

Brefeldin A (BFA) is an inhibitor of protein transport between the ER and Golgi apparatus. In yeast, deletion of *ERG6* leads to increased cell permeability and sensitivity to BFA. *BFR1* was first reported as a multi-copy suppressor of BFA induced lethality in *S.cerevisiae* (Jackson and Képès 1994). *BFR1* is a non-essential gene and cells deleted for *BFR1* (*bfr1*Δ) are viable but show cell shape alterations, increased cell size and defects in nuclear segregation (Jackson and Képès 1994). Furthermore, deletion of *BFR1* leads diploid cells to produce an ascus containing asci instead of spores (Xue et al. 1996). Two-hybrid interaction studies suggest that Bfr1p interacts with Bbp1p and proposed to play a role in cell cycle regulation (Xue et al. 1996). Bbp1p is a component of the spindle pole body (SPB) and together with the nuclear envelope protein Mps2p, Bbp1p controls the PB duplication (Schramm et al. 2000). Additionally, Bfr1p associates with the SESA (Sym2p-Eap1p-Scp160p-Asc1p) network via mRNAs (e.g. *POM34* mRNA) and inhibits its translation to regulate the SPB duplication (Senzen et al. 2009). Interestingly, Bfr1p only co-immunoprecipitated with the

Scp160p and Asc1p but not with the Sym2p and Eap1p of SESA network suggesting, Bfr1p interaction with SESA is possibly via Br1p-Bbp1p interactions and thus implicated in chromosomal mis-segregation and change of ploidy.

BFR1 encodes for a 55 kDa protein that contains three coiled-coil domains covering amino acids 17-178, 237-281, and 398-469 (**Results, Figure 2.3 A**). Bfr1p localizes predominantly to the endoplasmic reticulum (ER) but also shuttles between ER and cytoplasm (Lang et al. 2001). Furthermore, Bfr1p co-purifies with polysome complexes together with the RBP Scp160p. The interaction between Bfr1p and polysomes is dependent on RNA (Lang et al. 2001). Although Bfr1p does not contain canonical RNA-binding domains, Bfr1p binds to several hundreds of mRNAs that encode for endomembrane proteins or secretion proteins, but also binds to mRNAs encodes for ribosome biogenesis, ncRNA processing, protein glycosylation and glycoprotein biosynthesis (Hogan et al. 2008, Lapointe et al. 2015). Bfr1p binds to these mRNAs during translation at the ER (Lapointe et al. 2015) and PAR-CLIP data of Bfr1p-RNA interactions revealed that there are at least six residues in Bfr1p that cross-link to and therefore directly contact RNA (Kramer et al. 2014). These six residues (R38, H79, K138, F211, Y225, and F239) are found in the first two coiled-coil domains of Bfr1p suggesting these two domains are important for the RNA-binding functions of Bfr1 protein.

During cellular stress, the translation of mRNAs is repressed, and these mRNAs are localized to a membrane-less compartment in the cytoplasm known as processing bodies (P-bodies). P-bodies are formed by phase separation and store mRNAs and its degradation machinery components to regulate mRNA turnover. Bfr1p was shown to be a part of the P-bodies component and targets some mRNAs (eg. *RPS16A*) during late-phase of P-bodies formation when cells are stressed for extended periods of

glucose starvation (Simpson et al. 2014). Under normal growth conditions, Bfr1p together with Scp160p is proposed to protect mRNAs by blocking their access by P-body components (Weidner et. 2014).

Bfr1p has also proposed as a checkpoint for the UPR activation during elevated ER stress (Low et al. 2014). It was shown that the Bfr1 down-regulate the UPR and secretion pathway when a novel group of kinetochore genes (*CFT19* complex) is deleted (Low et al. 2014).

Taken together, Bfr1p binds RNA and loss of *BFR1* affects secretion pathway, ploidy maintenance, assembly of P-bodies.

1.4. Functional similarities between Bfr1p and Scp160p.

Scp160p (*Saccharomyces cerevisiae* protein involved in the control of ploidy) is a 160 kDa protein with 14 repeats of the highly conserved hnRNP K-homology (KH) domains and the yeast member of the vigilin protein family (Weber et al. 1997, Lang and Fridovich-Keil 2000, Cheng and Jansen 2017). Several studies have proposed that Scp160p and Bfr1p share functional similarities (Lang and Fridovich-Keil 2000, Senzen et al. 2009). The deletion of either *SCP160* or *BFR1* has similar consequences such as abnormal cell shape and cell size, issues with maintenance of ploidy suggesting that both proteins either function together and dependent on each other.

A microarray analysis from Hogan et al. (2008) showed that the mRNA interactome of Scp160p and Bfr1p overlap in terms of mRNA partners. In addition, Scp160p interacts with polysomes via Bfr1p and, in contrast to Bfr1p, in an RNA-dependent manner (Lang et al. 2001). Similarly, our lab has previously shown that Scp160p acts as a translational enhancer of a set of mRNAs by efficient recycling of tRNAs and preventing their diffusion (Hirschmann et al. 2014).

Also, studies have shown that under normal growth conditions, Bfr1p together with Scp160p prevents P-bodies formation by inhibiting access to the P-bodies components since the deletion of either *BFR1* or *SCP160* was shown to induce the formation of P-bodies (Weidner et al. 2014). This suggests that Bfr1p might also play a role in translation similar way as Scp160p since these two proteins bind to similar mRNAs during translation and share a similar set of functionalities.

1.5. Aims of this study

Since the first identification of Bfr1p in 1994, multiple functions have been proposed for Bfr1p, such as a multi-copy suppressor of brefeldin A exposure, roles in secretion, nuclear segregation, and RNA-binding. However, the function of Bfr1p at the molecular level remains unclear, especially since all the previous studies have been performed with the *BFR1* deletion (*bfr1*Δ) cells and have not excluded secondary effects resulting e.g. from nuclear mis-segregation.

Therefore, the present study focuses on two aspects;

1. **The functional relationship between the RNA-binding function of Bfr1p and the phenotypes associated with loss of *BFR1***. As a starting point, I created point mutations in the residues of Bfr1p that have been shown to UV-cross link with the RNA and investigated whether the loss of RNA-binding affects the known phenotypes such as cell ploidy, BFA resistance, and P-bodies induction.
2. **The function of Bfr1p in translational control of its mRNA targets and in protein translocation of the encoded proteins.** From the previously published high-throughput studies of Bfr1p-mRNA complexes, I characterized two RNA binding partners (*ERG4* and *OSH7*) via ribosome affinity purifications

and polysome profiling approaches to find how Bfr1p affects the translation of these mRNAs at the ER.

2. Results

2.1. The RNA-binding function of Bfr1p is important for its localization to the ER.

2.1.1. K138 and F239 residues of Bfr1p are highly conserved among *ascomycetes.*

Bfr1p has three coiled-coil domains but does not have any canonical RNA-binding domains. However, from previous studies (Hogan et al. 2008, Kramer et al. 2014, Laponite et al. 2014) it has been shown that Bfr1p binds to several hundreds of mRNAs. *In vivo* UV-crosslinking of Bfr1p with mRNAs revealed six crosslink sites (Kramer et al. 2014) that span within first two coiled-coil domains. To check whether these six residues are conserved in the phylum Ascomycota of the fungal kingdom, I performed a multiple sequence alignment. Among these six RNA-binding residues of Bfr1p (R38, H79, K138, F211, Y225 and F239), I found that K138, Y225 and F239 are highly conserved among *ascomycetes* for at least 8 species **(Figure 2.1),** and when compared to more than 10 species K138 and F239 remains highly conserved. However, all the six residues of Bfr1p are conserved and thus, I decided to mutate these residues to further characterize the Bfr1p interaction with mRNAs.

2.1.2. RNA-dependent localization of Bfr1p to the ER.

To confirm whether localization of Bfr1p to the ER is RNA-dependent, I constructed a yeast strain expressing Bfr1p with a yeast enhanced GFP (yeGFP) tag fused at the C-terminus (Bfr1p-yeGFP) and treated the lysates with RNase. The cytosolic and membrane fractions were separated by subcellular fractionation and proteins were detected by western blot. Lysates without RNase treatment were used as a negative control.

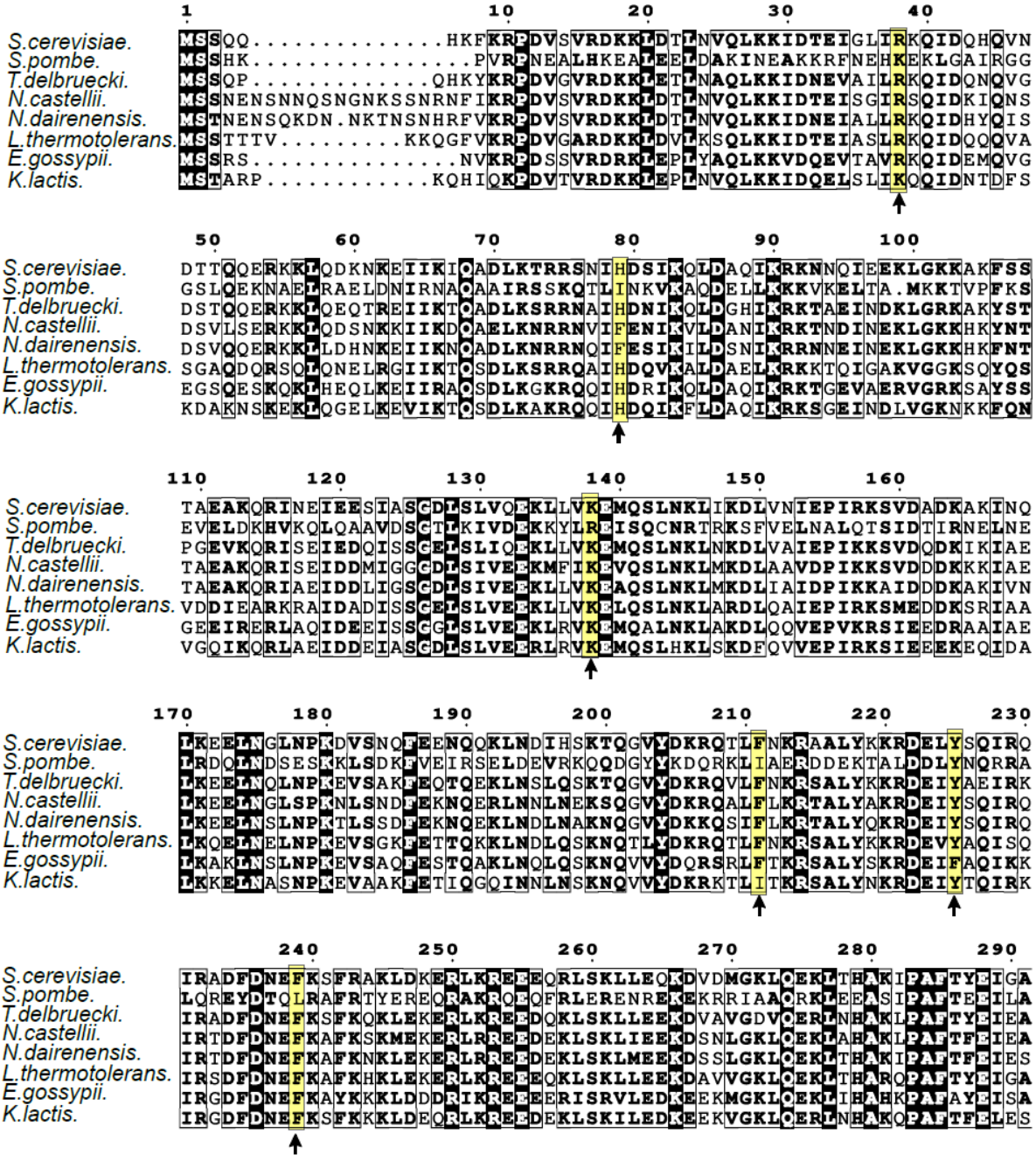

Figure 2.1. Multiple-sequence alignment of Bfr1p from various fungi reveals K138 and F239 RNA-binding residues are highly conserved. Alignment of Bfr1p was performed for 8 different species of the fungal kingdom with Clustal Omega (EMBL-EBI). The output file was prepared with ESprint 3 and manually edited for residues 1-291 of Bfr1p. UV cross-linked RNA-binding residues of Bfr1p are highlighted in yellow with arrows.

The western blots revealed that a majority of the Bfr1p co-fractionated with the membrane fraction only in lysates that are not treated with RNase, whereas a reduced Bfr1p level is observed in the membrane fraction after treatment with RNase **(Figure 2.2)**. However, Bfr1p can still be detected in the membrane fraction after RNase

treatment. The distribution of cytoplasmic fraction and membrane fractions were controlled using Pgk1p and Sec61p as a cytoplasmic and membrane marker, respectively.

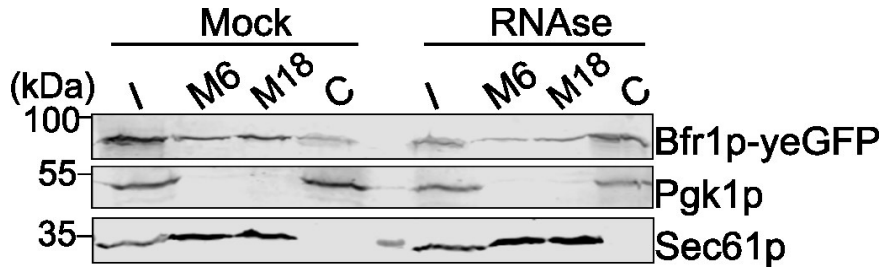

Figure 2.2. Bfr1p localize to the ER in RNA-dependent manner. Bfr1p redistributes between the membrane and cytosolic fractions upon RNAse treatment. (M6) membrane fraction (pellet from 6000g), (M18) membrane fraction (pellet from 18,000g), and (C) cytoplasmic fraction (supernatant from 18,000g). Pgk1p and Sec61p serves as a marker for cytoplasmic and membrane fractions respectively.

2.1.3. Mutating F239 alone or all the six RNA-binding residues to alanine results in the loss of Bfr1p localization to the ER.

After establishing RNA-dependent localization of Bfr1p to the ER, I next wanted to establish if all six RNA-binding residues of Bfr1p are important for its localization. To answer this, I generated strains with mutations in RNA-binding residues of Bfr1p-yeGFP either by creating single point mutations of these residues or mutating all six together by replacing them with alanine residues **(see Methods and Figure 2.3 A)**. Since it has been shown that all six cross linked residues are within first two coiled domains, I also generated a strain with a truncation of third coiled domain (Bfr1p(1-397)) to find out whether the first two coiled-coil domains are sufficient for the function of Bfr1p. Western blots and their quantification revealed that the expression of Bfr1p is not affected by either mutating the RNA-binding residues or truncating the third coiled-coil domain when compared to the wild type full length Bfr1p **(Figure 2.3 B, C)**. Since the expression of Bfr1p mutants was not altered by exchanging their RNA-

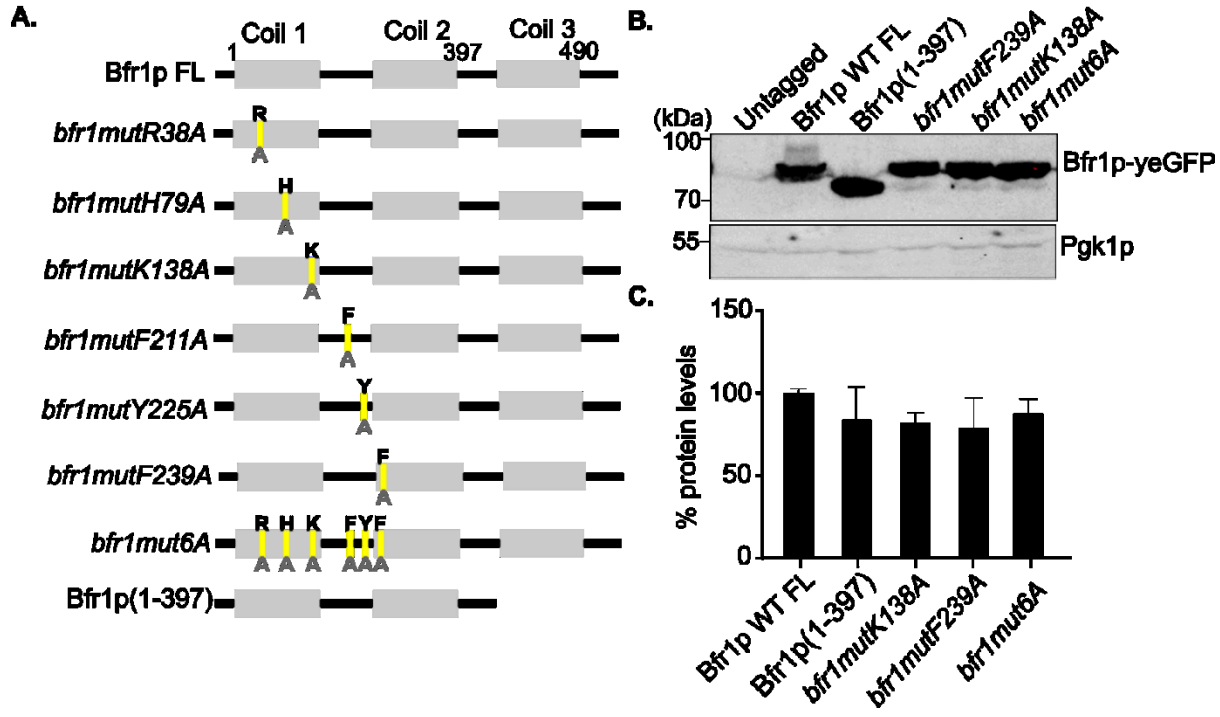

Figure 2.3. Mutations in RNA-binding residues of Bfr1p do not affects its expression. **A**. schematic view of the genomic *BFR1* locus. RNA-binding residues R38, H79, K138, F211, Y225, and F239 were replaced with alanine and cloned into a plasmid. The mutant *bfr1mut6A* contains all six mutations, Bfr1p(1–397) is a truncation lacking the third coiled-coil were introduced in genome. **B.** Westen blot of expression of Bfr1p constructs shows no change in the protein expression levels. Pgk1p served as a control for normalization of loading and untagged wild strain as a control for GFP antibody specificity. **C**. Quantification graph displayed as % protein levels of Bfr1p constructs normalized to Pgk1p levels from three biological replicates. Error bars show ±SD.

binding residues, I performed fluorescence microscopy analysis to find whether these mutations impact Bfr1p localization the ER. As suspected, I found that mutations in the highly conserved residue F239A alone or in all six RNA-binding residues, affects Bfr1p localization to the ER when compared to the wild type protein **(Figure 2.4A)**. Interestingly, Bfr1p with a truncation of the third coiled-coil domain and all the other individual mutations (R38A, H79A, K138A, F211A, Y225A) shows normal localization to the ER. **(Figure 2.4B)**. To further validate our results, I performed subcellular fractionation with strains expressing wild type full length Bfr1p, Bfr1p(1-397) and *bfr1mut6A.* Western blots from subcellular fractionations revealed similar results as

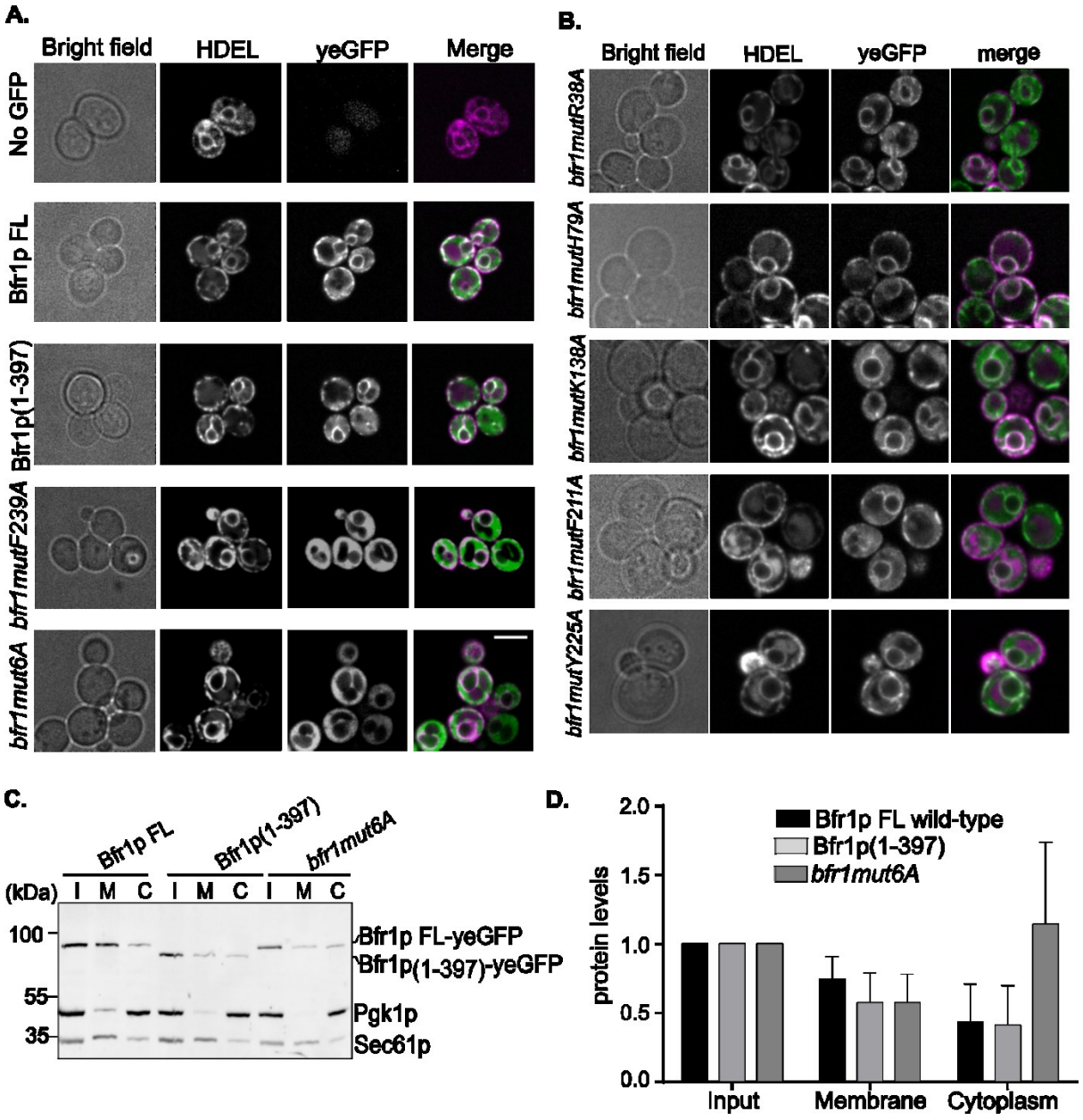

Figure 2.4. RNA-binding mutants affects ER localization of Bfr1p. **A. and B.** Intracellular distribution of yeGFP-tagged Bfr1p constructs. Plasmid-expressed HDEL-DsRed serves as an ER marker. Bfr1p variants of mutants *bfr1mutF239A* and *bfr1mut6A* show loss of colocalization between Bfr1p and the ER. None of individual mutants including Bfr1p(1-397) affect the distribution of Bfr1p. Scale bar, 8 µm. **C.** Distribution of Bfr1p constructs in subcellular fractionation. (I) input, (M) membrane fraction (pellet from 18,000g), (C) cytoplasmic fraction (supernatant from 18,000g). Pgk1p serves as cytosolic and Sec61p as ER markers. **D**. Quantification of subcellular fractionation of yeGFP-tagged Bfr1p constructs. Data are displayed as relative protein levels. Protein in the membrane fraction was normalized to Sec61p and in cytoplasmic fraction to Pgk1p. Results stem from three biological replicates. Error bars show ±SD.

observed with microscopy as Bfr1p shifts from membrane to the cytoplasmic fraction in *bfr1mut6A* **(Figure 2.4C)**. Quantification from subcellular fractions of three biological

replicates confirms the observation when normalizing against Pgk1p or Sec61p for cytoplasmic and membrane fractions, respectively **(Figure 2.4D)**. These data suggest that RNA-binding residues are important for Bfr1p to localize at the ER.

2.2. The known phenotypes of *bfr1Δ* are independent of its RNA interaction.

2.2.1. The RNA-binding mutants of Bfr1p does not induce P-bodies.

It has been shown in previous studies that loss of *BFR1* (*bfr1Δ)* induces P-bodies under normal growth conditions (Weidner et al. 2014) and that Bfr1p targets certain mRNAs to P-bodies during late phase of glucose stress (Simpson et al. 2014).

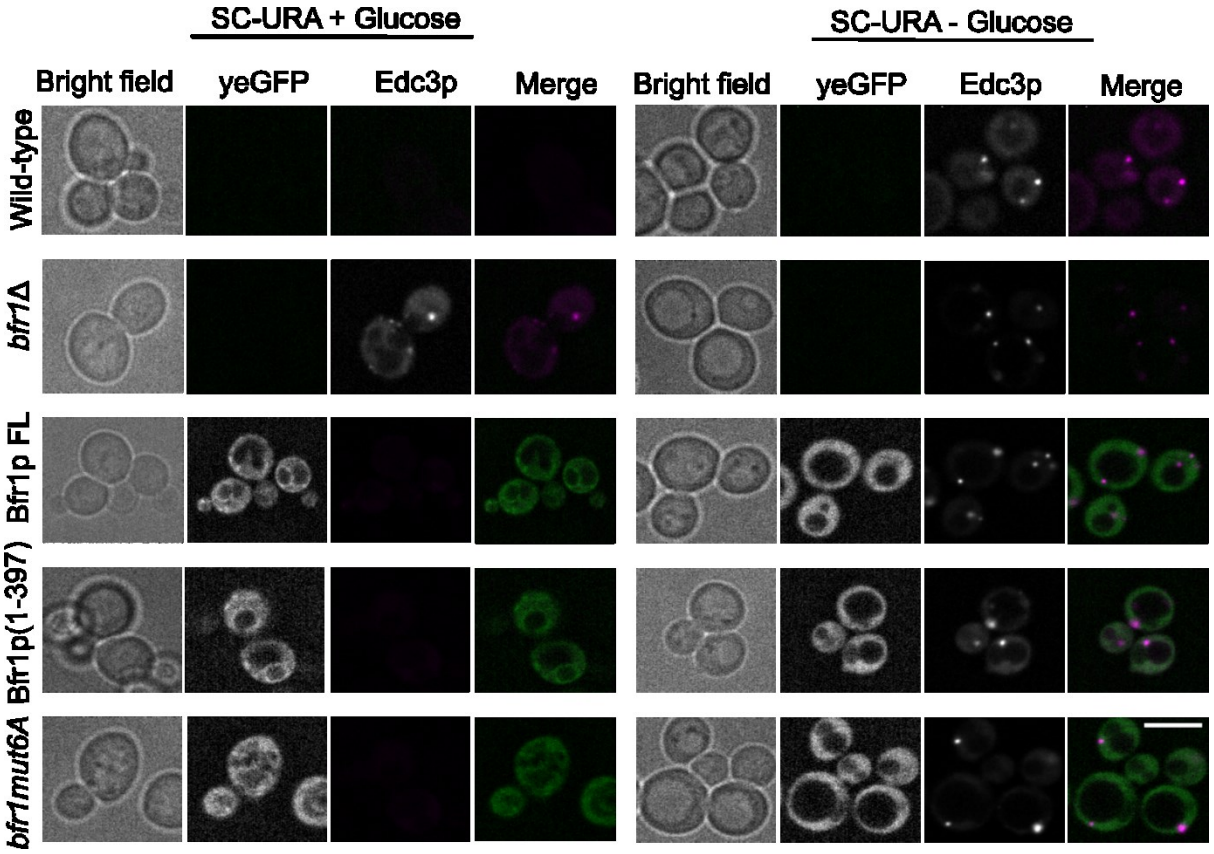

Figure 2.5. The RNA-binding mutants of Bfr1p does not induce P-bodies. Premature P-bodies are not induced by RNA-binding mutations of Bfr1p. Images were collected from logarithmically growing cells shifted for 30 minutes to media with or without glucose to induce P-bodies. Edc3p-mCherry serves as P-body marker. Unlike a *BFR1* deletion, neither RNA-binding mutations nor Bfr1p(1-397) show any P-body foci in cells growing in glucose-containing medium. Scale bar, 5 µm.

Therefore, I wanted to check whether the mutations in the RNA-binding residues of Bfr1p also induce P-body formation. To answer this, I performed fluorescence microscopy of cells growing in log phase that were shifted to medium lacking glucose for 30 minutes to induce P-body formation before proceeding to live cell imaging. Cells co-expressed Edc3p-mCherry that served as a P-bodies marker (Weidner et al. 2014). None of the RNA-binding mutant constructs nor the truncation of third coiled-coil domain of Bfr1p shows premature induction of P-bodies under normal conditions **(Figure 2.5, left panel)**. This suggests that the increase in P-bodies from *bfr1Δ* is possibly due to a loss of its interaction with other proteins and, thus is independent from the RNAs interaction of Bfr1p.

2.2.2. The RNA-binding mutants of Bfr1p does not alter cell ploidy.

One of the first reported phenotypes of loss of *BFR1* were changes in cell shape and size as well as an increase in DNA content (Jackson and Képès 1994). Flow-cytometry (FACS) analysis showed that the *bfr1Δ* cells turn from haploid to diploid or tetraploid cells and was later attributed to defects in nuclear segregation and nuclear spindle formation (Xue et al. 1996). Since these experiments were performed in *bfr1Δ* cells it remained unclear if RNA interactions of Bfr1p contribute to regulating the cell ploidy. To investigate this, I performed FACS analysis of the cells with mutations in RNA-binding residues of Bfr1p. Wild type haploid and diploid cells were used as a reference for this experiment. As previously shown, FACS histograms of *bfr1Δ* cells show peaks at 2C/4C (i.e. 2N to 4N cells) like wild type diploid cells whereas haploid wild type Bfr1p1 expressing cells show 1C/2C peaks (1N to 2N) like wild type haploid cells **(Figure 2.6)**. Interestingly, I did not find any change in ploidy for the cells with Bfr1p mutation constructs including truncation of third-coiled coil domain and all these constructs show 1C/2C condition like wild type Bfr1p. However, a small percentage of

cells (4-6 %) in *bfr1mut6A* show 2C/4C conditions. From this data I conclude that the Bfr1p can possibly have multiple roles and RNA-binding function of Bfr1p is independent from the ploidy of the cells.

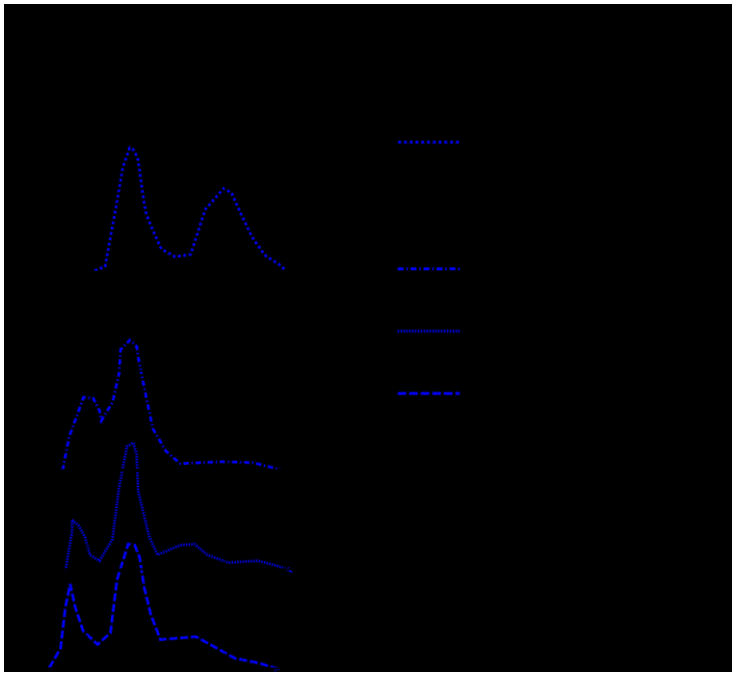

Figure 2.6. The ploidy phenotype of Bfr1p is not affected by RNA-binding mutants. Flow cytometry analysis of Bfr1p variants showing that ploidy is not changed by the mutations in RNA-binding residues of Bfr1p. Histograms show plots of DNA content after propidium iodide staining.

2.2.3. The RNA-binding mutants of Bfr1p are not sensitive to Brefeldin A.

Yeast cells that have lost the Erg6 protein (*erg6Δ)* are highly sensitive to the drug brefeldin A (Graham et al. 1993 and Vogel et al. 1993). Erg6p is an enzyme that functions as a catalyst in the biosynthesis of zymosterol. Normally, brefeldin A cannot enter yeast cells due to their low permeability for this drug. The loss of *ERG6* alters the sterol composition and increase permeabilization of brefeldin A. *BFR1* was originally reported as a multi-copy suppressor of brefeldin A sensitivity (Jackson and Képès 1994) and proposed to have a role in secretion. I wanted to find out whether the high-copy suppression of brefeldin A sensitivity is achieved via its interactions with

RNA, especially since the protein co-localizes with ER, the site of membrane protein synthesis. Therefore, I expressed RNA-binding mutants of Bfr1p in 2 *μm* plasmids

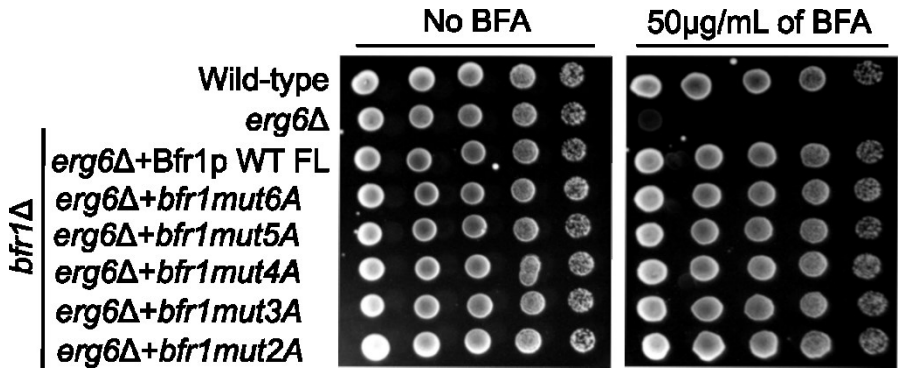

Figure 2.7. Brefeldin A sensitivity of *erg6Δ* is rescued by overexpression of wild-type Bfr1p and RNA-binding mutants. Bfr1p mutants (*bfr1mut5A*: R38A, K138A, F211A, Y225A, F239A; *bfr1mut4A*: R38A, K138A, F211A, F239A; *bfr1mut3A*: R38A, K138A, F239; *bfr1mut2A*: K138A, F239A) were expressed from YEplac181 (LEU2) plasmids in double knockout *erg6Δ bfr1Δ* cells. Wild type and *erg6*Δ cells with empty YEplac181 plasmids served as controls. Logarithmically growing cells were serially diluted and plated on dropout (-*leucine*) agar with or without 50 μg/ml brefeldin A (BFA), and grown for 72 h at 30 °C.

(YEplac181) in *erg6Δ bfr1Δ* double knockout cells and treated with or without 50 μg/ml brefeldin A. As previously reported, I could show that *erg6Δ* cells do not grow on media with 50 μg/mL of brefeldin A and that overexpression of the wild type Bfr1p rescues brefeldin A sensitivity in *erg6Δ bfr1Δ* double knockout cells (**Figure 2.7**). Surprisingly, all mutant constructs rescue cells from brefeldin A like wild type Bfr1p. Therefore, I conclude that RNA-binding function of Bfr1p is independent from its role in secretion.

2.3. Bfr1p interacts with *ERG4* mRNA via its known RNA-binding residues.

Recent studies on Bfr1p showed that it binds to several hundreds of mRNAs that are translated at the ER (Hogan et al. 2008, Mitchell et al. 2013, Lapointe et al. 2015). These mRNAs encode for proteins of the endomembrane system or secreted proteins (Lapointe et al. 2015). Bfr1p was also reported as a component of polysomes and has a potential role in translation of mRNAs (Lang et al. 2001). Therefore, I wanted to

address the physiological impact on these mRNAs of mutations in RNA-binding residues of Bfr1p. Based on previous studies (Hogan et al. 2008 and Lapointe et al. 2015) I selected mRNAs that were significantly enriched as bound by Bfr1p and whose encoded proteins are linked to known phenotypes of *bfr1Δ* or Bfr1p overexpression. From this list I chose five mRNAs encoding ER or Golgi proteins (*IMH1*, *RUD3*, *SGM1*), proteins involved in ER-Golgi transport (*IMH1*) or involved in sterol biosynthesis (*ERG4*), and sterol binding (*OSH7*) as targets of Bfr1p and characterized them further.

2.3.1. Loss of *BFR1* does not affect target mRNA levels.

Since these five mRNAs have been shown to bind Bfr1p, I wanted to verify whether in *bfr1Δ,* Bfr1p(1-397), and *bfr1mut6A* mutants their stability is affected compared to the wild type cells. Therefore, I extracted total RNA from logarithmically growing cells (three replicates) and quantified these mRNAs by qRT-PCR. Normalized (to *ACT1*) levels of target mRNAs revealed that none of the mRNAs demonstrated significant changes in their levels when compared to the wild type cells (**Figure 2.8**). Hence, I conclude that Bfr1p does not influence the stability of these mRNAs.

Figure 2.8. Stability of mRNAs does not change upon loss of *BFR1*. Quantification of mRNA levels of *IMH1*, *RUD3*, *ERG4*, *OSH7*, and *SGM1* by qRT-PCR in wild type, *bfr1Δ,* Bfr1p(1-397) and *bfr1mut6A* cells. Data are presented as mean values from three independent experiments with ±SD.

2.3.2. Mutating the RNA contact sites in Bfr1p reduces its interaction with *ERG4*.

Although, the levels of target mRNAs were unaffected in the Bfr1p mutants or in *bfr1*Δ (**Figure 2.8**), I wanted to test whether the interaction of these mRNAs with Bfr1p depends on the known RNA-binding residues. Using the Bfr1p constructs fused to yeGFP, I co-immunoprecipitated these mRNAs with Bfr1p wild-type, *bfr1mut6A* and Bfr1p(1-397) using anti-GFP nanobody-coupled magnetic beads (GFP-MA trap, Chromotek) and quantified them by qRT-PCR. The wild-type strain (mock) served as the negative control and *MID2* mRNA (an mRNA that binds to the RBP Khd1p (Syed et al. 2018)) served as a non-target control mRNA in the immunoprecipitation. The fold enrichment of immunoprecipitated fractions revealed that only *ERG4* mRNA shows significant binding to full length wild type Bfr1p (Bfr1p FL) compared to *MID2* mRNA (**Figure 2.9**).

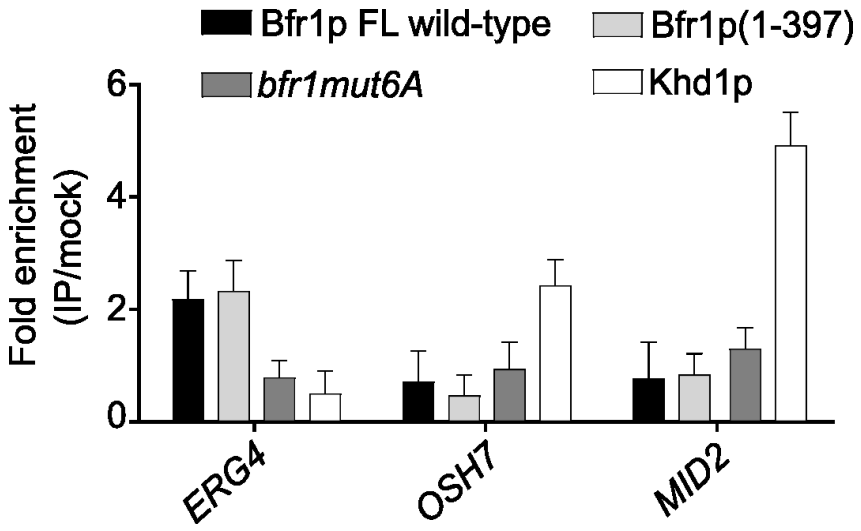

Figure 2.9. *ERG4* mRNA binding to Bfr1p is affected by mutating its RNA-binding residues. RNA binding of full-length Bfr1p (FL wild type), Bfr1p(1–397), and *bfr1mut6A* is assessed by coimmunoprecipitation of *ERG4* and *OSH7* mRNAs and qRT-PCR. *MID2* mRNA serves as a non-target for Bfr1p. Data are presented as mean values from three biological and two technical replicates, each with ±SD.

As expected, the RNA-binding mutant version *bfr1mut6A* strongly reduces this binding confirming that the *ERG4* mRNA directly interacts with Bfr1p. *OSH7* mRNA is more enriched in Khd1p immunoprecipitations than in those of Bfr1p, suggesting it to be a

potential target of Khd1p. Truncated Bfr1p(1-397) binds to *ERG4* mRNA similar to wild-type. This confirms that the first two coiled-coils of Bfr1p with their important RNA-binding residues are enough for the interaction with target mRNAs. Taken together, these results confirm that the *ERG4* mRNA is a direct binder of Bfr1p and that the mutations in RNA-binding residues affects this binding.

2.4. *ERG4* mRNA localization to ER is independent of Bfr1p.

In eukaryotes, mRNAs that encode membrane or secreted proteins are general co-translationally targeted to the ER by SRP pathway (Walter et al. 1981, Görlich et al. 1992). Previous studies from our and other labs show that mRNAs that are bound to RNA-binding proteins such as She2p (Schmid et al. 2006, Fundakowski et al. 2012) or Khd1p (Syed et al. 2018) can alternatively be targeted to the ER using these RNA-binding proteins. Erg4p is predicted to have seven transmembrane domains and localizes to ER (Zweytick et al. 2000). Since *ERG4* mRNA binds directly to Bfr1p, I wanted to test whether the RBP Bfr1p plays any role in localization of *ERG4* mRNA to ER. To follow *ERG4* mRNA *in vivo*, I used a recently improved MS2-tagging system (Tutucci et al. 2017) and tagged *ERG4* mRNA with 12 MS2 stem loops. The tagged mRNA was visualized by co-expressing a MS2 coat protein fused with GFP (MCP-GFP). I used a fusion of the Scs2p transmembrane domain and 2x RFP (Loewen et al. 2007) to detect ER in this experiment. Consistent with the previous studies that have shown that *ERG4* mRNA translates at the ER (Lapointe et al. 2015, Jan et al. 2014),, the majority of the wild type cells show *ERG4* mRNA localization to the ER (86.6+/-3.6%) whereas, the loss of *BFR1* has no significant impact on ER localization of *ERG4* mRNA (84+/-2.6 %) when compared to wild type cells **(Figure 2.10 A and B).** Therefore, I conclude that Bfr1p has no role in targeting of *ERG4* mRNA to the ER.

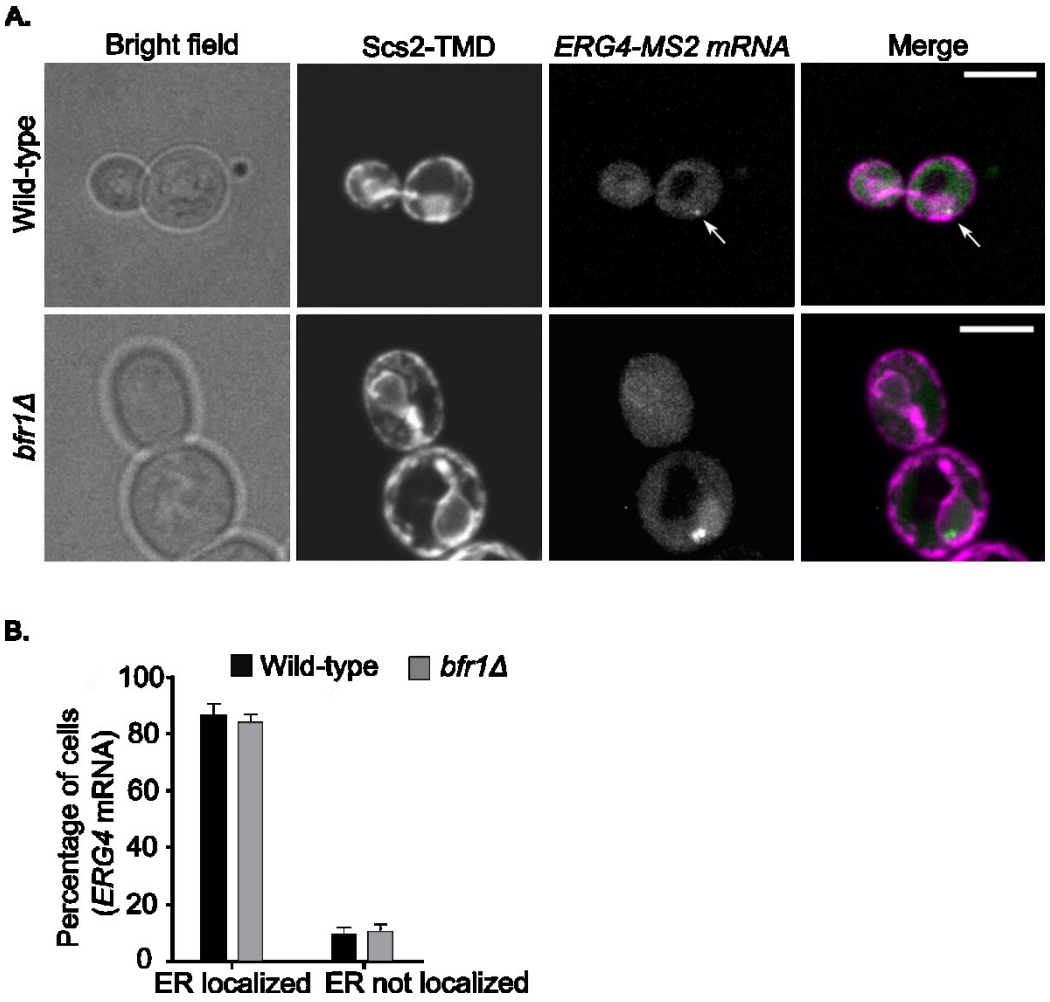

Figure 2.10. *ERG4* mRNA localization to the ER is not dependent of Bfr1p. **A.** Representative images of cells expressing MS2-tagged *ERG4* mRNA in wild-type and *bfr1*Δ. Scs2-TMD-2× RFP serves as an ER marker. White arrows indicate ERG4 mRNA particles. Scale bar, 8 µm. **B.** Quantification of *ERG4* mRNA colocalization with ER in wild type and *bfr1*Δ. Data are presented as mean values from at least 100 cells from three biological replicates with ±SD.

2.5. Erg4p expression and distribution is affected upon loss of *BFR1*.

Since the localization of *ERG4* mRNA to the ER does not depend on Bfr1p, I performed experiments to determine whether Bfr1p plays a role in the expression and localization of Erg4 protein at the ER. I generated a wild type, *bfr1*Δ and *bfr1mut6A* strains with Erg4p fused to yeGFP at the carboxy terminal end and performed fluorescence microscopy and western blot experiments to monitor the expression and localization. As previously published, I could see that in wild type, Erg4p predominantly localized at the ER (Zweytick et al. 2000) as gauged from expression of the ER marker

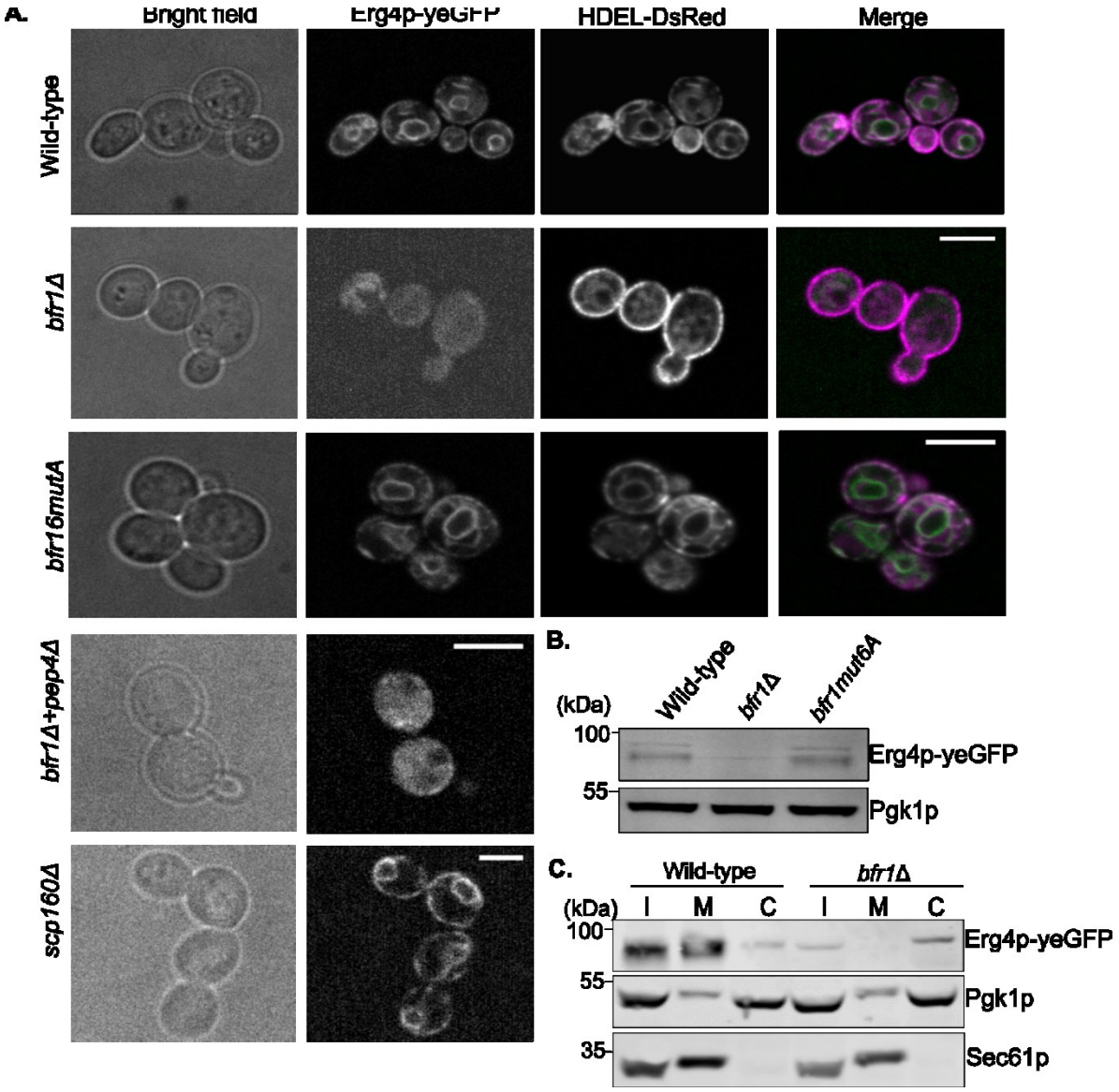

Figure 2.11. Erg4p expression is controlled by Bfr1p. **A.** Erg4p distribution changes upon deletion of *BFR1*. Representative images of cells from wild type, *bfr1Δ*, *bfr1mut6A*, *bfr1Δ pep4Δ*, and *scp160Δ* strains. HDEL-DsRed serves as an ER marker. Scale bar, 5 µm. **B.** Western blot showing down-regulation of Erg4p in *bfr1Δ* and *bfr1mut6A* compared to wild type. Total cell lysates were prepared from wild-type, *bfr1Δ*, and *bfr1mut6A* cells expressing a yeGFP-tagged Erg4p protein and Erg4p detected by an anti-GFP antibody. **C**. Erg4p shifts from ER to cytoplasm in *bfr1Δ* cells. Western blot following subcellular fractionation of wild-type and *bfr1Δ* cells expressing yeGFP-tagged Erg4p. (I) input, (M) membrane fraction, pellet 18,000g, and (C) cytoplasmic fraction, supernatant 18,000g. Pgk1p and Sec61p serve as a cytoplasmic or ER marker, respectively.

HDEL-DsRed. Surprisingly, the expression of Erg4p in *bfr1*Δ cells was strongly reduced and a faint signal was observed all over the cell, including the cytoplasm (**Figure 2.11 A, second row**). However, expression and localization of Erg4p was

very similar to wild type levels in *bfr1mut6A* suggesting that Bfr1p but not its RNA-binding residues are necessary for correct expression of Erg4p. Consistent with the microscopy data, a western blot of total cell lysates revealed that the Erg4p expression is strongly reduced in *bfr1*Δ **(Figure 2.11 B)**.

To test if the reduced Erg4p protein levels in *bfr1*Δ are due to increased vacuolar protein degradation, I generated a double knockout strain (*pep4*Δ *bfr1*Δ) expressing Erg4p fused to yeGFP. *PEP4* encodes the major vacuolar proteinase A (Woolford et al. 1986), and loss of *PEP4* should rescue Erg4p from degradation. However, Erg4p did not accumulate in the vacuole suggesting that the low levels of Erg4p is not due to targeting the protein to vacuolar degradation in *bfr1*Δ **(Figure 2.11 A, lower panel)**. Although, *ERG4* is a potential binder of Scp160p (Hogan et al. 2008), loss of *SCP160* does not affect the expression of Erg4p suggesting that this effect is specific for loss of Bfr1p.

To investigate if the weaker and diffuse signals of Erg4p-yeGFP in *bfr1*Δ cells are due to improper localization to ER, I also performed subcellular fractionation from total cell lysates of wild type and *bfr1*Δ cells to separate membrane and cytoplasmic fractions and processed them for western blot. Consistent with our fluorescence microscopy data, I detected a strong reduction of the presence of Erg4p in *bfr1*Δ cells compared to wild type cells and an enrichment of Erg4p in cytoplasmic fractions was also seen (**Figure 2.11 C**). The separation of membrane and cytoplasmic fractions were judged by using Sec61p as membrane marker and Pgk1p as cytoplasmic markers.

2.6. Loss of *BFR1* promotes degradation of Erg4p at ER by the ERAD pathway.

The ERAD (Endoplasmic Reticulum-Associated Degradation) pathway in cells targets misfolded proteins of the ER for degradation by *26S* proteasomes in the cytoplasm. In

yeast, proteins that are misfolded during translocation at the ER membrane are first ubiquitylated by the ubiquitin-ligase Hrd1p, which facilitates their re-translocation to cytoplasm for degradation by the 26S proteasomes (Hampton 2002, Baldridge and Rapaport 2016). As we already know that the *ERG4* mRNA is translated at the ER and that the localization of Erg4p in *bfr1*Δ cells shifts from membrane to cytoplasm, we hypothesized that loss of *BFR1* possibly leads to misfolding of Erg4p, initiating its degradation by the ERAD pathway.

To test our hypothesis, I generated a strain with a double deletion of *BFR1* and *HRD1* (*bfr1*Δ *hrd1*Δ) and expressing Erg4p-yeGFP. To inhibit 26S proteasome activity, I used the inhibitor MG132 for our experiments (Liu et al. 2007). Cells were treated with cycloheximide (CHX, 100µg/ml) to arrest the translation and harvested at different time points (0 mins, 30 mins, 60 mins) to check amounts of Erg4p-yeGFP in *bfr1*Δ and *bfr1*Δ *hrd1*Δ. The loss of *HRD1* should block the ubiquitination of misfolded Erg4p and

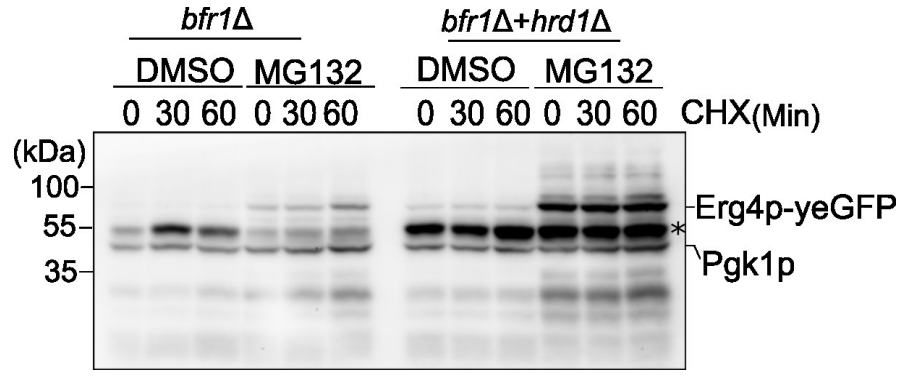

Figure 2.12. Erg4p is degraded by ERAD pathway in absence of *BFR1.* Representative western blot showing accumulation of Erg4p in an ERAD mutant upon treatment with MG132. Total cell lysates were prepared from *bfr1*Δ and *bfr1*Δ *hrd1*Δ cells expressing yeGFP-tagged Erg4p. Cells were harvested at 0, 30, and 60 min after adding cycloheximide (CHX). Pgk1p served as a loading control. The asterisk indicates an unspecific band at 55 kDa detected by the GFP antibody.

together with the inhibition of proteasomes should stabilize misfolded Erg4p. As expected, I can detect a small amount of Erg4p in *bfr1*Δ cells treated with MG132 **(Figure 2.12, lanes 4-6)**. In double knockout of *bfr1*Δ *hrd1*Δ cells a strong

accumulation of Erg4p was detected **(Figure 2.12, last 3 lanes)** which was further accumulated when proteasomes were blocked by MG132 from 0 mins to 60 mins. From this experiment, it was confirmed that the Erg4p is indeed misfolded during translocation at the ER in the absence of Bfr1p and eventually degraded by ERAD pathway. From our findings, I concluded that Bfr1p has a role in translation of *ERG4* mRNA at the ER and potentially in proper translocation of these proteins at the ER.

2.7. Bfr1p regulates *ERG4* translation at ER.

Bfr1p binds to mRNAs that are translating at the ER and Bfr1p is a component of polysome complex. From our experiments it was evident that and Bfr1p plays a role in translational control of *ERG4* mRNA. Our lab has previously shown that in yeast Scp160p also has a role in translation of a set of mRNAs by promoting efficient tRNA recycling during translation (Hirschmann et al. 2014). Therefore, I wanted to find out whether loss of *BFR1* has any consequences on *ERG4* translation at the ribosome level. To answer this, I performed a set of experiments to find either loss of *BFR1* or the mutation in RNA-binding sites of Bfr1p is important for this regulation.

2.7.1. Ribosomal occupancy on *ERG4* is reduced upon loss of *BFR1*.

Our lab has previously established Ribosome-affinity purifications (RAP) to analyse levels of ribosome occupancy on individual mRNAs (Hirschmann et al. 2014). Therefore, I decided to adopt this method to explore if loss of *BFR1* changes occupancy of ribosomes on candidate mRNAs. The experiment was performed as described in (Hirschmann et al. 2014). In brief, I fused Rpl16a protein with a TAP-tag in wild type and *bfr1*Δ cells and arrested translation with CHX (100µg/ml) before harvesting the cells. The lysates were then subjected to immunoprecipitation to purify ribosomes together with RNAs. After degrading the ribosomal proteins from the

complex, RNAs were reverse transcribed and quantified by real-time PCR. The wild type and *bfr1*Δ strains untagged are served as control strains (mock) to detect unspecific immunoprecipitations.

I tested ribosome occupancy for four different mRNA (*ACT1*, *ERG4*, *OSH7* and *MID2*) in wild type and *bfr1*Δ. The ribosomal occupancy on *ERG4* but not of *ACT1* or *MID2* was significantly reduced in *bfr1*Δ compared to wild type cells **(Figure 2.13)**. In contrast, no significant reduction was detectable for *OSH7* suggesting that its translation might not be under Bfr1p control. Hence, I concluded that the loss of *BFR1* reduces ribosomes *ERG4* mRNA during translation.

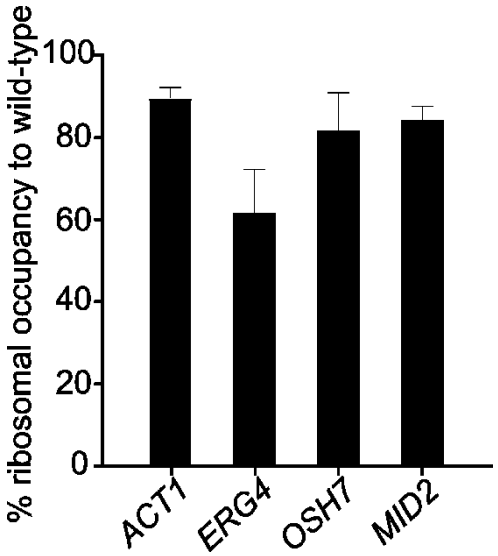

Figure 2.13. Loss of *BFR1* reduces the ribosomal occupancy on *ERG4* mRNA. Ribosome affinity purification (RAP) followed by qRT-PCR was performed to measure the ribosome association of *ACT1*, *ERG4*, *OSH7*, and *MID2* mRNAs in wild-type and *bfr1Δ* cells. An untagged (mock) strain was used to normalize the data. Quantification graphs show percentage of occupancy in *bfr1Δ* compared to the wild-type levels in three biological and two technical replicates of each with ±SD.

2.7.2. Polysomes are stalled on *ERG4* mRNA in *bfr1mut6A* and *bfr1*Δ strains.

The ribosome affinity purification only determines the overall association of ribosomes with mRNAs but does not give us any information on its distribution on mono- or polysomes. Since I have shown that the ribosome occupancy on *ERG4* mRNA is

reduced upon loss of *BFR1,* I next asked whether this reduction is due to the change in distribution between mono- or polysomes of this mRNA. Together with our collaborators in Biozentrum, University of Basel in Switzerland (Dr. Nitish Mittal and Prof. Dr. Anne Spang), we performed polysome profiling experiment to determine the role of Bfr1p in associating of monosome or polysome to its candidate mRNAs.

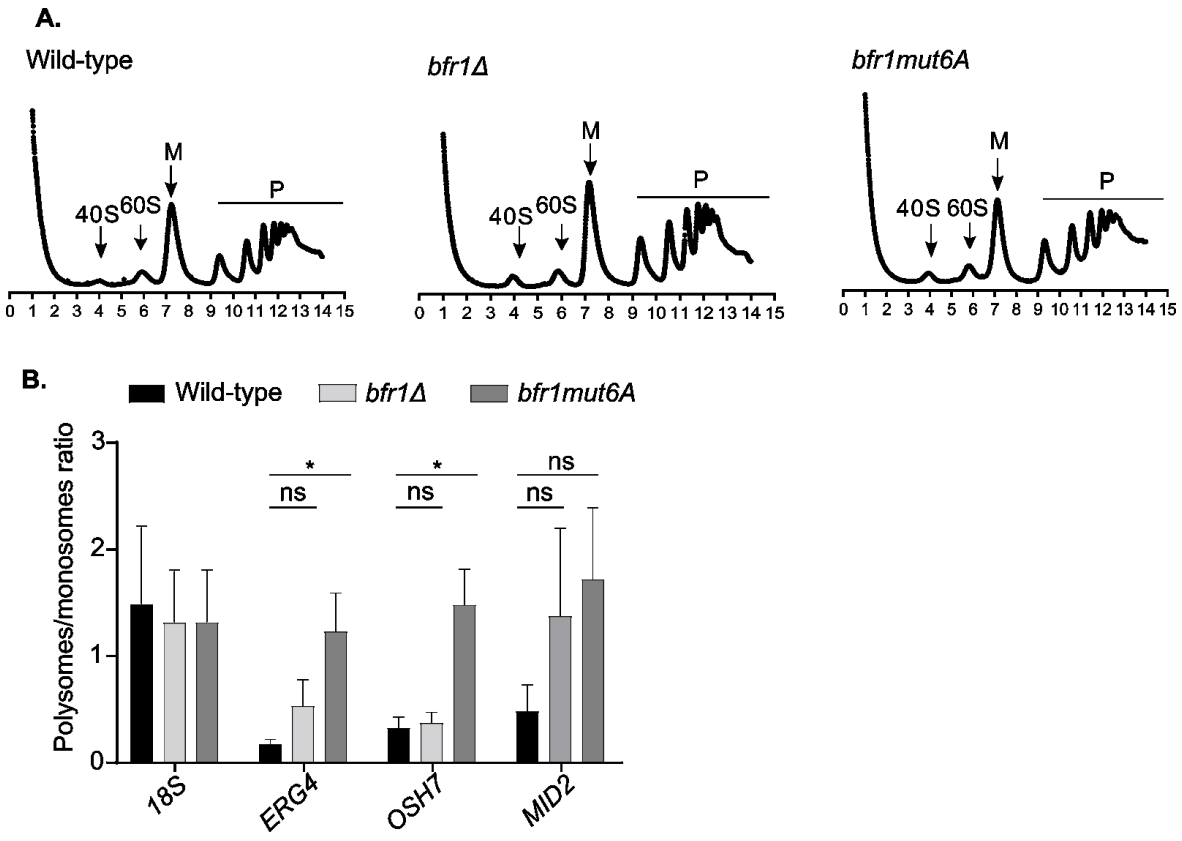

Figure 2.14. Bfr1p is required for efficient translation of *ERG4* mRNA. **A.** Polysome profiles from wild type, *bfr1mut6A* and *bfr1Δ* compared to wild-type cells. (M) monosomes, (P) polysomes. **B.** Polysome association of *ERG4* mRNA changes in *bfr1mut6A* and *bfr1Δ*. Sucrose density gradient fractionation was used to separate monosomes and polysomes, and RNAs from the fractions were quantified by qRT-PCR. Results are displayed as the fold change ratio of polysomes/monosomes for four mRNAs (normalized to *ACT1* levels) from three independent experiments with ±SD. An asterisk indicates P <0.05. (ns) nonsignificant.

Logarithmically growing cells of wild type, *bfr1*Δ and *bfr1mut6A strains* were treated with CHX (100µg/ml) before harvesting and lysates were prepared and processed for separation of mono- and polysome fractions by sucrose density gradients. The

mRNAs pooled from mono- and polysome fractions were then quantified by qRT-PCR. The distribution of free ribosomal subunits, monosomes and polysomes in wild type, *bfr1*Δ and *bfr1mut6A* is similar as judged by fractionation profiles **(Figure 2.14 A).** IN contrast, an increased distribution of *ERG4* ($p<0.0299$) and *OSH7* ($p<0.0178$) to the polysome fraction was observed in *bfr1mut6A* cells when compared to the wild type cells. A similar pattern was seen in *bfr1*Δ **(Figure 2.14 B)**. In addition, I have seen an increase of *MID2* mRNA on polysomes but with a lesser significance ($P<0.0708$). The low expression of Erg4p as seen by western blot and in microscopy experiments and the increase of ERG4 on polysomes suggest that the polysomes are stalled on these mRNAs in both *bfr1mut6A* and *bfr1*Δ. Therefore, I conclude that Bfr1p plays a role in efficient elongation of polysomes on *ERG4* mRNA during translation at ER.

2.7.3. Bfr1p interacts transiently with ribosomes.

The Bfr1 protein has been shown to co-purify with polysomes (Lang et al. 2001). However, it was unclear whether Bfr1p directly binds to ribosomes or it co-purifies with polysomes because it binds mRNAs during translation. To answer this, I performed co-immunoprecipitation of Rps3p, a small ribosomal subunit protein with Bfr1p. I performed immunoprecipitation using a commercially available GFP binder (GFP- MA Trap) system and co-immunoprecipitated Rps3p in Bfr1-yeGFP and *bfr1mut6A*-yeGFP cells. A wild type untagged strain served as a control for specificity of immunoprecipitations.

Although Bfr1p co-purifies with ribosomes, the western blot analysis of co-immunoprecipitations revealed that there is no direct interaction between Bfr1p and ribosomes as all the Rps3p was seen in flow through fractions but not in IP fractions **(Figure 2.16 A)**. Since I did not cross link the proteins in our lysates, I concluded that

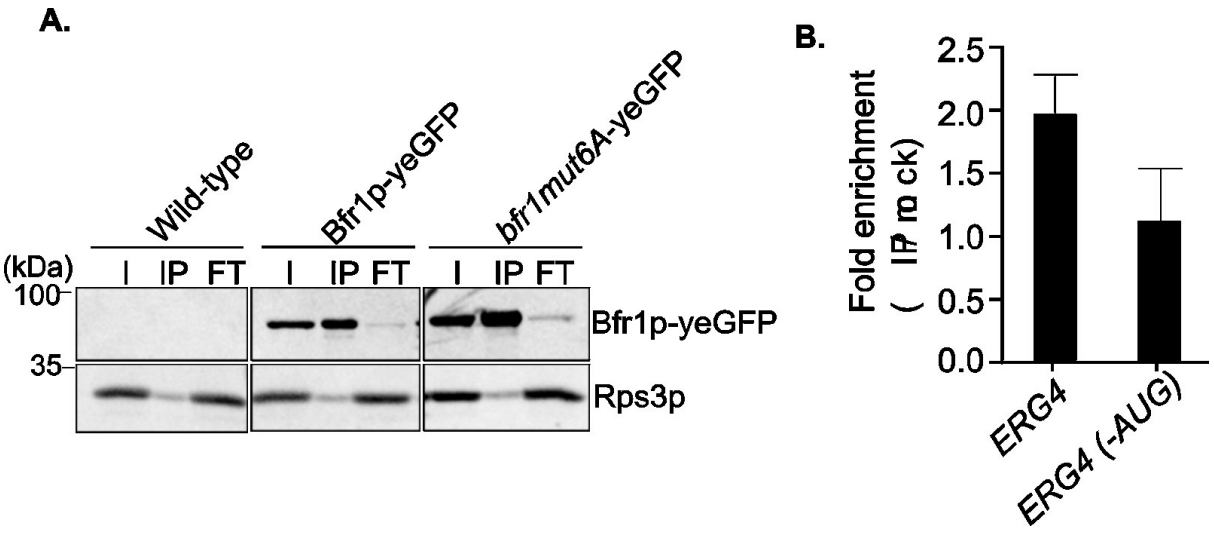

Figure 2.16. Bfr1p interaction with ribosomes is transient. **A.** Bfr1p does not coprecipitate the small ribosomal subunit protein Rps3p indicating Bfr1p interaction with ribosomes is unstable. A representative image of three independent experiments from Bfr1pyeGFP immunoprecipitations. (I) Input, (IP) immunoprecipitation, (FT) flow through. **B.** Bfr1p interaction with *ERG4* mRNA is increased upon translation. Immunoprecipitation was performed from the lysates of cells expressing Bfr1p-yeGFP and wild-type cells to co-precipitate *ERG4* mRNA with or without AUG and levels were quantified by qRT-PCR. Binding of *ERG4* mRNA lacking an AUG (-AUG) is reduced by 43%. Data are represented as fold change ratio of the IP versus mock from three independent replicates with ± SD.

Bfr1p possibly interacts with ribosomes in transient manner or indirectly via mRNA on translating ribosomes.

2.7.4. Bfr1p interacts with *ERG4* mRNA during translation.

So far, I have established that Bfr1p binds to *ERG4* mRNA and mutations in RNA-binding sites of Bfr1p reduces this binding. However, I did not find any evidence of direct interaction of Bfr1p with ribosomes or this interaction might be too transient to detect. Therefore, I wanted to investigate whether *ERG4* mRNA interaction with Bfr1p occurs during translation. To investigate this, I constructed a plasmid expressing *ERG4* lacking the start codon (-AUG) and transformed it into a strain expressing Bfr1-yeGFP. The co-immunoprecipitation of Bfr1p-yeGFP was performed for wild type *ERG4* mRNA and -AUG *ERG4* mRNA. A wild type untagged strain was used to control for non-specific immunoprecipitation.

The qRT-PCR revealed a reduction in -AUG *ERG4* mRNA compared to wild type *ERG4* mRNA suggesting that interaction of Bfr1p with *ERG4* is translation dependent **(Figure 2.16 B)**. However, a significant amount of -AUG *ERG4* mRNA is still bound to Bfr1p confirming that Bfr1p is part of *ERG4* mRNP complex during translation.

3. Discussion

The Bfr1 protein was first reported as a high-copy suppressor of brefeldin A with a possible role in secretion and ploidy maintenance (Jackson and Képès 1994). However, later studies emphasized its functions as an RNA-binding protein regulating mRNA metabolism (Lang et al. 2001, Hogan et al. 2008, Kramer et al. 2014, Lapointe et al. 2015). Recent high-throughput studies have revealed the interacting residues of Bfr1p cross-linked to RNAs (Kramer et al. 2014). Bfr1p was proposed to play a role in multiple pathways including secretion, ploidy control, mRNA binding, P-body formation, and translation, but all previous studies were performed in *BFR1* deletion cells (Jackson and Képès 1994, Xue et al. 1996, Weidner et al. 2014 and Simpson et al. 2014). Therefore, the RNA-binding functions of Bfr1p in terms of its physiological importance remains elusive.

Here, I report that Bfr1p acts as a translational regulator by efficiently elongating polysomes on mRNAs or efficient translocation proteins that are translating at the ER (e.g. *ERG4*). Additionally, I show that Bfr1p has at least two distinct functions; a) via Bfr1p-RNA interaction to control translational regulation and b) via Bfr1p-protein interaction to regulate cell ploidy, brefeldin A sensitivity and P-body formation.

3.1. The loss of interaction of Bfr1p with RNA does not explain the phenotypes of *bfr1*Δ.

Subcellular fractionations and fluorescence microscopy demonstrated that Bfr1p localizes to both the cytoplasm and the perinuclear endoplasmic reticulum (Lang et al. 2001). Here, the authors also report the association of Bfr1p with polysome complexes in an RNA-dependent manner. A similar distribution pattern was shown for another yeast RBP, Scp160p (Wintersberger et al. 1995). Our lab has previously shown that

Khd1p, yet another yeast RBP associated with the ER via binding to its RNA (Syed et al. 2018). Since Bfr1p interacts with mRNAs translating at the ER, I investigated whether the ER localization of Bfr1p is RNA dependent and demonstrated that Bfr1p localizes to the ER in an RNA dependent manner **(Figure 2.2)**. Further evidence for this was obtained from mutagenesis of either one of the conserved residues (F239) or all the six residues together, as Bfr1p's enrichment redistributes from ER to the cytoplasm **(Figure 2.4. A, C, D)**. This indicates that Bfr1p localizes to ER by binding to mRNAs that are translated on the surface of the ER.

3.1.1. RNA-binding of Bfr1p vs P-bodies induction in *bfr1*Δ.

Upon environmental stress, cells constantly regulate its proteome for its survival and to regain its normal growth conditions. The transcription is regulated to maintain the mRNA copy number protein abundance is determined by the mRNA translation and stability. To respond to the stress, the mRNAs are translationally attenuated stored in the membrane less bodies in the cytoplasm called P-bodies (Parker and Sheth 2007). During late phase of glucose starvation, Bfr1p was reported to target several mRNAs (e.g. *RPS16A*) to P-bodies (Simpson et al. 2014). Here, the authors also showed that Bfr1p localizes to P-bodies and interacts with the P-bodies components Dcp2 and Xnr1p via RNA.

Similarly, under normal growth conditions, Bfr1p together with Scp160p, protects mRNAs from translocating to P-bodies by blocking access to P-body components. Loss of *BFR1* induces P-body formation because mRNAs are now more accessible to the P-body components (Weidner et al. 2014). Surprisingly, mutations in RNA-binding residues do not induce premature P-bodies as seen in *bfr1*Δ, suggesting that loss of RNA-binding of Bfr1p is not important for the P-body formation **(Figure 2.5)**.

3.1.2. A role of RNA-binding of Bfr1p in ploidy maintenance?

One of the first observed phenotypes of *bfr1*Δ cells are defects in chromosome segregation and increased ploidy of the cells (Jackson and Képès 1994). A similar observation was also made cells deleted for *SCP160* and *WHI3* (Wintersberger et al. 1995, and Schladebeck and Mösch 2013). Whi3p is an RNA-binding protein with an RRM domain that binds, among others to the *CLN3* mRNA, which codes for a G1 cyclin that coordinates cell size and G1/S transition (Gari et al. 2001). Our lab has previously shown that the KH13-14 domains of Scp160 are necessary for the RNA-binding of Scp160p (Hirschmann et al. 2014). However, truncation of the KH10-14 domains of Scp160p does not alter the ploidy (Cheng Mathew HK, 2018). Similar to the Scp160p, the RNA-binding mutants of Bfr1p does not change the ploidy of cells remains haploid **(Figure 2.6)** suggesting the increase in ploidy upon loss of *BFR1* is independent from its RNA interactions. Bfr1p and Scp160p have also been identified as translational repressors of specific mRNAs (e.g. *POM34*) in the cells with defects in the spindle pole body duplications (SPB) (Sezen et al. 2009). Moreover, Bfr1p interacts with the Bbp1p, an SPB protein and this interaction is independent of RNA (Sezen et al. 2009). Taken together, this suggests that the role of Bfr1p in ploidy maintenance is based on protein-protein and not protein-RNA interactions.

3.1.3. RNA-binding of Bfr1p vs BFA sensitivity.

In eukaryotic cells, mRNAs encoding for secretory proteins are first translocated into the ER during translation for correct folding and modifications. Then most of these proteins are delivered to the Golgi apparatus for further modifications and to the plasma membrane for secretion (Guo et al. 2014, Guo et al. 2017). Since the majority of Bfr1p bound mRNAs encodes secreted or endomembrane proteins, I tested if the loss of interaction between Bfr1p and mRNAs has any consequence on the secretion

pathway. High-copy expression of Bfr1p rescues cells from brefeldin A sensitivity, and all RNA-binding mutants show a similar rescue **(Figure 2.7)**. This suggests that the proposed function of Bfr1p in secretion is not due to its interaction with translating mRNAs, rather it can be a consequence of interactions of Bfr1p with other RNAs or due to the protein-protein interactions of Bfr1p.

Taken together, my results suggest that loss of RNA-binding of Bfr1p is not associated with the published phenotypes that show up upon deletion of *BFR1,* including ploidy control, brefeldin A sensitivity and formation of P-bodies. This also suggests that the localization of Bfr1p at the ER is not required to achieve these functions.

3.2. *ERG4* mRNA binds to Bfr1p but localizes to the ER independently.

Several hundreds of Bfr1p-binding mRNAs were identified by high-throughput studies such as immunoprecipitations of RBPs followed by microarray analysis (RIP-Chip; Hogan et al. 2019), cross-linking and immunoprecipitation (CLIP; Mitchell et al. 2013), or RNA tagging (Lapointe et al. 2015). These studies investigated Bfr1p-mRNA interaction at a global level. However, no follow-up studies have been performed on Bfr1p's interaction with individual mRNAs. Therefore, I tested five mRNA binders of Bfr1p that are significantly enriched in these high-throughput analyses and encode proteins associated with the phenotypes of *bfr1*Δ cells. Although mRNA stability is not affected **(Figure 2.8)** by loss of Bfr1p, co-immunoprecipitation of Bfr1p coupled with qRT-PCR demonstrated that *ERG4* mRNA binds to Bfr1p at least in part via its known RNA contact sites, as mutations in these sites reduce this binding **(Figure 2.9)**. The *ERG4* mRNA is translated at the surface of the ER (Lapointe et al. 2015) and encodes an ER membrane protein with seven predicted transmembrane domains. Therefore, this mRNA must be targeted to the ER for its translation. mRNA localization to the ER

can be mediated by RBPs independent of their translation or by the SRP-targeting pathway. Our lab has previously demonstrated that two yeast proteins, She2p (Schmid et al. 2006) and Khd1p (Syed et al. 2018) are necessary for targeting their mRNA partners to the ER. In contrast, loss of *BFR1* has no implications on the localization of *ERG4* mRNA to the ER **(Figure 2.10 A, B)**. This indicates that the Bfr1p binds to *ERG4* mRNA at the ER and does not participate in its localization.

3.3. Bfr1p promotes local translation of mRNAs at the ER.

Translational control of mRNAs is one of the important mechanisms by which a cell regulates its proteome. For example, if an unfolded protein accumulates, the rate of protein synthesis is reduced as these unfolded proteins become toxic to the cells Walter and Ron 2011). Similarly, an increased translation of certain mRNAs is required when cells exposed to the stress conditions (e.g. heat shock response) (Liu and Chang 2008). RNA-binding proteins play a crucial role in regulating translation of mRNAs either by repressing or enhancing translation (Moore and von Lindern 2018, Abdelmohsen 2012). Since, Bfr1p binds to several ER translated mRNAs, its involvement in translation has already been proposed in previous studies (Lang et al. 2001 and Lapointe et al. 2015).

Although *ERG4* mRNA localization to the ER is not dependent on Bfr1p, Erg4p-yeGFP localization at ER is severely impacted in cells deleted in *BFR1* **(Figure 2.11 A, B, C)**. Erg4p-yeGFP predominantly localized at ER in wild type cells, whereas a faint signal from Erg4p-yeGFP was seen in the cytoplasm in *bfr1*Δ cells. However, replacing Bfr1p by the RNA-binding mutant (*bfr1mut6A*) has no effect on Erg4p expression and localization This implies that Bfr1p controls the expression of Erg4p independent from its interaction with the mRNA. The downregulation of Erg4p in *bfr1*Δ cells is not caused its vacuolar degradation as the deletion of *PEP4 and BFR1* together do not increase

Erg4p levels or result in accumulation in the vacuole. Since Bfr1p mimics several functions of Scp160p, and *ERG4* mRNA also binds to Scp160p (Hogan et al. 2008), I tested whether the loss of *SCP160* show similar effect on the expression of Erg4p. However, I did not find any effect on the expression of Erg4p in *scp160*Δ cells suggesting *ERG4* is a specific target of Bfr1p.

ER-Associated Degradation (ERAD) is a mechanism where misfolded proteins of the ER are ubiquitylated by Hrd1p before re-translocated to the cytoplasm and eventually degraded by *26S* proteasomes (Baldridge and Rapaport 2016). The Erg4p has seven predicted transmembrane domains and it is inserted into the ER membrane by simultaneously during translation. Therefore, the low expression of Erg4p in *bfr1*Δ cells is possibly due to misfolding of Erg4p in the absence of Bfr1p and hence it is redistributed to the cytoplasm for degradation. If this is true, the deletion of *HRD1* should result in the accumulation of misfolded Erg4p as it cannot be ubiquitylated for degradation. Here, I report that by inhibiting *26S* proteasomes and deleting *HRD1* (*bfr1*Δ *hrd1*Δ) a strong accumulation of Erg4p confirming that Erg4p is indeed misfolded in absence of Bfr1p and it is degraded by ERAD pathway **(Figure 2.12)**.

The rate of translation of mRNAs depends on the number of (poly) ribosomes occupied on that mRNA and how efficiently ribosomes are elongating on these mRNAs. One of the rate-limiting steps for translation is either by inhibiting translation initiation or inhibiting translational elongation by stalling polysomes on these mRNAs. To shed more light on the reduction in Erg4p levels in the absence of Bfr1p, I applied Ribosome-affinity purifications (RAP) to purify ribosomes together with actively bound mRNAs. Consistent with the low expression of Erg4p, I found that the ribosomal occupancy on *ERG4* mRNA is reduced suggesting Bfr1p might limit the ribosome

loading during translation **(Figure 2.13)**. However, with this approach, I can only determine the number of ribosomes on *ERG4* mRNAs but not the distribution of free-floating ribosomes, monosomes, and polysomes. Therefore, I performed polysome profiling to understand how Bfr1p is important for the distribution of ribosomes during translation. Contrasting to the low expression of Erg4p in *bfr1*Δ cells, the polysome profiles of *bfr1*Δ or *bfr1mut6A* clearly demonstrate a strong shift in the distribution from monosome to polysomes **(Figure 2.14 B)**. This is only possible if polysomes are stalled on these mRNAs resulting in less protein production. A similar observation was made for Scp160p where the number of polysomes on *PRY3* mRNA was increased while protein was down-regulated (Hirschmann et al. 2014).

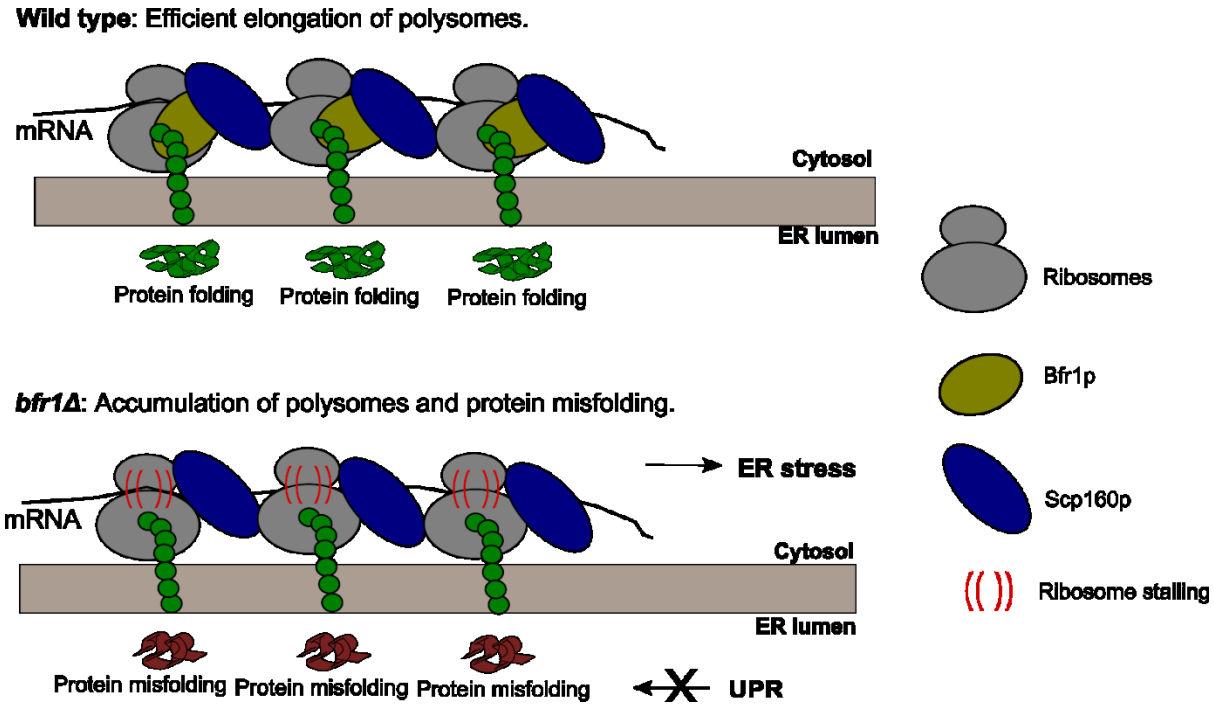

Figure 3. Working model of Bfr1p in translational regulation. The cytoplasmic Bfr1p interacts with mRNAs that are to be translated by ER-bound ribosomes as a complex together with Scp160p. Once at the ER membrane, Bfr1p and Scp160p support efficient elongation of the mRNA. Mutations in RNA-binding residues of Bfr1p or the loss of *BFR1* reduces the elongation efficiency, causing accumulation of polysomes on the mRNA, protein misfolding and elevated ER stress. In the absence of Bfr1p several proteins of the UPR pathway are down-regulated leading to degradation of misfolded proteins.

Consistent with the proposed role of Bfr1p in regulation of translation, a recent study from Castells-Ballester et al. (2019) showed that Bfr1p regulates the translation of Pmt1 and Pmt2, which are crucial for the unfolded O-mannosylation (UPOM). With ribosome profiling approach, the authors revealed that several mRNAs are translationally downregulated in *bfr1*Δ cells. Like PMT1 and PMT2, most of these mRNAs encode secretory proteins, proteins involved in ergosterol biosynthesis (including *ERG4*) and proteins of ER quality control.

In addition, Bfr1p has been linked to the UPR (Travers et al. 2000 and Low et al. 2014) and might act as a checkpoint for synthesis of several proteins during elevated ER stress (Low et al. 2014) by regulating their translational efficiency.

Taking together data from previous studies and from this study on Bfr1p, I propose that Bfr1p acts as a translational enhancer for mRNAs at the ER membrane either by increasing the efficiency of elongating polysomes or efficient folding of newly synthesized proteins (**Figure 3**).

4. Materials and Methods

4.1. Materials

4.1.1. Antibodies

Antibodies were diluted in PBS-T (1x PBS + 0.1% Tween-20) per blot, 3-5 ml of antibody solution was used.

Primary antibodies

Name	Host	Dilution	Source
GFP	Mouse	1:5000	Covance
GFP	Rabbit	1:2500	Invitrogen
HA (clone 3F10)	Rat	1:3000	Roche
Myc (9 E10)	Mouse	1:3000	Roche
Pgk1	Mouse	1:7500	Invitrogen
Scp160	Rabbit	1:10000	Gift from M. Seedorf, Heidelberg.
Sec61 (Serum)	Rabbit	1:7500	Gift from M. Seedorf, Heidelberg.
Rps3	Rabbit	1:10000	Gift from M. Seedorf, Heidelberg

Secondary antibodies

Name	Host	Dilution	Source
Anti-Mouse (IR)	Goat	1:10000	LI-COR
Anti-Rabbit (IR)	Goat	1:10000	LI-COR
Anti-Rat (IR)	Goat	1:10000	LI-COR
Anti-Mouse (HRP)	Sheep	1:10000	Amersham ECL
Anti-Rabbit (HRP)	Donkey	1:10000	Amersham ECL

4.1.2. Chemicals

Acros Organics	D-Glucose monohydrate
AppliChem	Bacto peptone Bacto yeast extract
Biomol	Salmon sperm DNA (ss DNA)

Carl Roth	1,4-Dithiothreitol (DTT) 2-mercaptoethanol Agarose ULTRA Acryl-Bisacrylamide Cycloheximide Dimethyl sulfoxide Glycerin Lithium Acetate Magnesium Chloride Hexahydrate Phenylmethylsulfonylfluoride (PMSF) Polyethylene glycol (PEG) Potassium Chloride TEMED Aminoacids Ammonium persulfate (APS) D-Galactose Ethylene Diamine Tetraacetic acid (EDTA) Sodium dodecyl sulfate (SDS) Sorbitol Sucrose Tris base Triton X-100 Tween-20
Fermentas	Deoxynucleotide triphosphate Mix (dNTPs)
FORMEDIUM	Yeast Nitrogen Base
Thermo Scientific	Brefeldin A (eBioscience)
Roche	cOMPLETE, Mini, EDTA-free Protease inhibitor Cocktail tablets
Sigma-Aldrich	Proclin-300, MG132, EDAC

4.1.3. Commercial Kits

Macherey and Nagel	NucleoSpin Gel and PCR clean up NucleoSpin Plasmid NucleoSpin RNA II isolation kit
Thermo Scientific	High-Capacity cDNA Reverse Transcription kit Fast SYBR Green Master Mix
Polysciences, Inc.	PolyLink Protein Coupling kit using EDAC

4.1.4. Consumables

Chromo Tek	GFP-Trap_MA beads
Carl Roth	Cover slips Objective slides Glass beads

GE Healthcare	Protein G Sepharose 4 Fast flow beads ECL Western blotting Substrate
LI-COR Biosciences	PVDF Membranes Nitrocellulose Membranes
SARSTEDT AG & Co.	Centrifuge tube 50 ml, 15 ml CryoPure Storage Systems High quality pipette tips High quality serological pipettes Micro Tubes SafeSeal 2 ml, 1.5 ml PCR reaction tubes Semi-micro cuvette

4.1.5. Enzymes

NEB	Restriction digestion enzymes
Agilent Technologies	Herculase II Fusion DNA Polymerase
Amsbio	Zymolse 20T, Zymolase 100T
GENAXXON	Taq Polymerase
Thermo Scientific/Fermentas	Proteinase K Fast-Digest Restriction enzymes RiboLock RNase Inhibitor T4 DNA Ligase PageRuler Prestained Protein Ladder PageRuler Unstained Protein Ladder PageRuler DNA ladder (100 bp, 1 Kb) RNse Inhibitor RNAse A
Promega	Q1-RNase free DNase

4.1.6. Equipment

Alpha Innotec	Fluorchem® FC2
Bio-Rad	Mini-PROTEAN Tetra Electrophoresis System PowerPac HC Power Supply ChemiDoc MP MyCycler Thermo Cycler SNAP i.d. ™ System
Eppendorf	Centrifuge 5415R Centrifuge 5702 Centrifuge 5810R Pippettes P1000, P200, P20, P10
BIO ER	ThermoCell Mixing Block MB-102

BECKMAN COULTER	Ultracentrifuge rotor SW 40 Ti Ultracentrifuge TLA-120.2 CytoFLEX Flow Cytometer
LI-COR Biosciences	Odyssey Infrared Imaging System
Stuart Scientific	Gyro rocker
Scientific Industries, Inc.	Vortex-Genie 2
SPEX® Inc	Bead mill
IKA	Vibrax VXR basic
VISITRON SYSTEMS	VisiScope Live Cell Imaging System
Thermo Scientific	The StepOne Plus Real-Time PCR System Ultracentrifuge rotor TH-641
ZEISS	Axio Examiner
SPEX Inc	Freezer Mill/Mixer Mill

4.1.7. Oligonucleotides

RJO	**Name**	**Sequence (5‘- 3‘)**	**Purpose**
5238	Bfr1_R38A_Fw	GAAATCGGTTTAATTGCCAAGCAAATCGATCAA	Mutation PCR
5239	Bfr1_R38A_Rw	TTGATCGATTTGCTTGGCAATTAAACCGATTTC	Mutation PCR
5240	Bfr1_H79A_Fw	CGTAGAAGCAACATTGCCGACTCTATTAAGCAA	Mutation PCR
5241	Bfr1_H79A_Rw	TTGCTTAATAGAGTCGGCAATGTTGCTTCTACG	Mutation PCR
5242	Bfr1_K138A_Fw	GAAAAACTACTAGTCGCCGAAATGCAATCTTTG	Mutation PCR
5243	Bfr1_K138A_Rw	CAAAGATTGCATTTCGGCGACTAGTAGTTTTTC	Mutation PCR
5244	Bfr1_F211A_Fw	AAAAGACAAACTTTAGCCAACAAACGTGCTGCC	Mutation PCR
5245	Bfr1_F211A_Rw	GGCAGCACGTTTGTTGGCTAAAGTTTGTCTTTT	Mutation PCR
5246	Bfr1_Y225A_Fw	AAGCGTGACGAATTAGCCAGTCAAATCAGACAG	Mutation PCR
5247	Bfr1_Y225A_Rw	CTGTCTGATTTGACTGGCTAATTCGTCACGCTT	Mutation PCR
5248	Bfr1_F239A_Fw	GACTTTGACAACGAAGCCAAATCATTCAGAGCC	Mutation PCR
5249	Bfr1_F239A_Rw	GGCTCTGAATGATTTGGCTTCGTTGTCAAAGTC	Mutation PCR
4924	Bfr1::HA C-terminal S3_Fw	AAAAGATTGAAAGAACAGGAAGAGTCTGAAAAAG ATAAAGAAAATCGTACGCTGCAGGTCGAC	Gene tagging
4925	Bfr1::HA C-terminal S2_Rw	AATGAAGAAAGATCAGGAGAAAAATTTTTTTCTAC TTCAGGTTTAATCGATGAATTCGAGCTCG	Gene tagging
5587	Eag1 Termi Bfr1_Fw	GGCCGGCCGACCTGAAGTAGAAAAAAATTTTTC	Cloning

5588	Terminator Bfr1 SacI_Rw	CGAGCTCGGAGGAAAGAATTGGCTGGTAAG	Cloning
6367	Bfr1 promotor_KpnI_Fw	GGGGTACCGGGCGTAAGAACGAATTTGAAG	Cloning
5432	yEGFP-Stop-NheI-Rw	GCCGCTAGCTTATTTGTACAATTCATCCATACC	Cloning
5589	S3_bfr1 1-397AA_Fw	ccaacactaattgctactttggccgaattagacgtaactgtcccaatcCG TACGCTGCAGGTCGAC	Gene tagging
5590	S2_bfr11-397AA_Rw	agtaatgaagaaagatcaggagaaaaatttttttctacttcaggtttaAT CGATGAATTCGAGCTCG	Gene tagging
3006	Bfr1_ko_S1_for	TCAACGTAATAGCATATTTTCTAACAACACAGCCA TTGCCCGTACGCTGCAGGTCGAC	Gene deletion
3007	Bfr1_ko_S2_rev	TGAAGAAAGATCAGGAGAAAAATTTTTTTCTACTT CAGGTATCGATGAATTCGAGCTC	Gene deletion
5828	ERG4 deltion Fw S1	CAGATACGGATATTTACGTAGTGTACATAGATTA GCATCGCTATGCGTACGCTGCAGGTCGAC	Gene deletion
5820	ERG4 C-term tag Fw S3	GAGTATTGTAAACATTGCCCTTACGTCTTTATTCC TTATGTTTTCCGTACGCTGCAGGTCGAC	Gene tagging
5821	ERG4 C-term tag Rw S2	ACTGTAAAATAAGTTAATGAAGTGGATAGAAAAA GAAAATAACTA ATCGATGAATTCGAGCTCG	Gene tagging
5826	ERG6 deltion Fw S1	AAAAAAACAAGAATAAAATAATAATATAGTAGGCA GCATAAGATGCGTACGCTGCAGGTCGAC	Gene deletion
5827	ERG6 deltion Rw S2	ATATATCGTGCGCTTTATTTGAATCTTATTGATCT AGTGAATTTAATCGATGAATTCGAGCTCG	Gene deletion
6320	ERG4_NewMS2_F:	ATGAGTATTGTAAACATTGCCCTTACGTCTTTATT CCTTATGTTTTCTAGccgctctagaactagtggat	Gene tagging
6321	ERG4_NewMS2_R:	ATATACAAACTGTAAAATAAGTTAATGAAGTGGAT AGAAAAAGAAAATAAgatatcacctaataacttcgtatag	Gene tagging
6603	PEP4 -del-S1-Fw	CTAGTATTTAATCCAAATAAAATTCAAACAAAAAC CAAAACTAACATGCGTACGCTGCAGGTCGAC	Gene deletion
6604	PEP4 -del-S2-Rw	TAGATGGCAGAAAAGGATAGGGCGGAGAAGTAA GAAAAGTTTAGCTCAATCGATGAATTCGAGCTCG	Gene deletion
2509	SCP160_ko_ fw S1	TAAAATATACTTCCCACACCCCCTCCTTCCATTAT AACTGCACGTACGCTGCAGGTCGAC	Gene deletion
2510	SCP160_ko_ rev S2	GCCAAAATCTATATTGAAAAAAATTGGTTTCAAAG AGCTTGTATCGATGAATTCGAGCTC	Gene deletion
6324	IMH1_qPCR_Fw_Set 2	ATTGACGACGCAGTGGATAC	qPCR
6325	IMH1_qPCR_Rw_Set 2	CTGGAATTTCCGAGTTCTGC	qPCR
6326	RUD3_qPCR_Fw_Set 1	TTTCGTGTCCATACCCAGAG	qPCR

6327	RUD3_qPCR_Rw_Set 1	CCGGCCTGTTGTTTCTTATC	qPCR
6332	ERG4_qPCR_Fw_Set 2	TGCCATGTGGACCTTGTATG	qRT-PCR
6333	ERG4_qPCR_Rw_Set 2	GTCATGATCCTCCCAAAACG	qRT-PCR
6334	OSH7_qPCR_Fw_Set 1	TGCAGAACAAACGAGTCACC	qPCR
6335	OSH7_qPCR_Rw_Set 1	CCATCATTGCAGCACTTGAG	qPCR
6338	SGM1_qPCR_Fw_Set 1	GGGAAGGGGAATCAATGAAC	qPCR
6339	SGM1_qPCR_Rw_Se t 1	GGCCGTTAGAATTCGATAGC	qPCR
2920	Act1_qPCR_1_Fw	TCAGAGCCCCAGAAGCTTTG	qPCR
2921	Act1_qPCR_1_Rw	TTGGTCAATACCGGCAGATTC	qPCR
4139	18S_qPCR_Fw	TCAACACGGGGAAACTCACC	qRT-PCR
4148	18S_qPCR_Rw	CTAAGAACGGCCATGCACCA	qRT-PCR
4488	MID2_qPCR_Fw	ATGGAGCAAAGCTCCCTTTT	qPCR
4489	MID2_qPCR_Rw	GCTCTCCACCGCTATTGGTA	qPCR
5568	Spike-qPCR_Fw	CACACTCATCAGCGACACGA	qPCR
5569	Spike-qPCR_Rw	CCAAAGCGGTGACTTTCTGC	qPCR
6527	BamHI_ERG4 _102_Fw	CGCGGATCCATTTGTGCGGAATTTTATCAC	Cloning
6528	ERG4_3UTR_Hindiii_ Rw	CCCAAGCTTGAATTTTCAAAGAATGACTTG	Cloning
3008	Bfr1_3'UTR_rev	CATGAGGAAAGAATTGGCTGG	Gene tagging
4918	bfr1_5'UTR_fw	TAACTGATCTCGACGACGTTG	Gene tagging

4.1.8. Plasmids

Name	**Short description**	**Source**
RJP1870	pRS415-HDEL-DsRED	(Bevis and Glick 2002)
RJP2121	pET296-YcpLac111-CYC1p-1xMCPNLSSV40-2-xyegfp	(Tutucci et al. 2017)
RJP1809	Edc3-mCh URA3 Cen	(Buchan et al. 2008)
RJP1686	YCp50-SCS2-TMD-2xRFP	(Loewen et al. 2007)
RJP2000	pRS316-pBFR1-Bfr1 FL-yeGFP	This study

RJP2199	pRS316-pBFR1-*bfr1mutR38A*-yeGFP	This study
RJP2200	pRS316-pBFR1-*bfr1mutH79A*-yeGFP	This study
RJP2061	pRS316-pBFR1-*bfr1mutK138A*-yeGFP	This study
RJP2201	pRS316-pBFR1-*bfr1mutF211A*-yeGFP	This study
RJP2202	pRS316-pBFR1-*bfr1mutY225A*-yeGFP	This study
RJP2062	pRS316-pBFR1-*bfr1mutF239A*-yeGFP	This study
RJP2209	pRS316-(-AUG) *ERG4*	This study
RJP2203	YEplac181-pBFR1-Bfr1 FL-yeGFP	This study
RJP2204	YEplac181-pBFR1-*bfr1mut6A*-yeGFP	This study
RJP2205	YEplac181-pBFR1-*bfr1mut5A*-yeGFP	This study
RJP2206	YEplac181-pBFR1-*bfr1mut4A*-yeGFP	This study
RJP2207	YEplac181-pBFR1-*bfr1mut3A*-yeGFP	This study
RJP2208	YEplac181-pBFR1-*bfr1mut2A*-yeGFP	This study
RJP148	pRS316 (URA3, CEN6)	(Janke et al. 2004)
RJP143	YEplac181 (LEU2), 2µm	(Gietz and Schiestl 2007)

4.1.9. Yeast (Saccharomyces cerevisiae) strains

Name	**Essential genotype**	**Plasmid(s)**	**Origin**
RJY358	*MATa ade2-1 trp1-1 can1-100 leu2-3,112 his3-11,15 ura3*	-	
RJY925	*MATa/MATalpha, ade2-1/ade2-1 trp1-1/trp1-1 can1-100/can1-100 leu2-3,112/leu2-3,112 his3-11,15/his3-11,15 ura3* GAL *psi+*	-	
RJY4680	*MATa Bfr1p-yeGFP::HIS3MX6*	-	This study
RJY5142	*MATa Bfr1p(1-397)-yeGFP::KanMX6*	-	This study
RJY5204	*MATa bfr1mut6A-yeGFP::HIS3MX6*	-	This study
RJY4626	*MATa bfr1::HIS3MX6*	-	This study
RJY5146	*MATa*	RJP1870	This study
RJY5148	*MATa Bfr1p-yeGFP::HIS3MX6*	RJP1870	This study
RJY5417	*MATa Bfr1p(1-397)-yeGFP::KanMX6*	RJP1870	This study
RJY5419	*MATa bfr1mut6A-yeGFP::HIS3MX6*	RJP1870	This study

RJY5145	*MATa bfr1::HIS3MX6*	RJP1870 RJP2062	This study
RJY5144	*MATa bfr1::HIS3MX6*	RJP1870 RJP2061	This study
RJY5421	*MATa bfr1::HIS3MX6*	RJP1870 RJP2199	This study
RJY5422	*MATa bfr1::HIS3MX6*	RJP1870 RJP2200	This study
RJY5423	*MATa bfr1::HIS3MX6*	RJP1870 RJP2201	This study
RJY5424	*MATa bfr1::HIS3MX6*	RJP1870 RJP2202	This study
RJY5434	*MATa*	RJP1809	This study
RJY5435	*MATa bfr1::HIS3MX6*	RJP1809	This study
RJY5436	*MATa Bfr1p-yeGFP::HIS3MX6*	RJP1809	This study
RJY5437	*MATa Bfr1p(1-397)-yeGFP::KanMX6*	RJP1809	This study
RJY5438	*MATa bfr1mut6A-yeGFP::HIS3MX6*	RJP1809	This study
RJY5425	*MATa erg6:KanMX6*	-	This study
RJY5426	*MATa erg6::KanMX6 bfr1::HIS3MX6*	RJP2203	This study
RJY5427	*MATa erg6::KanMX6 bfr1::HIS3MX6*	RJP2204	This study
RJY5428	*MATa erg6::KanMX6 bfr1::HIS3MX6*	RJP2205	This study
RJY5429	*MATa erg6::KanMX6 bfr1::HIS3MX6*	RJP2206	This study
RJY5430	*MATa erg6::KanMX6 bfr1::HIS3MX6*	RJP2207	This study
RJY5431	*MATa erg6::KanMX6 bfr1::HIS3MX6*	RJP2208	This study
RJY5260	*MATa ERG4-12xMS2V6::KanMX4*	RJP2121 RJP1686	This study
RJY5262	*MATa bfr1::HIS3MX6 ERG4-12xMS2V6::KanMX4*	RJP2121 RJP1686	This study
RJY5432	*MATa Erg4-yeGFP::klTRP1*	RJP1870	This study
RJY5433	*MATa Erg4-yeGFP::klTRP bfr1::HIS3MX6*	RJP1870	This study
RJY5439	*MATa Erg4-yeGFP::klTRP bfr1::HIS3MX pep4::KanMX6*	-	This study
RJY5440	*MATa Erg4-yeGFP::klTRP scp160::HIS3MX6*	-	This study
RJY4683	*MATa Bfr1p-6HA::KanMX Scp160-myc9::HIS3MX6*	-	This study
RJY3206	*MATa Khd1-GFP::KanMX4*	-	(Syed et al. 2018)
RJY3687	*MATa RPL16a-TEV-ProtA::HIS3MX6*	-	(Hirschmann et al. 2014)

RJY4855	*MATa RPL16a-TEV-ProtA::HIS3MX bfr1::KanMX4*	-	(Hirschmann et al. 2014)
RJY5441	*MATa Bfr1p-yeGFP::HIS3MX erg4::KanMX4*	RJP2209	This study
RJY5469	*MATa Erg4-yeGFP::klTRP bfr1mut6A-6HA::KanMX4*	RJP1870	This study
RJY5470	*MATa Erg4-yeGFP::klTRP bfr1::HIS3MX6 hrd1::KanMX4*	-	This study

4.2. Methods

All standard biochemical, microbiological and molecular biology techniques were based on Sambrook J. et al, 2001. Commercial Kits were used according to manufacturer's instructions. Standard buffers were prepared as described (Sambrook, 2001).

4.2.1. Basic Methods

4.2.1.1. Agarose gel electrophoresis and gel extraction

As a standard in most cases, I used 1.0 % of agarose gels. Agarose was added to TAE buffer to the required concentration and then heated in a microwave oven until agarose was completely melted. The solution was cooled to 60°C, then 2-3 µl of 10,000x stock solution of GelRed were added and the gel poured into a casting tray containing a multiwall comb. The gel was solidified at room temperature. For PCR product gel extraction, bands were cut out using 70% intensity of the UV illumination at 365 nm. DNA extraction was carried out by the NucleoSpin Gel and PCR clean up kit (Macherey & Nagel) according to manufacturer's instructions.

4.2.1.2. Restriction digestion

Vector and insert DNA were digested in a following reaction mixture. In most cases, Fast digest enzymes (Thermo Scientific) were used for reaction.

Insert DNA mix (20 µl):	*Vector DNA mix (30 µl):*
2 µl (0.2-0.5 µg)	2 µl (~1 µg)
2 µl 10x buffer	2 µl 10x buffer
1 µl enzyme 1	1 µl enzyme 1
1 µl enzyme 2	1 µl enzyme 2
14 µl sterile water	24 µl sterile water

The reaction mixtures were incubated at temperatures as described by the manufacturer's manual. After the incubation, DNA was extracted from the gel or PCR cleaned up by the NucleoSpin Gel and PCR clean up kit.

4.2.1.3. Ligation of DNA fragments

The molar ratio between vector and insert DNA was either 1:1, 1:2, 1:3 or 1:5 depending on the size of the insert and the presence of blunt ends in the insert. The online ligation calculator tool from NEB (https://nebiocalculator.neb.com/#!/ligation) was used for setting up the ligation reaction.

The ligation of digested DNA was performed as follows:

Ligation mix (20 µl):

10x ligation buffer 2 µl

T4 DNA ligase 2 µl

DNA vector 2-4 µl (~100-200 ng)

DNA insert 7 µl (~450-600 ng)

Sterile water 7-5 µl

The ligation mix was incubated overnight at 25°C for 30 min and afterwards directly used for *E. coli* transformation or stored at -20°C.

4.2.1.4. Overlap extension PCR

Some of the plasmids were constructed by the “Overlap Extension PCR” method (Bryksin, Matsumura 2010). This method allows ligation of linear DNAs which have at least 15-30 bp complementary sequences at their 5’ and 3’ ends by using *in vivo* homologous recombination in *E. coli*.

4.2.2. SDS-PAGE and Western blotting

4.2.2.1. SDS-PAGE

Sodium dodecyl sulfate polyacrylamide gel electrophoresis (SDS-PAGE) was performed using the Mini-Protean® Tetra System (BIO-RAD). In most cases, a 10% or 12% separating gel was used with 4% stacking gel. Samples were heated at 65ºC for 10 min or sometimes 95°C for 5 minutes before loading onto the gel. The samples were run at 100 V for 90-120 min and until the bromophenol blue reached the bottom of the gel. Afterwards, the gel was either prepared for Coomassie or Silver staining or for Western blotting.

4.2.2.2. Coomassie staining

For the staining of polyacrylamide gels using Coomassie Brilliant Blue R-250 the gel was immersed in Coomassie staining solution and warmed in a microwave oven for 20 to 30 seconds, then kept on shaker for at least 45 mins. Then stain was removed by shaking overnight until no more background was visible.

4.2.2.3. Western blotting

Protein transfer onto a polyvinylidene fluoride transfer membrane (PVDF; LI-COR) was performed using a wet blot procedure with a transfer cell (BIO-RAD). Both gel and Whatman-paper slices were covered with transfer buffer (0.25 M Tris, 1.92 M glycine, pH 8.6 ± 0.2) for 5 min. The PVDF membrane was activated by shortly rinsing it in

methanol. A transfer sandwich was set up (2 thin Whatman-papers sheets, membrane, gel, 2 thin Whatman-papers sheets) and the proteins were transferred for 45 min at 12 V. After disassembly, the membrane was blocked with 5% blocking buffer (5% non-fat dry milk powder in PBS-Tween 20; PBST) when directly using the SNAP i.d.TM system for immunoblotting. The antibodies for detection are listed in section 4.1. After blocking, the membrane was incubated with primary antibody for 10 min at room temperature, and then washed 3x with PBST to remove the unbound primary antibodies. Subsequently, incubation with the secondary antibody was performed for 10 min at room temperature. The membrane was washed 3x with PBST and visualization of proteins was performed using an enhanced chemiluminescence kit (ECL-kit, GE Healthcare) or IR fluorescence. Signals were detected using the Fluorchem® FC2 (Alpha Innotech) or ChemiDoc (Bio-Rad) chemiluminescence imaging system and for IR fluorescence LI-COR imaging system.

4.3. *E. coli*-specific techniques

4.3.1 Chemical competent *E. coli* cells preparation

Chemically competent *E. coli* cells were prepared from the strain One Shot™ TOP10 (Invitrogen), which was grown in 50 ml Luria Bertani (LB) medium (for 100ml: 0.8 g bacto peptone, 0.5 g yeast extract, 1 g NaCl pH 7.4) at 37°C in a shaking incubator until an optical density of 0.4-0.6 at OD_{600} was reached. Then the cells were cooled on ice for 15 min and collected by centrifugation (10 min, 4,500 rpm, 4°C). The pellet was resuspended in 1 ml ice-cold 50 mM $CaCl_2$/10% glycerol. After re-centrifugation, the pellet was resuspended in 2 ml of ice-cold calcium chloride solution. Then the cells were pelleted and resuspended in one fourth of the cell volume of 0.1 M $CaCl_2$/10% glycerol. Aliquots of 50 µl were shock-frozen in liquid Nitrogen (LN2) and stored at -80°C.

4.3.2 Plasmid-DNA extraction (Miniprep)

High-quality bacterial plasmid-DNA was extracted with the Macherey-Nagel Miniprep Kit according to the manufacturer's protocol.

4.3.3 Transformation of competent *E. coli* cells

The One Shot™ TOP10 competent cells were thawed on ice for about 5-10 min. Then the DNA (5-50 ng of plasmid DNA or 20 µl of the ligation mix) were added to 50 µl of cells and incubated on ice for 10-15 mins, then plated on antibiotic containing LB agar plates and incubated at 37°C overnight. Individual bacterial colonies were picked and inoculated in 3 ml of LB medium containing antibiotics (e.g. 100 µg/ml Ampicillin) and grown for 8 h or overnight (37°C, shaker) in order to perform plasmid extractions (Miniprep).

4.3.4 PCR for colony screening

Bacterial colony PCR was carried out by picking up a bacterial clone with the help of a 10 µl pipette tip and added to the master mix.

Reaction mixture (total volume 20 µl):

10x PCR buffer S with 15mM MgCl2 (Genaxxon)	2.0 µl
25 mM dNTPs	0.5 µl
Forward + Reverse primer (10 µM each)	1 + 1 µl
25 mM $MgCl_2$	0.5 µl
Taq polymerase	0.2 µl
Sterile water	14.8 µl

Program:

Step 1: 95°C – 5 min

Step 2: 95°C - 30 sec

Step 3: 54°C - 30 sec

Step 4: 68°C - (1 min/Kb)

Step 2-4: 30 cycles

Step 5: 68°C - 10 min

Step 6: 4°C ∞

4.3.5. Construction of specific plasmids

Plasmid RJP2000 (pRS316-pBFR1-Bfr1 FL-yeGFP) was created as follows. First, a PCR product spanning from the *BFR1* promoter region to the C-terminal yeGFP was generated using oligonucleotides RJO6367 and RJO5432 and genomic DNA of RJY4680 (Bfr1p-yeGFP::*HIS3MX6*) as a template. The product was digested with restriction enzymes *KpnI* and *NheI* whose sites were introduced by the oligonucleotides. RJP148 (pRS316) was digested with *KpnI* and *XbaI* and both fragments ligated. The 3'UTR region of *BFR1* was amplified separately with oligonucleotides RJO5587 and RJO5588 using genomic DNA of strain RJY358 and digested with restriction enzymes *EagI* and *SacI* whose restriction sites were introduced with the oligonucleotides. The intermediate construct was digested with restriction enzymes *EagI* and *SacI* and the digested PCR product was ligated in to generate RJP2000.

Plasmids containing the complete *BFR1* gene with point mutations (RJP2199; *bfr1mutR38A*-yeGFP, RJP2200; *bfr1mutH79A*-yeGFP, RJP2061; *bfr1mutK138A*-yeGFP, RJP2201; *bfr1mutF211A*-yeGFP, RJP2202; *bfr1mutY225A*-yeGFP and RJP2062; *bfr1mutF239A*-yeGFP) were created from a pRS316 vector carrying *BFR1* by an overlap extension PCR method (see 4.2.1.4) with respective oligonucleotides.

High copy number plasmids carrying *BFR1* or its mutant constructs were created as follows. Firstly, full-length *BFR1* fused to the yeGFP coding region was released from

RJP2000 (pRS316-pBFR1-Bfr1 FL-yeGFP) by digestion with *KpnI* and *SacI* and ligated into the vector YEplac181 to create plasmid YEplac181-pBFR1-Bfr1 FL-yeGFP (RJP2203). To generate plasmids carrying multiple mutations (RJP2208; YEplac181-pBFR1-*bfr1mut2A*-yeGFP, RJP2207; YEplac181-pBFR1-*bfr1mut3A*-yeGFP, RJP2206; YEplac181-pBFR1-*bfr1mut4A*-yeGFP, RJP2205; YEplac181-pBFR1-*bfr1mut5A*-yeGFP, RJP2204; YEplac181-pBFR1- *bfr1mut6A*-yeGFP), two-step overlap extension PCR was performed with oligonucleotides RJO6367 and RJO5432 together with mutation specific primers. The corresponding PCR products contained *KpnI* and *SacI* restriction sites at their ends. PCR products with lower numbers of mutations were used as templates for generation of additional mutations. The PCR products were then digested with *KpnI* and *SacI* and ligated into YEplac181.

Plasmid RJP2209 (carrying AUG-less *ERG4*) was created as follows. A PCR product of the *ERG4* coding region (lacking the part encoding the first 101 amino acids), together with the 3'UTR, was amplified by PCR with oligonucleotides RJY6527 and RJY6528, introducing *BamHI* and *HindIII* restriction sites. The digested product was ligated into vector pRS316.

4.3.6 Sequencing and analysis

Sequencing was done by Eurofins and GATC GmbH. The plasmids and primers were prepared and/or chosen as recommended by the company. The analysis of the sequences was done by using the software SnapGene (from GSL Biotech) and ApE-A plasmid Editor (by M. Wyane Davis).

4.3.7. Glycerol stocks and storage

To store bacteria for long-term, 500µl of cells from an overnight culture were transferred into a cryo-tube and mixed with 50% (w/v) glycerol to a final concentration of 15% (w/v). The cells were shock-frozen with liquid nitrogen and stored at -80°C.

4.4. *S. cerevisiae*-specific techniques

4.4.1 Polymerase chain reaction

Gene knock-out or introduction of tags in yeast were performed by PCR-based methods (Knop et al, 1999; Janke et al, 2004). Herculase (Agilent Technologies) was used for PCR reactions for its proof-reading ability and accuracy. PCR products were purified using the Macherey & Nagel PCR clean-up Kit.

4.4.1.1 Standard PCR for generation of deletion or tagging cassettes

The standard PCR reaction was prepared as follows:

Reaction mixture (total volume 50 µl): Program:

10x PCR buffer Herculase with 10mM MgCl2	5.0 µl
dNTPs 10 mM	2.5 µl
DMSO	2 µl
Forward + Reverse primer (10 µM each)	1 + 1 µl
Template (50-250 ng/µl)	1 µl
Herculase enzyme	0.5 µl
Sterile water	37 µl

Program:

Step 1: 95°C – 5 min

Step 2: 95°C - 30 sec

Step 3: 54°C - 30 sec

Step 4: 68°C - (1 min/Kb)

Step 2-4: 32 cycles

Step 5: 70°C - 10 min

Step 6: 4°C ∞

4.4.2 Yeast colony PCR

To identify correct colonies after the transformations, a single yeast colony was scraped off from a fresh plate and suspended in 100 µl of 200 mM lithium acetate containing 1% SDS. Then the mixture was incubated at 70°C for 15 min. After adding 300 µl of 100% ethanol and vortexing, the DNA was collected Methods 81 by centrifugation at 13,000 rpm for 3 min. The precipitated DNA was dissolved in 100 µl TE and cell debris were spun down at 13,000 rpm for 1 min. 1 µl of the supernatant was used for PCR (Looke et al, 2011; Balaji TM, 2014).

Reaction mixture (total volume 20 µl) Program:

10x PCR buffer S with 15mM MgCl2 (Genaxxon)	2.0 µl
25mM dNTPs	0.5 µl
Forward + Reverse primer (10 µM each)	1 + 1 µl
25mM MgCl2	0.5 µl
DNA template	1 µl
Taq polymerase	0.2 µl
Sterile water	13.8 µl

Program:

Step 1: 95°C – 5 min

Step 2: 95°C - 30 sec

Step 3: 54°C - 30 sec

Step 4: 68°C - (1 min/Kb)

Step 2-4: 20 cycles

Step 5: 68°C - 5 min

Step 6: 4°C ∞

4.4.3. Transformation of yeast cell

4.4.3.1 One-step yeast transformation with plasmids

Transformation of yeast with plasmids was done as described (Chen et al, 1992 and Balaji TM, 2014). Cells were inoculated in 5 ml of medium and incubated overnight or used directly by scraping off a fresh plate. The cell suspension (1 ml) was pelleted by centrifugation and the pellet was resuspended by vortexing briefly in 100 µl of one-step buffer (0.2 M lithium acetate, 40% PEG 4000, 100 mM DTT). An aliquot of single stranded salmon sperm DNA (ssDNA) was thawed on ice, heated for 5 min at 95°C, and directly cooled down on ice to make the DNA linear. 20 µg ssDNA and 100 - 500 ng plasmid DNA was added to the cell-buffer suspension and mixed by vigorous vortexing. Then the mixture was incubated for 30 min at 45°C. After this heat shock, 1 ml YEPD was added, cells were resuspended and pelleted at 10,000 rpm for 15 sec. The supernatant was discarded, and the pellet was carefully resuspended in 1 ml YPED medium. 100-200 µl of the suspension were plated onto the corresponding selective plate and incubated at 30°C. Colonies appeared after 2-3 days.

4.4.3.2 High-efficiency yeast transformation

Yeast cells were transformed with PCR products for genomic integration via homologous recombination by high efficiency transformation method (Schiestl & Gietz, 1989). A single colony of yeast was inoculated in 10 ml YEPD medium or drop out medium and rotated on a wheel overnight at 30°C. Subsequently 50 ml of YEPD medium or drop out medium was inoculated with an overnight culture to an OD_{600} of 0.2-0.3. Cells grew for two generations until OD_{600} reaches 1. The cells were then harvested by centrifugation at 2,500 rpm for 5 min. The supernatant was discarded,

the cells were washed with 10 ml water and the pellet was resuspended in 1 ml of freshly prepared 100 mM lithium acetate. After centrifugation at top speed for 30 sec, the supernatant was removed, and the cells were resuspended in 400 µl of 100 mM lithium acetate. An aliquot of ssDNA was thawed, boiled for 5 min at 95°C and quickly chilled on ice. For one transformation mix, 50 µl of the suspension was transferred into a new 1.5 ml reaction tube. After centrifugation lithium acetate was completely removed and the transformation mix (240 µl (50% w/v) PEG, 36 µl of 1 M lithium acetate, 25 µl of ssDNA (2 mg/ml), 50 µl water with 0.5-3 µg linear DNA) was added to the cell pellet. The mixture was vortexed vigorously until the pellet was completely resuspended. The mixture was then incubated for 30 min at 30°C, treated for 23 min at 42°C and centrifuged at 8,000 rpm for 30 sec. The transformation mix was removed, and the pellet resuspended in 1 ml of water or medium. 100-200 µl of the suspension was plated onto the corresponding selective medium. In the case of Kanamycin marker, cells were recovered on a YEPD plate overnight at 30°C and replica plated onto YEPD+G418 (geneticin) plates. Colonies appeared after 2-3 days.

4.4.4. Genomic DNA extraction from yeast cells

In order to use genomic DNA as a template for PCR, genomic DNA was extracted from yeast as the follows. A big loop of yeast was scraped off a fresh plate, resuspended in 1 ml of water and pelleted at 1,000 rpm for 5 min at 4°C. The pellet was resuspended in 200 µl of DEB (DNA extraction buffer, 1% SDS, 100 mM NaCl, 10 mM Tris-HCl pH 8.0, 1 mM EDTA pH 8.0 and 0.2% Triton X-100). 500 µl of acid-washed sterile glass beads (0.4 mm diameter) and 200 µl of Phenol/Chloroform/Isoamylalcohol (24:24:1) were added to the cells and the mixture was vigorously shaken using a vibrax shaker for 5 min (top speed, 4°C). The lysate was mixed with 200 µl of TE, vortexed for 30 sec and centrifuged at 12,000 rpm for 10

min at RT. After transferring 200 µl of the supernatant to a new Eppendorf cup filled with 750 µl of 100% ethanol and after vortexing the mixture, the genomic DNA was precipitated by centrifugation at 12,000 rpm for 10 min at RT. Ethanol was removed by aspiration. The tube was centrifuged again to remove residual ethanol. The pellet was dried for about 10 min by leaving the tube open and finally resuspended in 50 µl of TE buffer. The DNA was directly used for PCR or stored at -20°C.

4.4.5. Quick alkaline lysis of yeast cells

One loop of cells from fresh plates was mixed with 1 ml of water, 150 µl 1.85 M of NaOH and 7.5% β-Mercaptoethanol and chilled on ice for 15 min. 150 µl 50% TCA were added and the mixture centrifuged at 14,000 rpm for 15 min at 4°C. The supernatant was discarded and 50 µl of High Urea (HU) buffer (8 M urea, 5% SDS, 20 mM Tris pH 8.8, 1.5% DTT, bromophenolblue) was added to each pellet. The mixture was then incubated for 10 min at 65°C with shaking. The supernatant was collected by centrifugation at 14,000 rpm for 1 min and used for further experiments (e.g. Western blotting).

4.4.6. Construction of specific yeast strains

The strain with *BFR1* point mutations was generated as follows. We first mutated *F239A* using the genomic DNA from strain RJY4680 (Bfr1p-yeGFP::*HIS3MX6*) as a template and oligonucleotide pairs RJY4918 and RJY5248 (from the 5'UTR region of *BFR1* to F239 position), and RJY5249 and RJY3008 (from F239 position to 3'UTR region of *BFR1*). These two separate PCR products were then amplified in an overlap extension PCR reaction using the oligonucleotides RJY4918 and RJY3008. This intermediate PCR product served as a template for the subsequent introduction of individual mutations (R38A, H79A, K138A, F211A) using mutagenic oligonucleotides. After generating the final product with all six mutations, the linear DNA was

transformed into RJY358 to generate the strain RJY5204 (*bfr1mut6A-yeGFP::HIS3MX6*). Strains RJY5260 (*ERG4-12xMS2V6::KanMx4*) and RJY5262 (*bfr1Δ::HIS3MX6*, *ERG4-12xMS2V6::KanMx4*) were generated as described (Haim-Vilmovsky and Gerst 2009; Tutucci et al. 2017). *BFR1* gene deletion strains used to express Bfr1p from plasmids were created after transformation of the corresponding plasmids to avoid diploidization as often seen in *bfr1*Δ.

4.4.7. Yeast strains storage at -80°C

For long term storage of yeast, 500 µl of a cell suspension from an overnight culture were mixed in a cryo-tube with 50% (w/v) glycerol to a final concentration of 25% (w/v). Alternatively, some cells were scraped off from the fresh plate and transferred to 15% glycerol tubes. The cells were flash-frozen in liquid nitrogen and stored at - 80°C.

4.4.8. Yeast extract preparation and subcellular fractionation

50 OD_{600} units of logarithmically growing yeast cells were harvested and washed once with ice cold water. For subcellular fractionation into membrane and cytoplasmic fractions, we followed the protocol described in (Syed et al. 2018). In brief, cells were washed two times with cold potassium phosphate buffer (100 mM potassium phosphate pH 7.5, 1.2 M sucrose) and lysed using glass beads (four pulses of 60 seconds with breaks of 60 seconds on ice) in 500 µl low salt lysis buffer 1 (20 mM HEPES/KOH pH 7.5, 140 mM potassium acetate, 1 mM magnesium acetate, 1 mM DTT, 250 mM sucrose, 1x cOmpleteTM, Mini, EDTA-free Protease Inhibitor Cocktail). Cell debris was removed by centrifugation (twice at 800 *x*g for 5 minutes). The resulting whole cell extract (WCE) was diluted to 0.1 µg/µl of protein as determined by the Bradford assay and 200 µl was fractionated at 6,000 *x*g for 5 minutes (M6), 18,000 *x*g for 30 minutes (M18) and supernatant (C). Pellets M6 and M18 were resuspended in 200 µl low-salt lysis buffer 1 and 15 µl were used for SDS-PAGE followed by western

blotting. For RNAse A treatment experiments, after removing cell debris and dilution to 0.2 µg/µl, lysates were divided into two equal parts and one part was treated with RNAse A (100 µg/ml) for 30 minutes at room temperature. The other part was considered as a mock treatment.

4.4.9. Confocal microscopy

In vivo imaging of fluorescent labelled proteins was carried out from inoculation of single colonies into SC or SDC medium containing 2% glucose and overnight growth at 30° C. Logarithmically growing cells were harvested and re-suspended in 100µl of fresh medium. Cells were spread on thin agarose pads containing SC or SDC with 2% glucose and grown for 30 minutes at 30° C before observing in microscope (ZEISS AxioExaminer equipped with a CSU spinning disc confocal unit; Visitron Systems, Germany). Images were acquired with a 63x oil objective using VisiView software (Visitron Systems). Post image processing was performed using Fiji software as described (Syed et al. 2018; Hermesh et al. 2014). For *ERG4* mRNA localization, images were acquired with each containing at least 60 cells. For P-bodies analysis, logarithmically growing cells were harvested, washed once with sterile water before cells were spread on agarose pads containing SDC medium without glucose and grown at 30°C for 30 min to induce P-bodies.

4.4.10. Co-immunoprecipitations of protein and RNA

For protein-mRNA co-precipitations, experiments were performed as described (Syed et al. 2018) with the following changes. 100 OD_{600} units of cells were harvested and resuspended in 8-10 µl/OD_{600} of lysis buffer (10 mM Tris-HCl pH 7.5, 150 mM NaCl, 2 mM EDTA, 0.1% Triton X-100, 1x Protease inhibitor cocktail and 0.5 U/µL Ribolock RNase inhibitor). Glass bead lysis was performed, and cell debris was removed by 5 minutes centrifugation at 5000 *x*g at 4° C. Protein concentrations were measured and

200 µg of lysates were subjected to immunoprecipitation with GFP-Trap_MA magnetic beads (Chromotek) at 4° C for two hours on a rotating wheel. The beads were blocked prior to the immunoprecipitations with blocking buffer (10 mM Tris-HCl pH 7.5, 150 mM NaCl, 2 mM EDTA, 0.1% Triton X-100, 0.1 mg/ml *E.coli* tRNA and 0.4 mg/ml Heparin). Captured beads were washed 3x with 500 µl of wash buffer (10 mM Tris-HCl pH 7.5, 150 mM NaCl, 2 mM EDTA, and 0.1% Triton X-100) and resuspended beads with 125 µl of HPLC grade water (Sigma). 75µl of the bead slurry was used for SDS-PAGE and western blotting. RNA extraction was carried out with the remaining 50 µl of beads, to which 50 ng of spike RNA (*in vitro* transcribed *Arabidopsis* phosphoribulokinase RNA) had been added. For extraction 5 µl of 3 M Sodium acetate pH 5.2, 2.5 µl of 20% SDS and 50 µl of phenol/chloroform/isoamylalcohol (PCI) pH 4.5 (Roth, Germany) was added and the mixed sample centrifuged at maximum speed for 30 min at 4° C. Nucleic acids were precipitated overnight at -80° C with 20 µg of glycogen and 100 µl of 96% ethanol and RNA was resuspended in 20 µl of RNAse free water before continuing with cDNA synthesis and qPCR.

4.4.11. Co-immunoprecipitations of proteins

Co-immunoprecipitations of proteins were performed with Protein G Sepharose® 4 Fast Flow beads (GE Healthcare) or GFP-Trap_MA magnetic beads (Chromotek). 100 OD_{600} units of cells were harvested and resuspended in 8-10 µl/OD_{600} of lysis buffer (10 mM Tris-HCl pH 7.5, 150 mM NaCl, 2 mM EDTA, 0.1% Triton X-100, 1x Protease inhibitor cocktail and 0.5 U/µL Ribolock RNase inhibitor). Glass bead lysis was performed and cell debris was removed by 5 minutes centrifugation at 5000 *x*g at 4° C. Protein concentrations were measured and 200 µg of lysates were subjected to immunoprecipitation with GFP-Trap_MA magnetic beads or Protein G Sepharose® 4 Fast Flow beads at 4° C for two hours on a rotating wheel. The beads were blocked

prior to the immunoprecipitations with blocking buffer (10 mM Tris-HCl pH 7.5, 150 mM NaCl, 2 mM EDTA, 0.1% Triton X-100, 0.1 mg/ml *E. coli* tRNA and 0.4 mg/ml Heparin). For some experiments, prior to the immunoprecipitations RNAse treatment was performed with 100 µg/ml of RNAse A for 30 min at 37° C. Lysates were pre-cleared with the beads overnight 4° C on a rotating wheel. Beads were removed by centrifugation (twice at 1,000 x*g*) and then pre-cleared lysates were supplemented with respective antibody with beads and incubated at 4° C for 4 hours on a rotating wheel. After washing, the beads were resuspended in 1x Laemmli buffer and continued with SDS-PAGE and western blot analysis.

4.4.12. RNA extraction from yeast cells

Total RNA was extracted from 20 OD_{600} units of yeast cells. Glass beads lysis was performed in 500 µl of Cross buffer I (0.3 M NaCl, 10 mM Tris-HCl pH 7.5, 1 mM EDTA, 0.2 % SDS) and 400 µl of phenol:chloroform:isoamylalcohol by four pulses of 120 seconds with interrupts of 60 seconds on ice. After centrifugation for 10 minutes at full speed the upper phase was transferred to a new tube and nucleic acids precipitated with ethanol for 30 min at -20° C. Total RNA pellets were washed and resuspended in 20 µl of HPLC grade water before proceeding to cDNA synthesis and qPCR.

4.4.13. cDNA synthesis (RT-PCR)

Reverse transcription reactions for all the experiments were performed as described in (Syed et al. 2018) with some modifications. In brief, 1 µg of RNA samples were treated with RQ1 DNase (Promega) for 37°C for 30 minutes. 10x RT buffer, 10x Random primers, Reverse Transcriptase enzymes (all from Applied biosystems), 25mM dNTPs were mixed with 10 µl of DNAse treated RNA to the total reaction volume of 20 µl. 1 µl Ribolock was added to the reaction. A ‘minus RT’ reaction was carried

out by adding all the components except the reverse transcriptase. Reaction mixtures were placed in the PCR block.

PCR program:

25°C - 10 min

37°C - 2 h

85°C - 10 min

4°C - ∞

After PCR, cDNA samples were diluted to 1:10 and 1:100 with HPLC water for qRT-PCR analysis. For long term storage samples were stored at -20°C.and reverse transcription reactions performed using the High-Capacity cDNA Reverse Transcription Kit (Applied Biosystems).

4.4.14. Quantitative real time PCR (qRT-PCR)

Quantitative RT-PCR (qRT-PCR) was performed with a StepOnePlus Real-Time PCR System in 10 µl reactions containing 2.5 µl of cDNA samples at 1:25 or 1:50 dilutions. Target specific primers were designed with Primer3 software (Rozen and Skaletsky 2000). The PCR profile included an initial denaturation for 10 min at 95°C, followed by 35 cycles of amplification, comprising denaturation at 95°C for 15 sec and annealing/elongation at 60°C for 1 min. After each cycle, a single fluorescence measurement was taken. All reactions were run in duplicates and included a negative control (-RT). All reactions were performed from a minimum of three biological replicates and two technical replicates of each. Quantification was performed by comparative $\Delta\Delta_{ct}$ method (Livak and Schmittgen 2001; Syed et al. 2018) and values were normalized via the spiked-in RNA or via *ACT1* mRNA signals.

4.4.15. Ribosome affinity purifications (RAP)

Ribosome affinity purification (RAP-IP) to determine mRNAs or tRNAs bound to ribosomes was performed as described in (Hirschmann et al. 2014; and Hirschmann, 2015).

4.4.15.1. Coupling of microbeads to immunoglobulin using carbodiimide

Coupling of 0.75 µm microbeads (Polysciences) to PP-64K unspecific IgG (Millipore) using carbodiimide was performed essentially as prescribed by the manufacturer. Briefly, 12.5 mg of microparticles (or 500 µL) was pipetted into a microcentrifuge tube from a 2.5% w/v suspension solution of the beads. Particles were pelleted at 1,000 x*g* for 10 min, and the supernatant was evacuated. Particles were resuspended in 400 µL of Coupling buffer (50 mM MES pH 5.2,0.05% Proclin-300) and pelleted again as above. Then the particles were resuspended again in 170 µL of Coupling buffer, and a 200mg/mL EDAC (carbodiimide) solution which was prepared just before use by dissolving 5 mg EDAC in 25 µL coupling buffer. 20 µL of the EDAC solution was then added to the particle suspension and followed by brief maximal vortexing. A protein equivalent of 300 µg, e.g. from 30 µL of a 10 mg/mL solution, IgG was added immediately, followed by brief vortexing and incubation on a thermomixer for 1-1.5h at RT and 850 rpm shaking. After incubation, the tube was centrifuged as described above and supernatant of ~ 220 µL was used to determine the coupling efficiency. The remaining pellet was then resuspended in 400 µL of Washing buffer (10 mM Tris pH 8, 0.05% BSA, 0.05% Proclin-300) and used for the RAP experiments.

4.4.15.2. Ribosome-affinity purification followed by IP (RAP-IP)

100 mL of yeast cells were used to perform RAP experiments. One minute prior to harvest, cells were provided with 1mL of 10 mg/mL cycloheximide (CHX) stock added to 100 mL of culture to achieve translational arrest by a concentration of 0.1 mg/mL

CHX. 100 mL of yeast of each strain were harvested at OD_{600} of 0.5 in 50 mL Falcon tubes (Sarstedt) in aliquots of 50 mL and centrifuged for 5 mins at 3,000 rpm. Pellets were resuspended with a total of 10 mL of buffer A (20mM Tris–HCl, 140mM KCl, 2mM $MgCl_2$,1% Triton X-100, 0.2 mg/ml heparin, 0.1 mg/ml CHX) in two aliquots of 5 ml. The aliquots were then pooled in a 14 mL Corex-equivalent plastic tube (Sarstedt) and centrifuged again as described above. After discarding the supernatant, cells were flash-frozen using liquid nitrogen and stored at -80°C. For RAP analysis, cells were thawed on ice and resuspended in 1 mL of buffer B (buffer A plus 0.5mM dithiothreitol (DTT), 1mM phenylmethylsulfonylfluoride (PMSF), 0.5 µg/ml Leupeptin, 0.2 µg/ml Pepstatin, 20 U/ml DNase I, 100 U/ml RiboLock (Fermentas)) in 14 mL plastic tube, and lysed using 1/3 vol. of 0.4 µm glass beads (Roth) by four cycles of (20s vortex at max speed – 90s cooling on ice) each. Then, crude extracts were transferred to microcentrifuge tubes and cleared by three subsequent centrifugation steps at 2,600 – 8,600 – 13,500 *xg* at 4°C. Supernatants following the last centrifugation were brought to 1 mL with buffer B. The subsequent steps were performed in a cold room at 4°C. Four aliquots of IgG-coupled microbeads were used for each experiment. First, beads were blocked in 1 mL blocking buffer (buffer A supplemented with 0.4 mg/ml heparin, 0.1 mg/ml *Escherichia coli* tRNA , and 1% BSA) for each aliquot, and shaken at 850 rpm and RT for 10 mins and collected by centrifuging for 10 mins at 1,000 *xg*. Then, the beads are washed once using 500µL of buffer A per aliquot (10 mins, 850 rpm, RT). Prior to centrifugation (10 mins at 1,000 *xg*, RT) the four aliquots were pooled in a 2mL microcentrifuge tube. During centrifugation, a thermomixer was pre-incubated to 4°C in the cold room. 250 µL of lysate was secured and stored at -80°C and later used as a lysate control. The remaining 750 µL of lysate was batch-incubated with the pelleted beads for 2h at 4°C and 850 rpm in the cold room. Following batch incubation,

the beads were collected for 2 mins at 3,000 *xg*, 4°C. Then the beads were washed four times with 1.5 mL buffer C (20mM Tris–HCl [pH 8.0], 140mM KCl, 2mM $MgCl_2$, 5% glycerol, 0.5mM DTT, 40 U/ml RiboLock (Fermentas)) by shaking at 750 rpm and 4°C for 15 mins. Before the last washing step, the microcentrifuge tube was replaced with a fresh one to prevent nonspecific aggregation to tube walls. Beads were then resuspended in 207 µL of buffer C and Proteinase K (Thermo Fisher), and incubated for 40 minutes at 50°C. Following the cleavage, beads were pelleted for 5 mins at 13,400 *xg* and 4°C. The eluted beads were secured and stored at - 80°C and later used for RNA extractions

The RNA extraction was performed using phenol:chloroform (5:1) before re-extraction of the aqueous phase with chloroform and precipitation in ethanol overnight at -20°C. For the quantification of mRNAs bound to the ribosomes, qRT-PCR was performed, and the enrichment of mRNAs determined using the $\Delta\Delta_{CT}$ method. An enrichment of mRNAs from TAP purification (in wild-type and *bfr1*Δ) was considered only if at least two-fold greater than from mock purification (strains without TAP tags). The % ribosomal occupancy of *bfr1*Δ was then plotted against wild type.

4.4.16. Polysome profiling

Separation of mono- and polysomes was done as described in (Mittal et al. 2017) and performed with three biological replicates of wildtype, *bfr1*Δ and *bfr1mut6A* strains. Logarithmically growing cells were treated with 100µg/ml cycloheximide (CHX) for 1 minute, harvested by vacuum filtration and flash frozen with liquid nitrogen. Cells lysis was performed under cryogenic conditions using lysis buffer (20 mM Tris-HCl, pH 7.5, 100 mM NaCl, 10 mM $MgCl_2$, 1% Triton X-100, 0.5 mM DDT and 100 µg/ml of CHX) and a bead mill (Spex Inc., Metuchen, NJ, USA). Cell debris was removed by centrifugation for 3 min at 3,000 *x*g and 4 °C followed by 10,000 *x*g for 5 minutes at 4

°C. To separate monosomes and polysomes, 10 A_{260} units of lysates were loaded on pre-cooled 12 ml of 7% - 47% linear sucrose gradients (50 mM Tris-HCl, pH 7.5, 50 mM NH_4Cl, 12 mM $MgCl_2$, 0.5 mM DTT, and 100 µg/ml CHX) and centrifuged at 35,000 rpm for 3 hours at 4° C in a TH-641 rotor (Thermo Scientific) before collecting the monosome and polysome peaks. RNA was isolated by adding 5µl of glycogen and phenol:chloroform (5:1) before re-extraction of the aqueous phase with chloroform and precipitation in ethanol overnight at -20°C. RNA pellets were resuspended in 30 µl of HPLC grade water and processed for cDNA synthesis and qRT-PCR.

4.4.17. Brefeldin A sensitivity drop assay

A single colony of yeast cells was inoculated in 10 mL of YEPD or drop out medium and grown at 30°C overnight before diluting it into fresh medium of 20 mL in flask to grow until logarithmic phase. Cells were harvested by centrifugation at 2500 rpm, and room temperature. After that cells were washed once with sterile water. 1 OD_{600} units of cells was used for serial dilution and 3 µl of dilutions were plated on SDC-leu medium with or without 50 µg/ml brefeldin A. Cells were grown for 72 hrs at 30°C.

4.4.18. Proteasomes inhibition by MG132

To block the proteasomes, we have used commercially available proteasome inhibitor MG132 as described in Liu et al. (2007). Briefly, cells from a single colony was inoculated overnight in a synthetic medium containing 0.17% yeast nitrogenous base without ammonium sulfate and supplemented with 0.1% proline, appropriate amino acids, and 2% glucose as the carbon source. Cultures were reinoculated in 30 mL fresh media with 0.003% of SDS for 3 h at 30°C. Then 75 µM MG132 dissolved in DMSO or DMSO alone as a control was added to the cultures and grown for 30 min at 30°C before adding 100 µg/mL of CHX to the cultures to stop the translation. Cells

were harvested at 0, 30, and 60 min and processed for cell lysis and western blot to analyse the protein levels.

5. References

Abdelmohsen K, Gorospe M. 2012. RNA-binding protein nucleolin in disease. *RNA Biol* **9**: 799–808.

Ann L Coker, Woalder. 2017. Cell-Free Formation of RNA Granules: Low Complexity Sequence Domains Form Dynamic Fibers Within Hydrogels. *Physiol Behav* **176**: 139–148.

Ast T, Cohen G, Schuldiner M. 2013. A network of cytosolic factors targets SRP-independent proteins to the endoplasmic reticulum. *Cell* **152**: 1134–1145. http://dx.doi.org/10.1016/j.cell.2013.02.003.

Ast T, Schuldiner M. 2013. All roads lead to Rome (but some may be harder to travel): SRP-independent translocation into the endoplasmic reticulum. *Crit Rev Biochem Mol Biol* **48**: 273–288.

Aviram N, Ast T, Costa EA, Arakel EC, Chuartzman SG, Jan CH, Haßdenteufel S, Dudek J, Jung M, Schorr S, et al. 2016. The SND proteins constitute an alternative targeting route to the endoplasmic reticulum. *Nature* **540**: 134–138. http://dx.doi.org/10.1038/nature20169.

Balaji T. 2014. The role of the budding yeast RNA-binding proteins Khd1p and Loc1p in mRNA targeting. *Doctoral dissertation*. *Eberhard Karls Universität Tübingen*.

Baldridge RD, Rapoport TA. 2016. Autoubiquitination of the Hrd1 Ligase Triggers Protein Retrotranslocation in ERAD. *Cell* **166**: 394–407. http://dx.doi.org/10.1016/j.cell.2016.05.048.

Bays NW, Gardner RG, Seelig LP, Joazeiro CA, Hampton RY. 2001. Hrd1p/Der3p is a membrane-anchored ubiquitin ligase required for ER-associated degradation. *Nat Cell Biol* **3**: 24–29.

Bhamidipati A, Denic V, Quan EM, Weissman JS. 2005. Exploration of the topological requirements of ERAD identifies Yos9p as a lectin sensor of misfolded glycoproteins in the ER lumen. *Mol Cell* **19**: 741–751.

Bordallo J, Plemper RK, Finger A, Wolf DH. 1998. Der3p/Hrd1p is required for endoplasmic reticulum-associated degradation of misfolded lumenal and integral membrane proteins. *Mol Biol Cell* **9**: 209–222.

Braakman I, Hebert DN. 2013. Protein folding in the endoplasmic reticulum. *Cold Spring Harb Perspect Biol* **5**.

Brodsky JL, Schekman R. 1993. A Sec63p-BiP complex from yeast is required for protein translocation in a reconstituted proteoliposome. *J Cell Biol* **123**: 1355–1363.

Bryksin A V., Matsumura I. 2010. Overlap extension PCR cloning: A simple and

reliable way to create recombinant plasmids. *Biotechniques* **48**: 463–465.

Butter F, Scheibe M, Mörl M, Mann M. 2009. Unbiased RNA-protein interaction screen by quantitative proteomics. *Proc Natl Acad Sci U S A* **106**: 10626–10631.

Caetano-Anollés G, Hee SK, Mittenthal JE. 2007. The origin of modern metabolic networks inferred from phylogenomic analysis of protein architecture. *Proc Natl Acad Sci U S A* **104**: 9358–9363.

Carvalho P, Goder V, Rapoport TA. 2006. Distinct Ubiquitin-Ligase Complexes Define Convergent Pathways for the Degradation of ER Proteins. *Cell* **126**: 361–373.

Chaytow H, Huang YT, Gillingwater TH, Faller KME. 2018. The role of survival motor neuron protein (SMN) in protein homeostasis. *Cell Mol Life Sci* **75**: 3877–3894. https://doi.org/10.1007/s00018-018-2849-1.

Chen DC, Yang BC, Kuo TT. 1992. One-step transformation of yeast in stationary phase. *Curr Genet* **21**: 83–84.

Cheng MHK. 2018. An Investigation of the role of the S . cerevisiae RNA- binding protein Scp160p / vigilin in the aggregation of Q / N-rich proteins. *Doctoral dissertation. Eberhard Karls Universität Tübingen.*

Cheng MHK, Jansen RP. 2017. A jack of all trades: the RNA-binding protein vigilin. *Wiley Interdiscip Rev RNA* **8**: 1–15.

Christianson JC, Olzmann JA, Shaler TA, Sowa ME, Bennett EJ, Richter CM, Tyler RE, Greenblatt EJ, Wade Harper J, Kopito RR. 2012. Defining human ERAD networks through an integrative mapping strategy. *Nat Cell Biol* **14**: 93–105.

Clapham DE. 2007. Calcium Signaling. *Cell* **131**: 1047–1058.

Cox JS, Walter P. 1996. Cell-Free Formation of RNA Granules: Low Complexity Sequence Domains Form Dynamic Fibers Within Hydrogels. **87**: 1–14. papers3://publication/uuid/1C5E757F-7771-4F4A-BECB-43A63139AB55.

Craig Venter J, Adams MD, Myers EW, Li PW, Mural RJ, Sutton GG, Smith HO, Yandell M, Evans CA, Holt RA, et al. 2001. The sequence of the human genome. *Science (80-)* **291**: 1304–1351.

De Boulle K, Verkerk AJMH, Reyniers E, Vits L, Hendrickx J, Van Roy B, Van Den Bos F, de Graaff E, Oostra BA, Willems PJ. 1993. A point mutation in the FMR-1 gene associated with fragile X mental retardation. *Nat Genet* **3**: 31–35.

Deng M, Hochstrasser M. 2006. Spatially regulated ubiquitin ligation by an ER/nuclear membrane ligase. *Nature* **443**: 827–831. doi:10.1038/nature05170.

Denic V, Quan EM, Weissman JS. 2006. A Luminal Surveillance Complex that Selects Misfolded Glycoproteins for ER-Associated Degradation. *Cell* **126**: 349–359.

Deshaies RJ, Schekman R. 1987. A yeast mutant defective at an early stage in import of secretory protein precursors into the endoplasmic reticulum. *J Cell Biol* **105**: 633–645.

Deshaies RJ, Schekman R. 1989. SEC62 encodes a putative membrane protein required for protein translocation into the yeast endoplasmic reticulum. *J Cell Biol* **109**: 2653–2664.

DONG L, LÜ L-B, LAI R. 2013. Molecular cloning of Tupaia belangeri chinensis neuropeptide Y and homology comparison with other analogues from primates. *Zool Res* **33**: 75–78. http://pub.chinasciencejournal.com/article/getArticleRedirect.action?doiCode=10.3724/SP.J.1141.2012.01075.

Dreyfuss G, Kim VN, Kataoka N. 2002. Messenger-RNA-binding proteins and the messages they carry. *Nat Rev Mol Cell Biol* **3**: 195–205. http://www.nature.com/articles/nrm760.

Eichler J, Moll R. 2001. The signal recognition particle of Archaea. *Trends Microbiol* **9**: 130–136.

English AR, Voeltz GK. 2013. Endoplasmic reticulum structure and interconnections with other organelles. *Cold Spring Harb Perspect Biol* **5**: 1–16.

Fagone P, Jackowski S. 2009. Membrane phospholipid synthesis and endoplasmic reticulum function. *J Lipid Res* **50**: 311–316.

Favaloro V, Spasic M, Schwappach B, Dobberstein B. 2008. Distinct targeting pathways for the membrane insertion of tail-anchored (TA) proteins. *J Cell Sci* **121**: 1832–1840.

Feng Y, Absher D, Eberhart DE, Brown V, Malter HE, Warren ST. 1997. FMRP associates with polyribosomes as an mRNP, and the I304N mutation of severe fragile X syndrome abolishes this association. *Mol Cell* **1**: 109–118.

Fundakowski J, Hermesh O, Jansen RP. 2012. Localization of a subset of yeast mRNAs depends on inheritance of endoplasmic reticulum. *Traffic* **13**: 1642–1652.

Garí E, Volpe T, Wang H, Gallego C, Futcher B, Aldea M. 2001. Whi3 binds the mRNA of the G1 cyclin CLN3 to modulate cell fate in budding yeast. *Genes Dev* **15**: 2803–2808.

Görlich D, Hartmann E, Prehn S, Rapoport TA. 1992. A protein of the endoplasmic reticulum involved early in polypeptide translocation. *Nature* **357**: 47–52.

Graham TR, Scott PA, Emr SD. 1993. Brefeldin A reversibly blocks early but not late protein transport steps in the yeast secretory pathway. *EMBO J* **12**: 869–877.

Guo Y, Sirkis DW, Schekman R. 2014. Protein Sorting at the trans -Golgi Network .

Annu Rev Cell Dev Biol **30**: 169–206.

Habeck G, Ebner FA, Shimada-Kreft H, Kreft SG. 2015. The yeast ERAD-C ubiquitin ligase Doa10 recognizes an intramembrane degron. *J Cell Biol* **209**: 261–273.

Hafner M, Landthaler M, Burger L, Khorshid M, Hausser J, Berninger P, Rothballer A, Ascano M, Jungkamp AC, Munschauer M, et al. 2010. PAR-CliP - A method to identify transcriptome-wide the binding sites of RNA binding proteins. *J Vis Exp* 2–6.

Hampton RY. 2002. ER-associated degradation in protein quality control and cellular regulation. *Curr Opin Cell Biol* **14**: 476–482.

Han TW, Kato M, Xie S, Wu LC, Mirzaei H, Pei J, Chen M, Xie Y, Allen J, Xiao G, et al. 2012. Cell-free formation of RNA granules: Bound RNAs identify features and components of cellular assemblies. *Cell* **149**: 768–779. http://dx.doi.org/10.1016/j.cell.2012.04.016.

Hann BC, Walter P. 1991. The signal recognition particle in S. cerevisiae. *Cell* **67**: 131–144.

Hebert DN, Garman SC, Molinari M. 2005. The glycan code of the endoplasmic reticulum: Asparagine-linked carbohydrates as protein maturation and quality-control tags. *Trends Cell Biol* **15**: 364–370.

Hennig S, Kong G, Mannen T, Sadowska A, Kobelke S, Blythe A, Knott GJ, Iyer SS, Ho D, Newcombe EA, et al. 2015. Prion-like domains in RNA binding proteins are essential for building subnuclear paraspeckles. *J Cell Biol* **210**: 529–539.

Hentze MW. 1994. Enzymes as RNA-binding proteins: a role for (di)nucleotide-binding domains? *Trends Biochem Sci* **19**: 101–103.

Hermesh O, Genz C, Yofe I, Sinzel M, Rapaport D, Schuldiner M, Jansen RP. 2014. Yeast phospholipid biosynthesis is linked to mRNA localization. *J Cell Sci* **127**: 3373–3381.

Hetz C, Chevet E, Harding HP. 2013. Targeting the unfolded protein response in disease. *Nat Rev Drug Discov* **12**: 703–719. http://dx.doi.org/10.1038/nrd3976.

Hetz C, Papa FR. 2018. The Unfolded Protein Response and Cell Fate Control. *Mol Cell* **69**: 169–181. https://doi.org/10.1016/j.molcel.2017.06.017.

Hirschmann WD. 2015. Novel Protein and Coding Determinants of Protein Biosynthesis Speed and Accuracy. *Doctoral dissertation. Eberhard Karls Univ Tübingen*.

Hirschmann WD, Westendorf H, Mayer A, Cannarozzi G, Cramer P, Jansen RP. 2014. Scp160p is required for translational efficiency of codon-optimized mRNAs in yeast. *Nucleic Acids Res* **42**: 4043–4055.

Hoffman AM, Chen Q, Zheng T, Nicchitta C V. 2019. Heterogeneous translational

landscape of the endoplasmic reticulum revealed by ribosome proximity labeling and transcriptome analysis. *J Biol Chem* **294**: 8942–8958.

Hogan DJ, Riordan DP, Gerber AP, Herschlag D, Brown PO. 2008. Diverse RNA-binding proteins interact with functionally related sets of RNAs, suggesting an extensive regulatory system. *PLoS Biol* **6**: 2297–2313.

Hu J, Li J, Qian X, Denic V, Sha B. 2009. The Crystal Structures of Yeast Get3 Suggest a Mechanism for Tail-Anchored Protein Membrane Insertion. *PLoS One* **4**: 1–7.

Huyer G, Piluek WF, Fansler Z, Kreft SG, Hochstrasser M, Brodsky JL, Michaelis S. 2004. Distinct machinery is required in Saccharomyces cerevisiae for the endoplasmic reticulum-associated degradation of a multispanning membrane protein and a soluble luminal protein. *J Biol Chem* **279**: 38369–38378.

Jackson CL, Kepes F. 1994. BFR1, a multicopy suppressor of brefeldin A-induced lethality, is implicated in secretion and nuclear segregation in Saccharomyces cerevisiae. *Genetics* **137**: 423–437.

Jan CH, Williams CC, Weissman JS. 2014. Principles of ER cotranslational translocation revealed by proximity-specific ribosome profiling. *Science (80-)* **346**: 1257521–1257521. http://www.sciencemag.org/cgi/doi/10.1126/science.1257521.

Janke C, Magiera MM, Rathfelder N, Taxis C, Reber S, Maekawa H, Moreno-Borchart A, Doenges G, Schwob E, Schiebel E, et al. 2004. A versatile toolbox for PCR-based tagging of yeast genes: New fluorescent proteins, more markers and promoter substitution cassettes. *Yeast* **21**: 947–962.

Joan Castells-Ballester, Natalie Rinis, Ilgin Kotan, Lihi Gal, Daniela Bausewein, Ilia Kats, Ewa Zatorska, Günter Kramer, Bernd Bukau, Maya Schuldiner SS. 2019. Translational regulation of Pmt1 and Pmt2 by Bfr1 affects unfolded protein O-mannosylation. *bioRxiv* **1**: 1–51. https://doi.org/10.1101/847095.

Keenan RJ, Freymann DM, Stroud RM, Walter P. 2001. The Signal Recognition Particle. *Annu Rev Biochem* **70**: 755–775. http://www.annualreviews.org/doi/10.1146/annurev.biochem.70.1.755.

Kim W, Spear ED, Ng DTW. 2005. Yos9p detects and targets misfolded glycoproteins for ER-associated degradation. *Mol Cell* **19**: 753–764.

Knop M, Siegers K, Pereira G, Zachariae W, Winsor B, Nasmyth K, Schiebel E. 1999. Epitope tagging of yeast genes using a PCR-based strategy: More tags and improved practical routines. *Yeast* **15**: 963–972.

Kramer K, Sachsenberg T, Beckmann BM, Qamar S, Boon KL, Hentze MW, Kohlbacher O, Urlaub H. 2014. Photo-cross-linking and high-resolution mass spectrometry for assignment of RNA-binding sites in RNA-binding proteins. *Nat*

Methods **11**: 1064–1070.

Lang BD. 2000. Scp160p, a multiple KH-domain protein, is a component of mRNP complexes in yeast. *Nucleic Acids Res* **28**: 1576–1584.

Lang BD. 2001. The brefeldin A resistance protein Bfr1p is a component of polyribosome-associated mRNP complexes in yeast. *Nucleic Acids Res* **29**: 2567–2574.

Lapointe CP, Wilinski D, Saunders HAJ, Wickens M. 2015. Protein-RNA networks revealed through covalent RNA marks. *Nat Methods* **12**: 1163–1170.

Lewis HA, Musunuru K, Jensen KB, Edo C, Chen H, Darnell RB, Burley SK. 2000. Sequence-specific RNA binding by a Nova KH domain: Implications for paraneoplastic disease and the fragile X syndrome. *Cell* **100**: 323–332.

Liao Y, Castello A, Fischer B, Leicht S, Föehr S, Frese CK, Ragan C, Kurscheid S, Pagler E, Yang H, et al. 2016. The Cardiomyocyte RNA-Binding Proteome: Links to Intermediary Metabolism and Heart Disease. *Cell Rep* **16**: 1456–1469.

Liu C, Apodaca J, Davis LE, Rao H. 2007. Proteasome inhibition in wild-type yeast Saccharomyces cerevisiae cells. *Biotechniques* **42**: 158–162.

Liu Q, Fischer U, Wang F, Dreyfuss G. 1997. The spinal muscular atrophy disease gene product, SMN, and its associated protein SIP1 are in a complex with spliceosomal snRNP proteins. *Cell* **90**: 1013–1021.

Liu Y, Chang A. 2008. Heat shock response relieves ER stress. *EMBO J* **27**: 1049–1059.

Livak KJ, Schmittgen TD. 2001. Analysis of relative gene expression data using real-time quantitative PCR and the 2-ΔΔCT method. *Methods* **25**: 402–408.

Loewen CJR, Young BP, Tavassoli S, Levine TP. 2007. Inheritance of cortical ER in yeast is required for normal septin organization. *J Cell Biol* **179**: 467–483.

Low YS, Bircham PW, Maass DR, Atkinson PH. 2014. Kinetochore genes are required to fully activate secretory pathway expansion in S. cerevisiae under induced ER stress. *Mol Biosyst* **10**: 1790–1802.

Lu D, Searles MA, Klug A. 2003. Crystal structure of a zinc-finger-RNA complex reveals two modes of molecular recognition. *Nature* **426**: 96–100.

Lunde BM, Moore C, Varani G. 2007. RNA-binding proteins: Modular design for efficient function. *Nat Rev Mol Cell Biol* **8**: 479–490.

Mitchell SF, Jain S, She M, Parker R. 2013. Global analysis of yeast mRNPs. *Nat Struct Mol Biol* **20**: 127–133. https://doi.org/10.1038/nsmb.2468.

Moore KS, von Lindern M. 2018. RNA binding proteins and regulation of mRNA translation in erythropoiesis. *Front Physiol* **9**: 1–17.

Morl K, Ma W, Gething MJ, Sambrook J. 1993. A transmembrane protein with a cdc2+ CDC28-related kinase activity is required for signaling from the ER to the nucleus. *Cell* **74**: 743–756.

Murakami T, Qamar S, Lin JQ, Schierle GSK, Rees E, Miyashita A, Costa AR, Dodd RB, Chan FTS, Michel CH, et al. 2015. ALS/FTD Mutation-Induced Phase Transition of FUS Liquid Droplets and Reversible Hydrogels into Irreversible Hydrogels Impairs RNP Granule Function. *Neuron* **88**: 678–690.

Nakatsukasa K, Huyer G, Michaelis S, Brodsky JL. 2008. Dissecting the ER-Associated Degradation of a Misfolded Polytopic Membrane Protein. *Cell* **132**: 101–112. 10.1016/j.cell.2007.11.023.

Niaki AG, Sarkar J, Cai X, Rhine K, Vidaurre V, Guy B, Hurst M, Lee JC, Koh HR, Guo L, et al. 2019. Loss of Dynamic RNA Interaction and Aberrant Phase Separation Induced by Two Distinct Types of ALS/FTD-Linked FUS Mutations. *Mol Cell*. http://www.sciencedirect.com/science/article/pii/S1097276519307270.

Oubridge C, Ito N, Evans PR, Teo C-H, Nagai K. 1994. Crystal structure at 1.92 Å resolution of the RNA-binding domain of the U1A spliceosomal protein complexed with an RNA hairpin. *Nature* **372**: 432–438. http://www.nature.com/articles/372432a0.

Paget-Bailly P, Meznad K, Bruyère D, Perrard J, Herfs M, Jung AC, Mougin C, Prétet JL, Baguet A. 2019. Comparative RNA sequencing reveals that HPV16 E6 abrogates the effect of E6*I on ROS metabolism. *Sci Rep* **9**: 5938.

Parker R, Sheth U. 2007. P Bodies and the Control of mRNA Translation and Degradation. *Mol Cell* **25**: 635–646.

Pickart CM. 2001. Mechanisms Underlying Ubiquitination. *Annu Rev Biochem* **70**: 503–533. http://www.annualreviews.org/doi/10.1146/annurev.biochem.70.1.503.

Plath K, Rapoport TA. 2000. Spontaneous release of cytosolic proteins from posttranslational substrates before their transport into the endoplasmic reticulum. *J Cell Biol* **151**: 167–178.

Plemper RK, Böhmler S, Bordallo J, Sommer T, Wolf DH. 1997. Mutant analysis links the translocon and BIP to retrograde protein transport for ER degradation. *Nature* **388**: 891–895.

Rapoport TA. 2007. Protein translocation across the eukaryotic endoplasmic reticulum and bacterial plasma membranes. *Nature* **450**: 663–669.

Reithinger J. 2013. *Membrane Protein Biogenesis in Saccharomyces cerevisiae*. http://www.diva-portal.org/smash/record.jsf?pid=diva2:661735.

Reithinger JH, Kim JEH, Kim H. 2013. Sec62 Protein mediates membrane insertion and orientation of moderately hydrophobic signal anchor proteins in the endoplasmic reticulum (ER). *J Biol Chem* **288**: 18058–18067.

Robert X, Gouet P. 2014. Deciphering key features in protein structures with the new ENDscript server. *Nucleic Acids Res* **42**: 320–324.

Rossmann MG, Moras D, Olsen KW. 1974. Chemical and biological evolution of a nucleotide-binding protein. *Nature* **250**: 194–199.

Rothblatt JA, Deshaies RJ, Sanders SL, Daum G, Schekman R. 1989. Multiple genes are required for proper insertion of secretory proteins into the endoplasmic reticulum in yeast. *J Cell Biol* **109**: 2641–2652.

Ruggiano A, Foresti O, Carvalho P. 2014. ER-associated degradation : Protein quality control and beyond. **204**: 869–879.

Ryter JM, Schultz SC. 1998. Molecular basis of double-stranded RNA-protein interactions: Structure of a dsRNA-binding domain complexed with dsRNA. *EMBO J* **17**: 7505–7513.

Sadler I, Chiang A, Kurihara T, Rothblatt J, Way J, Silver P. 1989. A yeast gene important for protein assembly into the endoplasmic reticulum and the nucleus has homology to DnaJ, an Escherichia coli heat shock protein. *J Cell Biol* **109**: 2665–2675.

Scherrer T, Mittal N, Janga SC, Gerber AP. 2010. A screen for RNA-binding proteins in yeast indicates dual functions for many enzymes. *PLoS One* **5**.

Schiestl RH, Gietz RD. 1989. High efficiency transformation of intact yeast cells using single stranded nucleic acids as a carrier. *Curr Genet* **16**: 339–346.

Schladebeck S, Mösch HU. 2013. The RNA-binding protein Whi3 Is a key regulator of developmental signaling and ploidy in Saccharomyces cerevisiae. *Genetics* **195**: 73–86.

Schmid M, Jaedicke A, Du TG, Jansen RP. 2006. Coordination of Endoplasmic Reticulum and mRNA Localization to the Yeast Bud. *Curr Biol* **16**: 1538–1543.

Schmidt HB, Barreau A, Rohatgi R. 2019. Phase separation-deficient TDP43 remains functional in splicing. *Nat Commun* **10**: 1–14. http://dx.doi.org/10.1038/s41467-019-12740-2.

Schramm C. 2000. The Bbp1p-Mps2p complex connects the SPB to the nuclear envelope and is essential for SPB duplication. *EMBO J* **19**: 421–433.

Schuldiner M, Metz J, Schmid V, Denic V, Rakwalska M, Schmitt HD, Schwappach B, Weissman JS. 2008. The GET Complex Mediates Insertion of Tail-Anchored Proteins into the ER Membrane. *Cell* **134**: 634–645. http://dx.doi.org/10.1016/j.cell.2008.06.025.

Sezen B, Seedorf M, Schiebel E. 2009. The SESA network links duplication of the yeast centrosome with the protein translation machinery. *Genes Dev* **23**: 1559–1570.

Shorter J. 2019. Phase separation of RNA-binding proteins in physiology and disease: An introduction to the JBC Reviews thematic series. *J Biol Chem* **294**: 7113–7114.

Simpson CE, Lui J, Kershaw CJ, Sims PFG, Ashe MP. 2014. mRNA localization to P-bodies in yeast is bi-phasic with many mRNAs captured in a late Bfr1p-dependent wave. *J Cell Sci* **127**: 1254–1262.

Stefanovic S, Hegde RS. 2007. Identification of a Targeting Factor for Posttranslational Membrane Protein Insertion into the ER. *Cell* **128**: 1147–1159.

Swanson R, Locher M, Hochstrasser M. 2001. degradation signal. Doa10 functions with two E2s, Ubc6 and Ubc7, to ubiquitinate. *Genes Dev* **2**: 2660–2674.

Syed MI, Moorthy BT, Jenner A, Fetka I, Jansen RP. 2018. Signal sequence-independent targeting of MID2 mRNA to the endoplasmic reticulum by the yeast RNA-binding protein Khd1p. *FEBS Lett* **592**: 1870–1881.

Szathmary R, Bielmann R, Nita-Lazar M, Burda P, Jakob CA. 2005. Yos9 protein is essential for degradation of misfolded glycoproteins and may function as lectin in ERAD. *Mol Cell* **19**: 765–775.

Tabara K, Iwata Y, Koizumi N. 2018. The Unfolded Protein Response. In *Methods in Molecular Biology*, Vol. 1691 of, pp. 223–230 http://link.springer.com/10.1007/978-1-4939-7389-7_17.

Taxis C, Hitt R, Park SH, Deak PM, Kostova Z, Wolf DH. 2003. Use of modular substrates demonstrates mechanistic diversity and reveals differences in chaperone requirement of ERAD. *J Biol Chem* **278**: 35903–35913.

Topisirovic I, Siddiqui N, Lapointe VL, Trost M, Thibault P, Bangeranye C, Pĭol-Roma S, Borden KLB. 2009. Molecular dissection of the eukaryotic initiation factor 4E (eIF4E) export-competent RNP. *EMBO J* **28**: 1087–1098.

Travers KJ, Patil CK, Wodicka L, Lockhart DJ, Weissman JS, Walter P. 2000. Functional and genomic analyses reveal an essential coordination between the unfolded protein response and ER-associated degradation. *Cell* **101**: 249–258.

Tutucci E, Vera M, Biswas J, Garcia J, Parker R, Singer RH. 2018. An improved MS2 system for accurate reporting of the mRNA life cycle. *Nat Methods* **15**: 81–89. https://www.ncbi.nlm.nih.gov/pmc/articles/PMC5843578/pdf/nihms913718.pdf.

Valverde R, Edwards L, Regan L. 2008. Structure and function of KH domains. *FEBS J* **275**: 2712–2726.

Van Puyenbroeck V, Vermeire K. 2018. Inhibitors of protein translocation across membranes of the secretory pathway: novel antimicrobial and anticancer agents. *Cell Mol Life Sci* **75**: 1541–1558. https://doi.org/10.1007/s00018-017-2743-2.

Vashist S, Ng DTW. 2004. Misfolded proteins are sorted by a sequential checkpoint mechanism of ER quality control. *J Cell Biol* **165**: 41–52.

Vogel JP, Lee JN, Kirsch DR, Rose MD, Sztul ES. 1993. Brefeldin a causes a defect in secretion in Saccharomyces cerevisiae. *J Biol Chem* **268**: 3040–3043.

Walter P, Ibrahimi I, Blobel G. 1981. Translocation of proteins across the endoplasmic reticulum. I. Signal recognition protein (SRP) binds to in-vitro-assembled polysomes synthesizing secretory protein. *J Cell Biol* **91**: 545–550.

Wang C, Schmich F, Srivatsa S, Weidner J, Beerenwinkel N, Spang A. 2018. Context-dependent deposition and regulation of mRNAs in P-bodies. *Elife* **7**: 1–25. https://elifesciences.org/articles/41300.

Waters MG, Blobel G. 1986. Secretory protein translocation in a yeast cell-free system can occur posttranslationally and requires ATP hydrolysis. *J Cell Biol* **102**: 1543–1550.

Weber V, Wernitznig A, Hager G, Harata M, Frank P, Wintersberger U. 1997. Purification and nucleic-acid-binding properties of a Saccharomyces cerevisiae protein involved in the control of ploidy. *Eur J Biochem* **249**: 309–317.

Weidner J, Wang C, Prescianotto-Baschong C, Estrada AF, Spang A. 2014. The polysome-associated proteins Scp160 and Bfr1 prevent P body formation under normal growth conditions. *J Cell Sci* **127**: 1992–2004.

Wild K, Rosendal KR, Sinning I. 2004. A structural step into the SRP cycle. *Mol Microbiol* **53**: 357–363.

Wintersberger U, Kühne C, Karwan A. 1995. Scp160p, a new yeast protein associated with the nuclear membrane and the endoplasmic reticulum, is necessary for maintenance of exact ploidy. *Yeast* **11**: 929–944.

Woolford CA, Daniels LB, Park FJ, Jones EW, Van Arsdell JN, Innis MA. 1986. The PEP4 gene encodes an aspartyl protease implicated in the posttranslational regulation of Saccharomyces cerevisiae vacuolar hydrolases. *Mol Cell Biol* **6**: 2500–2510.

Wu H, Ng BSH, Thibault G. 2014. Endoplasmic reticulum stress response in yeast and humans. *Biosci Rep* **34**: 321–330.

Xiao Y, Chen J, Wan Y, Gao Q, Jing N, Zheng Y, Zhu X. 2019. Regulation of zebrafish dorsoventral patterning by phase separation of RNA-binding protein Rbm14. *Cell Discov* **5**. http://dx.doi.org/10.1038/s41421-019-0106-x.

Xue Z, Shan X, Sinelnikov A, Mélèse T. 1996. Yeast mutants that produce a novel type of ascus containing asci instead of spores. *Genetics* **144**: 979–989.

Yang F, Wilkinson T. 2015. Enhancing viewing angle of computer generated hologram by Multi-channel technology. *Adapt Opt Anal Methods Syst AO 2015*

289.

Zhang T, Xu Y, Liu Y, Ye Y. 2015. Gp78 functions downstream of Hrd1 to promote degradation of misfolded proteins of the endoplasmic reticulum. *Mol Biol Cell* **26**: 4438–4450.

Zhao X, Fay J, Lambkin H, Schwartz S. 2007. Identification of a 17-nucleotide splicing enhancer in HPV-16 L1 that counteracts the effect of multiple hnRNP A1-binding splicing silencers. *Virology* **369**: 351–363.

Zimmermann R, Eyrisch S, Ahmad M, Helms V. 2011. Protein translocation across the ER membrane. *Biochim Biophys Acta - Biomembr* **1808**: 912–924. http://dx.doi.org/10.1016/j.bbamem.2010.06.015.

Zweytick D, Hrastnik C, Kohlwein SD, Daum G. 2000. Biochemical characterization and subcellular localization of the sterol C-24(28) reductase, Erg4p, from the yeast Saccharomyces cerevisiae. *FEBS Lett* **470**: 83–87.

6. Publication

Most part of this thesis published as a research article in *RNA* journal.

1. **Manchalu, S.**, Mittal, N., Spang, A. & Jansen, R. P. (2019). Local translation of yeast *ERG4* mRNA at the endoplasmic reticulum requires the brefeldin A resistance protein Bfr1. *RNA* 25, 1661–1672. doi:10.1261/rna.072017.119

7. Acknowledgements

First and foremost, I would like to express my deep sense of gratitude to my supervisor Prof. Dr. Ralf-Peter Jansen for giving me the opportunity to carry out my doctoral research work in his lab. I am thankful to him for his continuous motivation, encouragement and mentorship, and for always supporting me, both professionally and personally.

A special thanks to my second supervisor Prof. Dr. Doron Rapaport for his helpful suggestions and inputs during my TAC meetings, for reviewing my thesis and for his valuable time and efforts.

I would also like to thank Prof. Dr. Dirk Schwarzer and Prof. Dr. Thorsten Stafforst for agreeing to be part of my Ph.D. examination committee and for their valuable time.

I am thankful to Dr. Nitish Mittal and Prof. Dr. Anne Spang for their successful collaboration and contributions to this work.

I am grateful to the present members of Jansen group- Dr. Birgit Singer-Krüger, Dr. Orit Hermesh-Rau, Jonathan Feicht, Lisa Heinold, Saira Akram, and the previous members- Dr. Joyita Mukherjee, Dr. Muhammad Ibrahim Syed, Nidhi Kanwal, Dr. Matthew Cheng and Dr. Wolf Hirschmann for their valuable insights on this project and for creating a healthy and friendly environment in the lab. A special thanks to Ruth Schmid, Ulrike Thieß, and Ingrid Fetka for their technical support and Claudia Heberle for the administrative support during this work.

Many thanks to my friends- Shweta, Phani, Joyita, Ibrahim, Nidhi, Aarthi, Karthika, Kiran, Santoshi, Bhavesh, and Gandhi for motivating me during low times of my Ph.D. and giving me wonderful memories during my stay in Tübingen that I would cherish for life.

A special thanks to my friend Sai Prasanna for believing in me and supporting me in my all scientific and personal pursuits.

Last but not the least, I would like to thank my Mom, Dad, my sisters and my brothers-in-law for their unconditional love and support, and always encouraging me to pursue my dreams.